Effects of silicon nutrition on wheat growth and quality in upland soils of Hokkaido

2023

Vilayphone Sourideth

Doctoral Program in Animal Science and Agriculture

Graduate School of Animal and Veterinary Science and Agriculture

Obihiro University of Agriculture and Veterinary Medicine

北海道の普通畑土壌におけるコムギのケイ素吸収が生育や品質に及ぼす影響

令和 5 年
（2023）

帯広畜産大学大学院畜産学研究科
畜産科学専攻博士課程

スリデイ　ヴィーライフォン

TABLE OF CONTENT

LIST OF TABLES

CHAPTER 2.

CHAPTER 3.

CHAPTER 4.

LIST OF FIGURES

CHAPTER 1. INTRODUCTION

1.1. Silicon and its benefits

Silicon (Si) is the second most abundant element after oxygen in the Earth's (Wedepohl, 1995). Even though Si is not a confirmed essential nutrient for plant growth, Si is a very useful nutrient for many cereal crops where it can enhance and increase the resistance against many biotic and abiotic stresses (Datnoff et al., 2001; Epstein, 1994; Liang et al., 2015; Rodgers‐Gray and Shaw, 2004; Rodrigues and Datnoff, 2015). Especially, for rice (*Oryza sativa*), Sugarcane (*Saccharum officinarum*), maize (*Zea mays*) and wheat (*Triticum aestivum*) those are categorized as Si accumulators (plants accumulate more than 1 % Si concentration of shoot biomass and a Si/Ca ratio greater than 1) (Ma and Takahashi, 2002).

The studies of relationship between soil available Si and plant Si uptake in rice and sugarcane have been well expanded (Camargo and Keeping, 2021; Frazão et al., 2020; Guntzer et al., 2012; He et al., 2015; Liang et al., 2015; Ma and Takahashi, 2002; Majumdar and Prakash, 2022). Rice is a staple food in Japan and many Asian countries, the relationship between soil available Si and plant Si uptake has been studied in detail, particularly for paddy rice (Liang et al., 2015). Increase of soil Si availability could improve Si uptake by rice (Kato and Owa, 1997; Liu et al., 2014). Although there have not been many studies on upland soil cropping system. Soil Si availability for sugarcane production areas in Okinawa was recently reported (Yanai et al., 2019).

In wheat production, applying Si amendment could reduce the severity of some diseases such as powdery mildew (*Blumeria graminis*), tan spot (*Pyrenophora tritici-repentis*) and blast caused by *Pyicularia Oryzae* (Debona et al., 2014; Dorneles et al., 2017; Rodgers‐Gray and Shaw, 2004). Furthermore, Si could also increase wheat nutrients (N, P) uptake,

enhance the growth and reduced heavy metals (Cadmium) accumulation (Ali et al., 2019; Hellal et al., 2012; Kostic et al., 2017; Wu et al., 2016). Si application also helps to mitigate the salt and drought stress condition (Alzahrani et al., 2018; Neu et al., 2017).

1.2. Wheat and soil in Tokachi, Hokkaido

Hokkaido is one of the major food production areas in Japan, and Tokachi district is the major upland crop production area for wheat, potatoes (*Solanum tuberosum L.*), soybeans (*Glycine max*), adzuki beans (*Vigna angularis*), and sugar beets (*Beta vulgaris ssp. Vulgaris*). Wheat is the most important upland crop in the Tokachi district, covering 42,600 ha and accounting for 20 % of the whole production area of Japan (Department of Agriculture, Hokkaido Goverment, 2022). About 90 % of wheat produced in Hokkaido is winter wheat. The average wheat grain yield in this region is about 4700 kg $ha^{-1}$and lower than average yield for Hokkaido (5780 kg ha^{-1}). Low wheat production maybe resulted from abiotic and biotic stresses such us lodging and diseases (Figure 1.1).

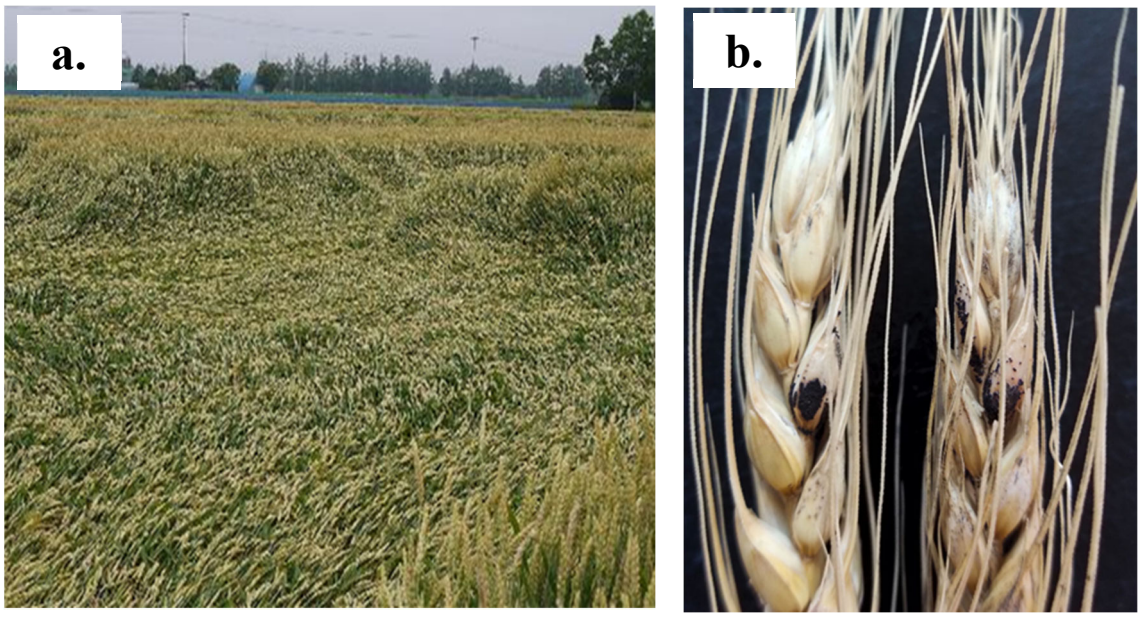

Figure 1.1. Wheat plant lodging (a) and affected by Fusarium head blight (b)

In Tokachi district, regional scale variation of soil types has been studied extensively. The surface topography of the Tokachi plain is surrounded by the Daisetsu mountains in the north and in the west bounded by the Hidaka mountains range (Figure 1.2). composed of alluvial fans and floodplains on various river terraces formed in different ages (Kikuchi, 2008). The formation age of the river terrace is known to affect the types of parent materials found in the soil profiles ranging from alluvial materials to volcanic ash of different origins. (Hatano et al., 2021; Kikuchi, 2008; Tani, 2010). About 50 % of the arable soils in the Tokachi district are classified as Andosols and 34 % are classified as Lowland soils according to the Hokkaido soil classification system (Kanda et al., 2016; Obara et al., 2016).

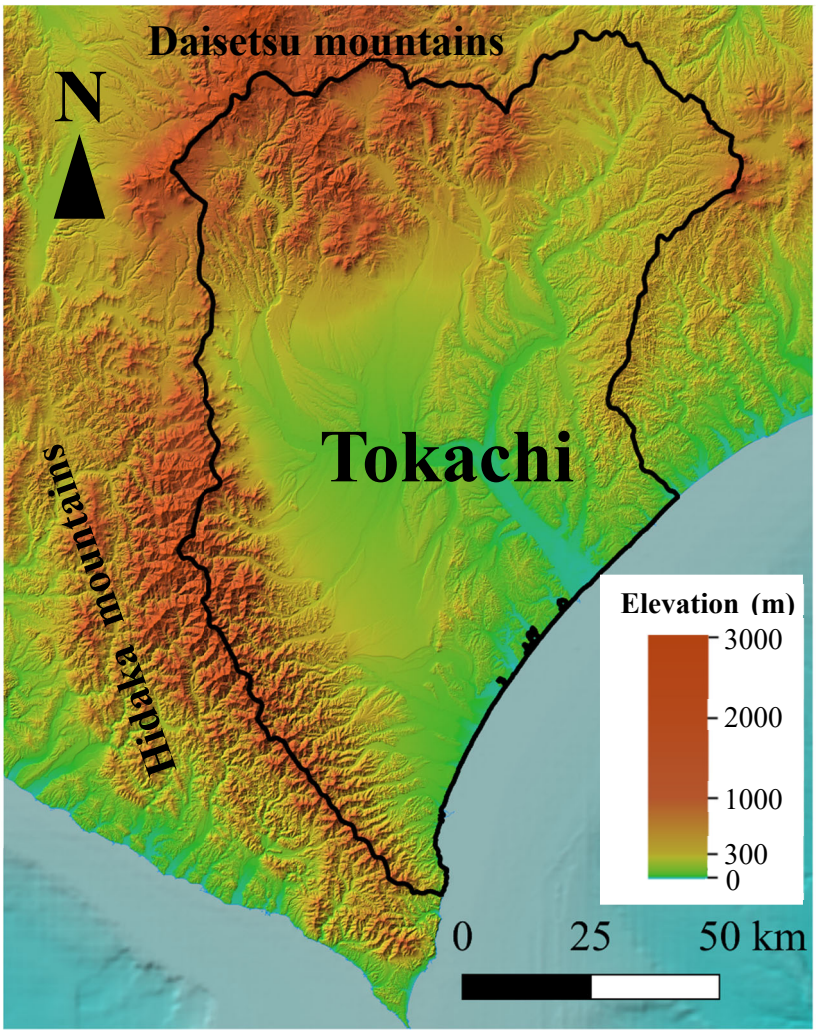

Figure 1.2. Topography map of Tokachi, Hokkaido.

1.3. Objectives

Wheat is known to take up a large amount of silicon (Si), which functions to improve productivity of wheat (Ma and Takahashi, 2002; Powell et al., 2005). In Japan, the Si studies mainly focused on rice and paddy fields (Ma and Takahashi 2002, Yoshida et al. 1962, Ma and Yamaji 2006) and there are very few studies that were done in upland areas.

Plant availability of Si is known to be different from total Si in the soils. Available Si in paddy soil is evaluated by measuring the concentration of Si that dissolves into the solution when the soil is incubated under flooded conditions, though the method is time-consuming and requires effort. Several extraction methods have been introduced to estimate plant-available Si using a buffer solution of phosphate and acetate but only for rice paddy soils (Kitta and Mizuochi, 1997; Shigezumi et al., 2002). However, the methodology estimating plant available Si in upland soils is still not clarified.

In upland soils, the soil available Si has been studied across Japan, and it varied from 12.0 to 572 mg kg^{-1} using an acetate buffer method (Yanai et al., 2016). The large variation was attributed to the difference in both parent materials as well as soil pH. Soils with higher amounts of amorphous clay minerals (i.e. allophane and imogolite) showed higher Si availability and higher pH also increased plant available Si since more orthosilicic acid adsorption on soil colloids at a higher pH range (Yanai et al., 2016; 2019).

Nevertheless, the previous studies showed only Si from the soils and very few samples from Hokkaido, and there have not been any studies focusing on the availability of Si in upland soils for upland crops information on plant available Si in upland soil. Therefore, the overall goals of this study were to improve crop production in upland soil in Tokachi, Hokkaido. To achieve to this goal the study had the following objectives;

- To assess the availability of soil Si in upland soils while considering the impact of other soil properties
- To evaluate the level of Si absorption and concentration in wheat and their correlation with the Si availability of the soil and other nutrients
- To evaluate soil Si solution extraction methods that could be used to determine available Si for wheat grown in upland soil

CHAPTER 2. VERTICAL DISTRIBUTION OF AVAILABLE SILICON IN THE SOILS ALONG THE RIVER TERRACE OF TOKACHI, HOKKAIDO

2.1. Objectives

The previous chapter showed the in Tokachi area, many different soil types occur and these differences in soil types are known to affect their physicochemical and mineralogical properties. There are several soil profile sties were done in the Tokachi however, they mainly focused on soil formation processes and phosphate availability (Kato et al., 2019; Kikuchi, 2008; Tani et al., 2010) and there have not been any studies focusing on the availability of Si in the soils for crop production.

In addition, previous studies on soil Si under upland crops have solely focused on topsoil (Yanai et al., 2016; 2019), no studies have been done to evaluate Si reserve in the subsoils. Wheat roots may be distributed not only in the topsoil but also in the subsoil (Thorup-Kristensen et al., 2009; White and Kirkegaard, 2010), and the vertical distribution of available nutrients is also important for clarifying nutrient uptake by plants (Jackson et al., 2000; Jobbágy and Jackson, 2001).

In this chapter, the objectives of this study were to (i) clarify the soil morphological features and characteristics of soil profiles on river terraces developed in different ages in the Tokachi district, (ii) classify the soils developed on the river terraces using the Japanese Soil Classification System (The Fifth Committee for Soil Classification and Nomenclature, 2017) and Soil Taxonomy (Soil Survey Staff, 2014), and (iii) evaluate the amount of available Si in each horizon of the soil profiles and determine the soil factors that affect the available Si in the soil profiles.

2.2. Materials and methods

2.2.1. Study site and samplings

The study was conducted in Shimizu town, which located in the western part of Tokachi district at the base of the Hidaka Mountain Range, Hokkaido, Japan (Figure 2.1.). Upland fields cover 14,900 ha in Shimizu town and the major crops are wheat, sugar beets, potatoes and beans (Hokkaido Agriculture Policy Office, 2022).

Four soil profile survey sites were intentionally placed in river terraces of different formation ages. Four levels of river terraces with different elevations have developed, Lowland, Low terrace, Middle terrace, and High terrace in the order of lower to higher elevations with younger to older formation age. The average elevation was 105 m, 128 m, 153 m, and 196 m for Lowland, Low terrace, Middle terrace and High terrace respectively.

The soil profile survey was conducted in August 2021 right after winter wheat harvest. The morphological evaluations were done according to the Soil Survey Handbook (Japanese Society of Pedology, 2021). The soil samples were collected from each horizon, and they were air-dried, sieved through a 2-mm mesh, and any visible plant roots and remains were removed as much as possible.

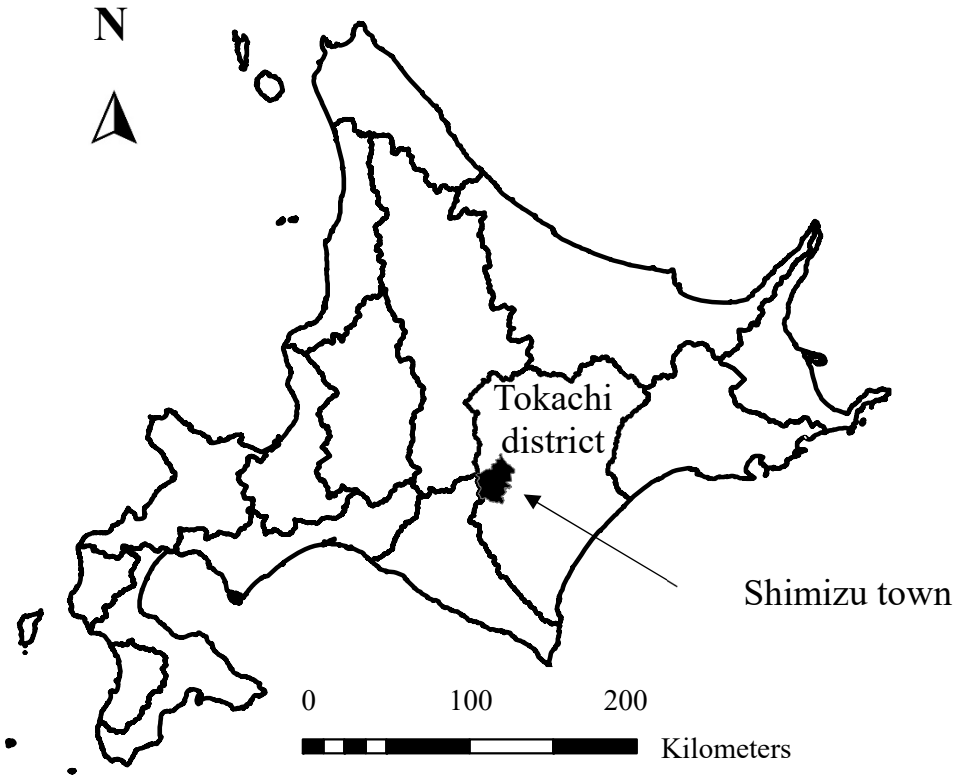

Figure 2.1. Location of Shimizu town and Tokachi district, Hokkaido.

2.2.2. Soil analysis

Acid-oxalate extractable aluminum (Al_o), iron (Fe_o), and silicon (Si_o) were determined using a 0.2 mol L^{-1} acid ammonium oxalate solution at pH 3. 0 (Blakemore et al., 1987). Pyrophosphate extractable aluminum (Al_p) and iron (Fe_p) were determined using a 0.1 mol L^{-1} sodium pyrophosphate solution at pH 10 (Blakemore et al., 1987). The concentrations of aluminum (Al), iron (Fe), and Si in the extracts were measured by a simultaneous inductively coupled plasma atomic emission spectrometer (ICP-AES; ICPE-9820, Shimadzu Corporation, Kyoto, Japan).

Available phosphate (P) was determined by the Truog method, and the concentration of phosphate in the extract was measured using the colorimetric molybdate blue method with a spectrophotometer (UV mini-1240; Shimadzu Corporation, Kyoto, Japan) and the data was showed in element base. The pH (H_2O) and pH (KCl) were measured using a 1:2.5 soil/water and soil/1 mol L^{-1} KCl ratio, respectively. Total carbon (Total C) was measured by the dry combustion method with a CHN automated elemental analyzer (Vario EL III, Elementar Analysensysteme, Hanau, Germany). The phosphate absorption coefficient (PAC) was determined by reacting soil with a solution containing 13.44 mg-P_2O_5 mL^{-1} for 24 hours. After the reaction, remaining concertation of phosphate in the solution was measured using the vanadomolybdate yellow method with a spectrophotometer (UV mini-1240; Shimadzu Corporation, Kyoto, Japan). Cation exchange capacity (CEC) and exchangeable cations were measured using a 1 mol L^{-1} ammonium acetate extraction method buffered at pH 7. The CEC was determined using a formal titration method. The concentration of exchangeable cations was measured by an atomic adsorption spectrophotometer (AAS; Z-5010, Hitachi High-Tech Corporation, Tokyo, Japan). Base saturation (BS) was calculated from the CEC and exchangeable cations.

In this chapter, the acetate buffer extraction method was selected to evaluate available Si in the soils (Imaizumi and Yoshida, 1958; Kitta and Mizuochi, 1997; Yanai et al., 2016). Two grams of air-dried soil sample was mixed with a 0.1 molL^{-1} acetate buffer solution (pH 4.0) in a 50 mL centrifugation tube at a soil/solution ratio of 1:10. The tubes were continuously shaken for 5 h at 40°C in the hot water bath. The solution was then filtered with a filter paper (ADVANTEC No. 6). The concentration of Si in the solution was measured using an ICP-AES (ICPE-9820; Shimadzu Corporation, Kyoto, Japan) and showed in element base. Although we have not verified whether the aetate buffer extraction developed for paddy soils can be applied to upland soils where wheat is cultivated, we

decided to denote Si extracted by the acetate buffer as “available Si” in this study as the previous study has also used it to evaluate available Si in upland soils (Yanai et al., 2016). Statistical analyses were conducted using JMP Pro 16.1 (SAS Institute Inc., Cary, North California). Pearson correlations were performed to determine the extent of relationships between available Si and soil properties.

2.3. Results and discussion

2.3.1. Soil morphological features

The four soil profiles showed distinctly different morphological features (Figure 2.2). Especially, the differences in the colors of the topsoil and subsoil were remarkable. They might be affected by variable content of soil organic matter in the topsoil and drainage in the subsoil. Some of the descriptions of the soil profiles were selected and shown in Table 2.1.

The Lowland soil profile showed the lightest color (10YR 4/3) in the topsoil followed by the High terrace (10YR 3/3) and the Low terrace (10YR 2/2). The Middle terrace showed the darkest color (10YR 1.7/1) among the soil profiles. Fe mottling was observed in the Lowland, the Low terrace, and the Middle terrace indicating poor drainage in the subsoil. Fe mottling appeared at the depth closest to the surface in the Low terrace.

In the Lowland, the soil texture was relatively coarse with sandy loam to loamy sand. The Tokachi river, which starts from the Hidaka mountain range, flows through the Tokachi plain and into the Pacific Ocean. Since Shimizu town is located relatively upstream of the Tokachi river, coarse alluvial sediments are deposited in the lowland of this area due to flooding. In the Low terrace and the Middle terrace, the topsoil was loam and the subsoils

Table 2.1. Soil profile description of four soil profiles.

Horizon	Depth (cm)			Moist soil color[a]	Mottling and concretion[b]	Field texture[c]	Rock structure[d]	Active aluminum
Lowland								
Ap1	0	~	15	10YR 4/3	N		SL	N	-
Ap2	15	~	30	10YR 4/3	N		SL	N	-
Ap3	30	~	39	2.5Y 4/4	N		SL	N	-
C	39	~	69	2.5Y 5/4	N		LS	N	-
Cg1	69	~	100	10YR 4/6 (30%) 2.5Y 5/2 (70%)	FA TU FeM FA CL FeM	(30%)	S/LS	N	-
Cg2	100	~	120+	10YR 4/6 (30%) 2.5Y 5/2 (70%)	FA TU FeM FA CL FeM	(30%)	LS	N	±
Low terrace								
Ap1	0	~	15	10YR 2/2	N		L	F G SR (2%)	++
Ap2	15	~	30	10YR 2/2	N		L	F G SR (2%)	++
Ap2/2B/ 2A	30	~	38	10YR 2/2 (Ap2) 10YR 4/6 (2B) 10YR 2/1 (2A)	N		L (Ap2) SL (2B) CL (2A)	N	++ (Ap2) +++ (2B) +++ (2A)
2Cg1	38	~	48	10YR 4/6 (50%) 10YR 5/1 (50%)	DI TU FeM	(50%)	CL	F G SR (1%)	-
2Cg2	48	~	80	10YR 4/6 (10%) 2.5Y 5/1 (90%)	DI TU FeM	(10%)	LiC	F S SR (5%)	-
2Cg3	80	~	100+	10YR 4/6 (50%) 10YR 5/1 (50%)	FA TU FeM	(30%)	CL	F S/LS SR (30%)	-
Middle terrace								
Ap1	0	~	15	10YR1.7/1	N		L	N	++
Ap2	15	~	35	10YR1.7/1	N		L	N	++
2A	35	~	46	N 1.5/0	N		L	N	++
3B	46	~	61	10YR5/4	N		CL	N	+++
4Cg1	61	~	91	2.5 Y 6/1 (90%) 7.5YR 5/6 (10%)	DI TU FeM	(10%)	LiC	N	-
4Cg2	91	~	110+	2.5 Y 5/2 (90%) 7.5YR 5/6 (10%)	DI TU FeM	(10%)	CL	N	-
High terrace								
Ap1	0	~	13	10YR 3/3	N		L	N	++
Ap2	13	~	32	10YR 3/3	N		L	N	++
2B	32	~	42	10YR 4/6	N		L	N	+++
3B1	42	~	72	10YR 5/6	N		L	N	+++
3B2	72	~	104+	10YR 5/6	N		L	F G SR (1%)	+++

[a]Based on Munsell color chart. [b]N, none; FA, faint; DI, distinct; TU, tubular; CL, cloudy; FeM, Fe mottling. [c]SL, sandy loam; LS, loamy sand; S, sand; L, loam; CL, clay loam; LiC, light clay. [d]N, none; F, fresh; G, gravel; S, stone; LS, large stone; SR, subrounded.

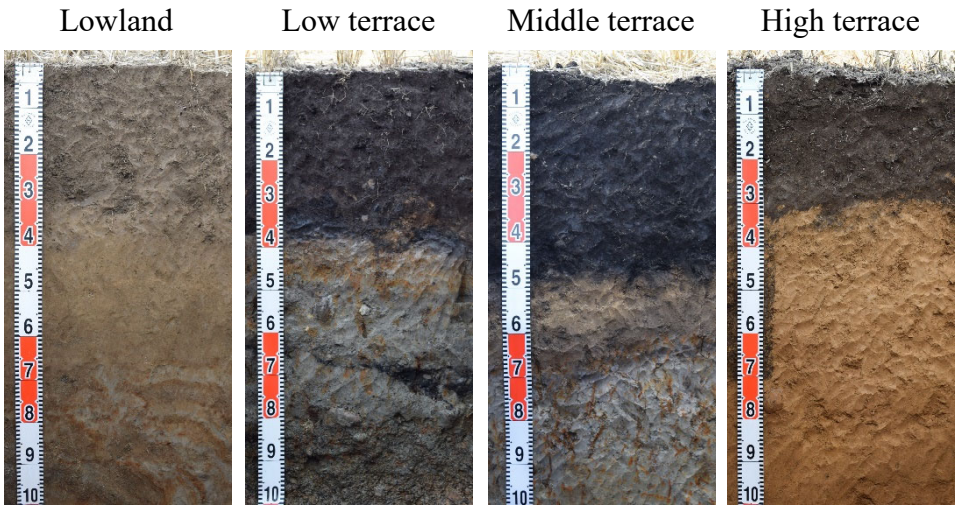

Figure 2.2. Four soil profiles surveyed from different topographical positions along the river terraces.

were clay loam to light clay. The High terrace showed loamy textures in the entire soil profile, which is typical of volcanic ash soils in the area.

Based on the morphological characteristics of each profile and the results of active Al test, it is likely that these four soil profiles were developed from distinctly different parent materials. The schematic diagram of the parent materials was shown in Figure 2.3. In the

Lowland, the whole profile was formed by the alluvial deposit of the Tokachi river, with no indication of active Al (Table 2.1). In the Low terrace and Middle terraces, it is assumed that the surface soils were derived from the volcanic ashes with active Al (Table 2.1) and the subsoils were formed from alluvial deposits. These volcanic ashes are presumed to have been deposited in the Holocene, including Tarumae-a tephra erupted in 1739 (Ta-a), Komagatake-c2 tephra erupted in 1694 (Ko-c2), and Tarumae-b tephra erupted in 1667 (Ta-

b) (Machida and Arai, 1992), which were mixed by plowing in the Ap horizons (Table 2.1). Both 2A and 2B horizons of the Low terrace and the 2A horizon of the Middle terrace were identified as originating from Tarumae-c tephra (Ta-c), a wide spread volcanic ash estimated to have erupted 2,500 to 3,000 years ago, due to its high active Al content and loamy soil texture (Table 2.1).

The 3B horizon of the Middle terrace was supposed to have originated from Tarumae-d tephra (Ta-d), which erupted 8,000 to 9,000 years ago, based on the remarkable reaction of the active Al test and the appearance of a pumice-like morphology (Machida and Arai, 1992). In the High terrace, the entire soil profile was derived from volcanic materials, with the surface soil forming from the Holocene volcanic ashes, and the subsoil originating from the late Pleistocene volcanic ash. The Holocene volcanic materials might be similar to the Low and the Middle terraces, while the late Pleistocene volcanic materials were identified as Eniwa-a loam (En-a) deposited 18,000 years ago.

The differences in the morphological features of these profiles was considered to reflect the uplifting age of each river terrace. All the river terraces were located in the floodplain of the Tokachi river in the past, due to repeated uplifting and river erosion, the oldest uplifted High terrace had formed a stable terrace surface in the Late Pleistocene. On the other hand, in the Lowland located in the current river floodplain, the volcanic ashes that fell and deposited was washed away by the flooding of the river and the soil was derived only from alluvial sediments (Kato et al., 2019; Kikuchi, 2008).

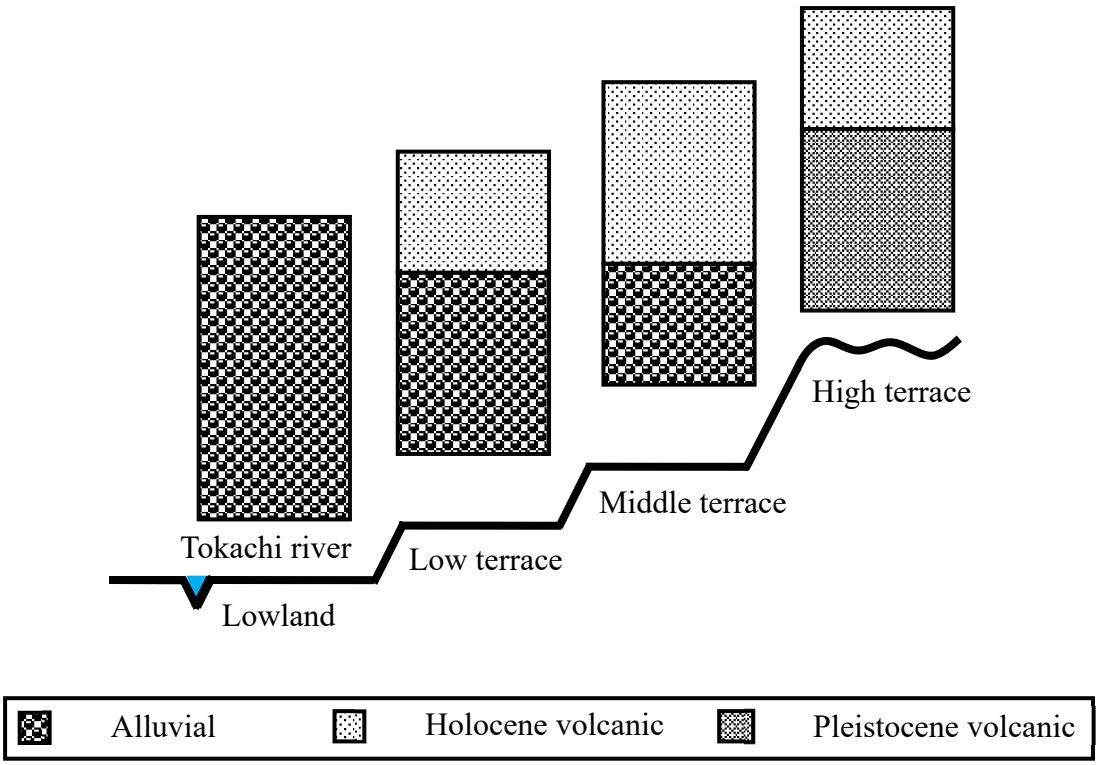

Figure 2.3. Schematic diagrams of different parent materials deposited in the soil profiles along the river terraces.

The Lowland soil profile is young and immature with little weathering or soil formation, and showed a typical A-C profile without B horizons (Table 2.1). Faint tubular and cloudy mottling were observed in the Cg1 and Cg2 horizons that implied slightly poor drainage. Due to its coarse texture, the mottling is thought to be caused by a seasonal movement of groundwater level. There was no indication of active Al confirming the absence of volcanic ash materials.

The soil profile of the Low terrace was also relatively immature, similar to the Lowland soils, and little development of B horizons was observed (Table 2.1). There was a distinct tubular mottling in 2Cg1 and 2Cg2 horizons indicating the presence of high seasonal groundwater level and poor drainage. The soil texture of the subsoils was clay loam to light

clay indicating that these sediments could be deposited when the area was under back swamp or a little far from the river. Subrounded rocks were also observed in the subsoils, suggesting that alluvial materials transported by the river were deposited. The active Al test showed strong reactions only in the topsoil (0-38 cm depth) whereas there was no reaction in the subsoils. These confirmed that the topsoil was originated from volcanic ash materials and the subsoils were derived from alluvial deposits.

In contrast to the Lowland and the Low terrace, a thick B horizon was observed in the soil profile of the Middle terrace, indicating that soil formation is relatively advanced (Table 2.1). In the subsoils below 61 cm depth, the soil texture was clay loam to light clay, and a distinct tubular mottling was also observed, suggesting that there was a seasonal rise in the ground water level and poor drainage. Since poor drainage could inhibit the decomposition of organic matter and contribute to the accumulation of humic substances, the blackness of the surface soils was conspicuous.

In the soil profile of the High terrace, brown B horizons (10YR 4/6 or 10YR 5/6) with a well-developed structure were observed under the Ap horizons, indicating that the soil has been formed for a relatively long time unlike the soil profiles on other terraces (Table 2.1) The active Al test showed strong reactions in all horizons from surface to the subsoils.

2.3.2. Soil mineralogical and physiochemical properties

The four soil profiles were noticeably different in soil mineralogical and physicochemical properties as well as morphological features (Table 2.2). These differences could be influenced by the differences in soil parent materials, pedogenesis, and their formation time at each location.

Al_o and Si_o originating from amorphous to para-crystalline clay (Blakemore et al., 1987) were significantly different in the soil profile of each terrace. These values decreased in the order of the High terrace, the Middle terrace, the Low terrace, and the Lowland, strongly reflecting the influence of volcanic ash described in the previous section. On the other hand, Fe_o was relatively abundant in the soil profile of the Low terrace, which might be affected by the redox potential under poor drainage conditions.

The $Al_o + 1/2Fe_o$ content is used for the criteria of andic soil properties, and if this value is 2 % or more, it meets the criteria in the Soil Taxonomy (Soil Survey Staff, 2014). These values in soil horizons ranged between 0.40 to 7.97 % reflecting differences in the parent materials (Table 2.2). In the soil profile of the Lowland, $Al_o + 1/2Fe_o$ values were less than 2 % in all horizons. As well as the Lowland, the subsoils of the Low terrace (2Cg1, 2Cg2, and 2Cg3) and Middle terrace (4Cg1 and 4Cg2) also showed $Al_o + 1/2Fe_o$ smaller than 2 %. In contrast, all horizons in the High terrace as well as upper horizons of the Low terrace and the Middle terrace showed $Al_o + 1/2Fe_o$ values greater than 2 %. These results clearly agreed with the differences in the morphological features and the parent materials of the profiles described in the previous section.

In Japanese soil classification, phosphate absorption coefficient (PAC), which is an index of the soil fixing ability of phosphate, has traditionally been used to define the Andosols (The Fifth Committee for Soil Classification and Nomenclature, 2017).

Table 2.2. Selected mineralogical and physicochemical properties of four soil profiles.

Horizon	Al_o[a]	Fe_o[a]	Si_o[a]	Al_p[b]	Fe_p[b]	$Al_o + 1/2Fe_o$	PAC[c]	pH	CEC[d]	BS[e]
			(g kg^{-1})			(%)		(H_2O)	($cmol_c$ kg^{-1})	(%)
Lowland										
Ap1	4.59	8.62	2.24	0.92	2.60	0.89	600	6.1	16.9	83.3
Ap2	3.80	7.91	1.67	0.77	2.50	0.78	630	6.2	17.4	92.0
Ap3	4.55	8.05	2.28	0.63	2.35	0.86	630	6.3	16.2	89.9
C	4.02	8.30	2.20	0.36	1.64	0.82	750	6.3	16.0	94.8
Cg1	2.73	8.75	1.88	0.08	0.83	0.71	590	6.5	14.1	82.6
Cg2	3.14	7.65	2.13	0.10	0.78	0.70	490	6.6	12.1	86.4
Low terrace										
Ap1	11.5	20.7	3.16	5.94	6.30	2.18	1390	5.3	30.1	40.8
Ap2	12.4	23.2	3.51	6.08	5.61	2.40	1440	5.3	29.6	39.6
Ap2/2B/ 2A	11.6	42.5	4.82	4.20	4.60	3.29	1650	5.6	31.6	47.8
2Cg1	2.72	10.6	1.89	0.06	0.70	0.80	810	6.0	16.9	98.5
2Cg2	2.12	3.84	1.16	0.09	0.52	0.40	610	6.1	13.6	95.3
2Cg3	4.45	7.04	2.54	0.46	1.11	0.80	300	5.9	8.08	68.9
Middle terrace										
Ap1	23.8	11.7	6.71	9.48	5.46	2.97	2150	5.7	40.6	50.3
Ap2	23.5	12.0	6.53	10.1	6.03	2.94	2090	5.7	42.4	45.6
2A	24.6	15.7	6.75	11.0	6.74	3.24	2310	5.7	45.2	42.3
3B	77.2	4.54	32.1	8.73	1.36	7.95	2680	5.4	42.7	16.1
4Cg1	2.88	7.37	1.01	0.25	1.10	0.66	980	4.9	22.8	64.7
4Cg2	2.82	8.19	1.66	0.01	1.09	0.69	1050	4.9	25.1	70.9
High terrace										
Ap1	39.6	14.3	16.5	4.95	1.67	4.67	2210	5.6	26.0	45.5
Ap2	40.9	17.6	17.0	4.80	1.71	4.97	2190	5.8	25.5	42.2
2B	40.6	12.7	19.6	3.28	0.31	4.69	2280	6.2	16.9	40.3
3B1	40.9	17.6	17.0	2.89	0.21	4.97	2260	6.4	15.4	34.4
3B2	40.9	17.6	17.0	3.40	0.25	4.97	2610	6.4	17.6	27.8

[a]Al_o, Fe_o, and Si_o; oxalate-extractable Al, Fe, and Si, respectively. [b]Al_p and Fe_p; pyrophosphate-extractable Al and Fe, respectively. [c]PAC; phosphate absorption coefficient. [d]CEC; cation exchange capacity. [e]BS; base saturation.

In the Japanese taxonomy, if the PAC is 1,500 or higher, it is defined as showing andic soil properties. For the top four horizons of the Middle terrace and all horizons of the High terrace, the PAC values were all 1,500 or more, which satisfied the andic soil properties together with $Al_o + 1/2Fe_o$. The Ap horizons of the Low terrace had less than 1,500 PAC but more than 2 % $Al_o + 1/2Fe_o$, which is probably due to the mixing of alluvial deposits into the volcanic ash by plowing. Since it is defined that the criterion of PAC of 1,500 or more can be replaced with the criterion of $Al_o + 1/2Fe_o$ of 2 % or more in the Soil Classification System of Japan (The Fifth Committee for Soil Classification and Nomenclature, 2017), the Ap horizons of the Low terraces also meets the requirements for andic soil properties.

Al_p and Fe_p extracted from metal-humus complexes were also significantly different in the soil profile of each terrace (Blakemore et al., 1987). In the Lowland soil profile, Al_p and Fe_p were significantly lower than in other profiles (Table 2.2), which was attributed to the formation of metal-humus complexes occurring in soils derived from volcanic materials (Takahashi and Dahlgren, 2016). In the horizons derived from volcanic ash in the soil profile on each terrace, Al_p and Fe_p were most abundant in the Middle terrace, followed by the Low terrace and then the High terrace (Table 2.2). The surface soils of the Middle terrace showed the highest accumulation of metal-humus complexes, reflecting the darkest color among the four soil profiles. The higher concentration of metal-humus complexes in the surface volcanic soils of the Middle and Low terraces might be resulted from hydro sequence factor under poor drained conditions, suggesting that the decomposition of organic matter by microorganisms was suppressed under oxygen-deficient conditions, and humic substances that were stabilized by combining with metals derived from volcanic ash were more likely to accumulate in the surface soils (Kikuchi, 1981; Saigusa et al., 1991).

Soil pH of these four profiles was acidic to slightly acidic ranging from 4.9 – 6.6 (Table 2.2). Cation exchange capacity (CEC) was significantly different in the soil profiles of each

terrace. The CEC of the surface horizons was highest in the Middle terrace, followed by the Low terrace, the High terrace, and the Lowland, indicating the CEC was strongly affected by humic substances in these profiles. BS might be influenced by both soil improvement by application of lime materials and soil formation processes. The BS in the Ap horizons reflected the effects of soil management by growers and CEC, and was as high as 80 % or more in the Lowland and around 40 – 50 % on the terraces.

The vertical distribution of total C and allophane contents, which were soil inherent properties, were significantly different in the soil profiles of each terrace, reflecting the effects of parent materials and soil formation processes (Figure 2.4). The allophane contents were calculated and estimated by Parfitt and Wilson (1985). The vertical distribution of the total C contents in the soil profiles of each terrace was significantly different in the layers from the surface to a depth of 40 cm. The total C contents of the surface horizons were highest in the Middle terrace, followed by the Low terrace, the High terrace, and the Lowland, similar to the morphological features of the soil profiles and the Al_p derived from the metal-humus complexes, which have already been discussed in the previous results.

On the other hand, the vertical distribution of allophane contents was quite different from that of the total C. The allophane contents from the surface to a depth of 40 cm was remarkably higher on the High terrace, slightly high on the Middle terrace, but significantly lower on the Low terrace and the Lowland. In the subsoils, the 3B horizon derived from Ta-d on the Middle terrace and 3B2 horizons derived from En-a on the High terrace showed extremely high allophane contents. Although amorphous and para-crystalline clay minerals, such as allophane and imogolite are synthesized through weathering and soil formation processes of volcanic materials, the formation of the minerals can be perturbed by humic substances, such as humic and fulvic acids (Inoue and Huang, 1985, 1990). The allophane contents were only high throughout the profile on the High terrace whereas the surface

horizons of the Low terrace and the Middle terrace originated from the Holocene volcanic ash, showed low allophane contents, which might be affected by accumulation of humic substances.

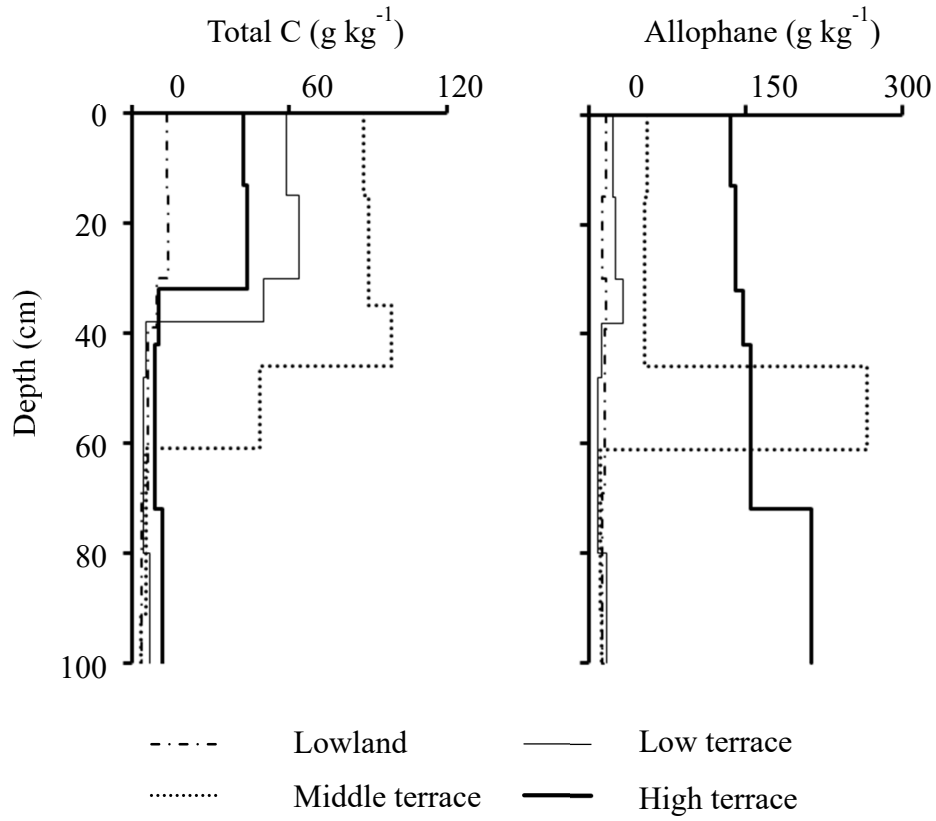

Figure 2.4. Vertical distribution of total carbon (C) and allophane in the soil profiles along the river terraces.

Based on the morphological features in the soil profiles, and the mineralogical and physicochemical properties analyzed for each horizon, we tried to classify the soils according to the Soil Classification System of Japan (The Fifth Committee for Soil

Classification and Nomenclature, 2017) and Soil Taxonomy by USDA (Soil Survey Staff, 2014).

The soil of the Lowland was classified as Aquic Brown Fluvic soils by the Soil Classification System of Japan, because the thickness of alluvial deposits was 25 cm or more within 50 cm of the surface layer, the color of the subsurface soil was brown, and wet characteristics by ground water appeared within 50 – 75 cm depth from the soil surface. The soil was classified as Oxyaquic Udifluvents by the Soil Taxonomy, because no diagnostic subsurface horizons were observed, the soil was formed from alluvial sediments under an udic moisture regime, and the subsoils were influenced by seasonal ground water within 100 cm depth from the surface soil.

The soil of the Low terrace was classified as Endofluvic Wet Andosols by the Soil Classification System of Japan, because the thickness of horizons, which showed andic soil properties was 25 cm or more within 50 cm of the surface layer, wet characteristics by ground water appeared within 50 cm depth from the soil surface, and alluvial deposits with a thickness of 25 cm or more accumulated within 75 cm from the soil surface. The soil was classified as Andic Oxyaquic Humudepts by the Soil Taxonomy, because the thickness of horizons, which showed andic soil properties was 18 cm or more but less than 60 % of the soil profile, umbric epipedon was observed, and the subsoils were influenced by seasonal ground water within 100 cm depth from the surface soil.

The soil of the Middle terrace was classified as Humic Allophanic Andosols by the Soil Classification System of Japan, because the thickness of horizons, which showed andic soil properties was 25 cm or more within 50 cm of the surface layer, main clay mineral was allophane, and organic carbon content of the surface soils was 6 % or more. The soil was classified as Aquic Melanudands by the Soil Taxonomy, because the thickness of horizons,

which showed andic soil properties was 60 % or more of the soil profile, melanic epipedon was observed, and the subsoils were influenced by seasonal ground water within 100 cm depth from the surface soil.

The soil of the High terrace was classified as Haplic Allophanic Andosols by the Soil Classification System of Japan, because the thickness of horizons, which showed andic soil properties was 25 cm or more within 50 cm of the surface layer, main clay mineral was allophane, and organic carbon content of the surface soils was 3 % or more and less than 6 %. The soil was classified as Typic Hapludands by the Soil Taxonomy, because the thickness of horizons, which showed andic soil properties was 60 % or more of the soil profile, umbric epipedon was observed, and the soil was developed under udic moisture regime.

2.3.3. Vertical distribution of available Si and affecting factors

Available Si contents extracted by the acetate buffer extraction method in this study ranged from 40.8 to 377 mg kg^{-1} with a mean of 119 mg kg^{-1} (Figure 2.5). These values were within the range of available Si in upland soils of Japan reported by Yanai et al. (2016). The vertical distribution of available Si in the soil profiles at each location was significantly different. In particular, it was remarkable that the available Si contents were mostly high through all horizons in the soil profile of the High terrace, whereas they were considerably low in the soil profiles of the Lowland and the Low terrace.

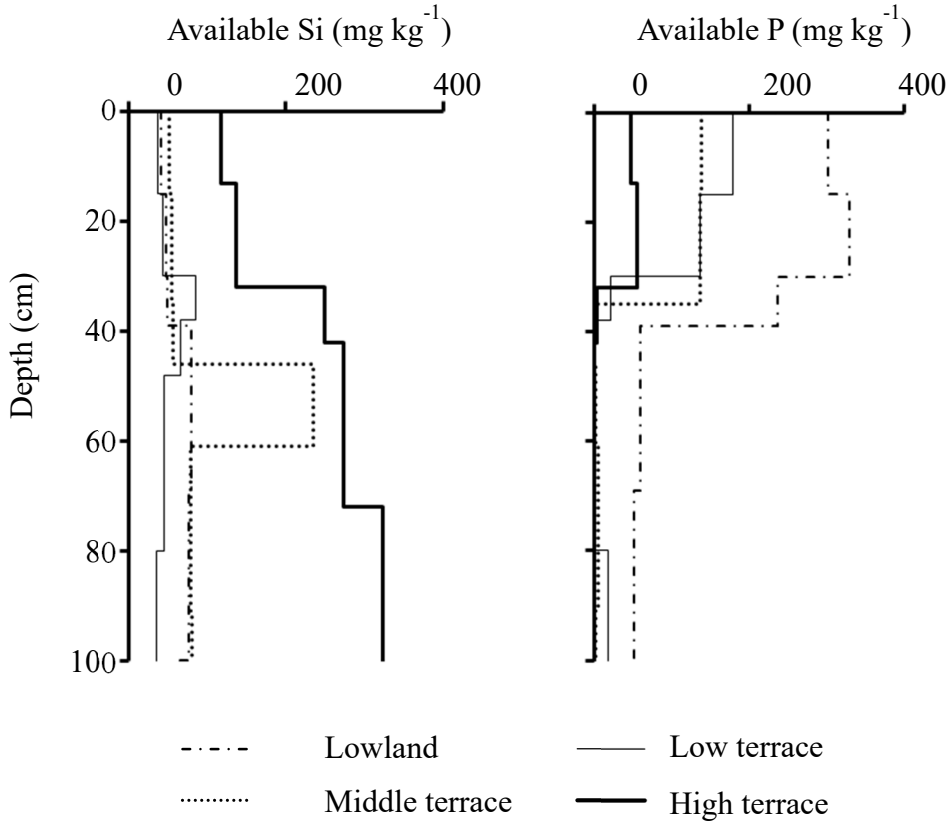

Figure 2.5. Vertical distribution of available silicon (Si) and phosphorous (P) in the soil profiles along the river terraces.

In the soil profile of the Middle terrace, the available Si contents were generally low in the most horizons and similar to those of the Lowland and the Low terrace, but the 3B horizon derived from Ta-d showed a distinctly high content. The available Si contents in the Ap horizons might be important, assuming that crops could absorb most of the Si from the surface horizons as same as other soil nutrients. In the Ap horizons, available Si contents were generally lower than the mean value (117 mg kg^{-1}) and below 70.1 mg kg^{-1} in the Lowland, the Low terrace and the Middle terrace. On the other hand, the available Si contents were relatively high around 140 mg kg^{-1} in the Ap horizons of the High terrace. Since Si

fertilization is not common in the study area, the factors that differ in the available Si in the surface Ap horizons could depend on the soil inherent properties, not an anthropogenic input.

In this region, one of the major factors limiting crop yields has been available phosphorous (P) and the heavy P fertilizer application has been recommended to maintain optimum yields because most of the soils have been originated by volcanic ashes which can fix a noticeable amount of P onto active Al present in the form of Al-humus complexes as well as non- and para-crystalline clay minerals (Hashimoto et al., 2012). In contrast to the available Si, available P was abundant in the surface horizons and very scarce in the lower horizons (Figure 2.5). The available P contents in the Ap horizons were significantly higher in the Lowlands (327 – 358 mg kg^{-1}), followed by the Middle terrace and the Low terrace (148 – 196 mg kg^{-1}), and the lowest in the High terrace (52.4 – 61.1 mg kg^{-1}). The available P contents in these soils could be affected by the PAC and agricultural inputs, such as P fertilizers and livestock manure. In particular, it was reported that a heavy application of P fertilizers to the upland Andosols in the Tokachi district could lead to a huge accumulation of total and available P in the Ap horizons (Tani et al., 2010). Thus, the available P contents were high in the Ap horizons because P had been enriched by continuous fertilization, but non-artificial factors that determined available Si contents should be clarified.

It was reported that a small portion of wheat roots could grow into deeper soil horizons below 60 cm depth (Thorup-Kristensen et al., 2009; White and Kirkegaard, 2010). If the roots could absorb Si from the lower horizons, the available Si below the Ap horizons should be evaluated. In the soil profile of the High terrace, the available Si contents increased with increasing soil depth and the subsoils had nearly double the amount of the Ap horizons. In the other profiles, the available Si contents were generally low at less than 93.5 mg kg^{-1}, but that was significantly higher at 234 mg kg^{-1} or more in the 3B horizon of the Middle terrace. Thus, the high available Si contents in the subsoils were consistent with the vertical

distribution of allophane contents (Figure 2.4 and Figure 2.5), suggesting that Si contained in amorphous minerals could be the source of available Si.

When the correlation between the available Si contents, and the soil physicochemical and mineralogical properties for all horizons of the four soil profiles was investigated, a significant positive correlation was found between the available Si contents and the allophane contents ($r = 0.895$; $p < 0.001$, n = 23), indicating that the available Si contents of the upland soils in the present study could be strongly influenced by the soil parent materials and soil formation processes, especially by amorphous and para-crystalline minerals. In addition, a weak positive correlation was observed between the available Si contents and pH (KCl) ($r = 0.477$, $p < 0.05$, n = 23) similar to the previous studies, suggesting the possibility that soil pH might be involved in dissolution of the minerals and a subsequent release of Si (Haynes, 2019; Huang and Hseu, 2021; Yanai et al., 2016; Yanai et al., 2019).

Furthermore, a decision tree analysis was performed using the available Si contents as the objective variable and the physicochemical and mineralogical properties as the explanatory variables (JMP Pro. 17, SAS Institute Inc. Japan, Tokyo, Japan). In the first step, Si_o was selected as an explanatory variable, and the soils were divided into two groups based on $Si_o > 16.9$ g kg^{-1} (mean of the available Si was 284 mg kg^{-1}) and $Si_o < 16.9$ g kg^{-1} (mean of the available Si was 71.2 mg kg^{-1}). Si_o was 17 g kg^{-1} or more in the four horizons below the Ap1 horizon of the High terrace and the 3B horizon of the Middle terrace. As a second step, the group with $Si_o < 17$ g kg^{-1} was further divided into two groups with $Si_o > 4.82$ g kg^{-1} (mean of the available Si was 85.2 mg kg^{-1}) and $Si_o < 4.82$ g kg^{-1} (mean of the available Si was 65.8 mg kg^{-1}) (Figure 2.6). The results of decision tree analysis indicated that the available Si contents in the soils could be explained only by Si_o ($R^2 = 0.837$), suggesting that amorphous minerals contributed as a source of available Si in the upland soils of Shimizu town, Hokkaido.

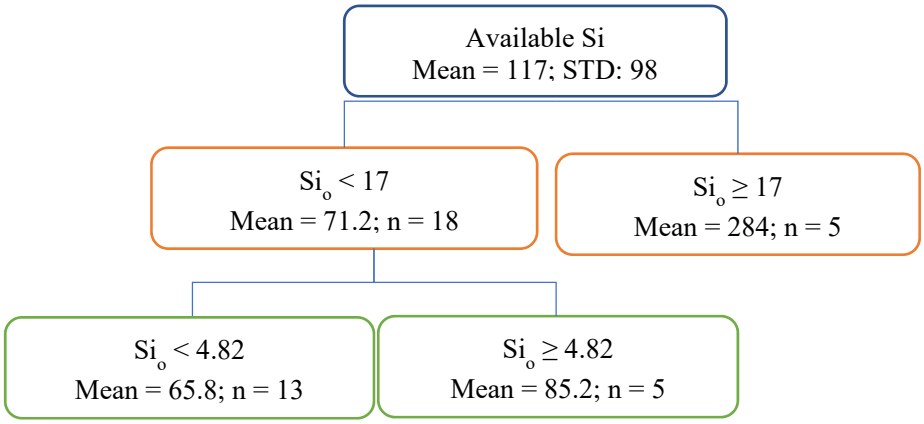

Figure 2.6. Decision tree analysis for available Si. Si_o, silicon extracted by acid oxalate

2.4. Summary

The four soil profiles on the river terraces in Shimizu town, Tokachi district, Hokkaido exhibited completely different morphological features and remarkably different physicochemical and mineralogical properties. The differences in the parent materials, such as alluvial and volcanic deposits, and water environment in the lower horizons had strong effects on the soil formation processes, and significant differences in the vertical distribution of humic substances and amorphous minerals. One soil profile was classified as Fluvic soils and three soil profiles were classified as Andosols according to the Japanese Soil Classification System, but one of the Andosols was classified as Inceptisols in the Soil Taxonomy due to a subtle difference in the criteria of the andic soil properties. The available Si content in each horizon of these soil profiles differed markedly, and was higher in the horizons where allophane formation was advanced. Although a strong positive correlation was observed between acid-oxalate soluble Si contents (Si_o) and available Si contents in the soils, further studies might be needed to clarify the relationship of Si between the soils and crops in the study area. Further studies might be necessary to compare the available Si contents of the upland soils with the Si uptake by crops such as wheat in the study area to clarify the relationship between Si in the soil and the crop.

CHAPTER 3. AVAILABLITY OF SI IN SOIL SURFACE ALONG RIVER TERRACE OF TOKACHI, HOKKAIDO

3.1. Objectives

In the Tokachi district, the alluvial fans and floodplains on various river terraces formed in different ages contributed to the formation of the surface topography of the Tokachi plain (Kikuchi, 2008). The formation age of the river terrace is known to affect the types of parent materials found in the soil profiles ranging from alluvial materials to volcanic ash of different origins (Hatano et al., 2021; Kato et al., 2019; Kikuchi, 2008; Tani, 2010).

The previous chapter evaluated the soil available Si and its vertical distribution under upland crops. The available Si contents in the Ap horizons might be important, assuming that crops could absorb most of the Si from the surface horizons as same as other soil nutrients. More than 50 % of wheat root distributes in 30 cm depth of the soil profile (White and Kirkegaard, 2010), hence majority of soil nutrients wheat may uptake from this soil layer.

Besides the acetate buffer extraction method (Imaizumi and Yoshida, 1958; Kitta and Mizuochi, 1997), there are several methods have been proposed for the evaluation of the soil available content in soils, particularly paddy soils, such as the submerged incubation method by Takahashi and Nonaka (1986), the readily dissoluble silica evaluation method by Sumida (1991) and the phosphate extraction methods (Kato, 1998; Shigezumi et al., 2002) which among them the acetate buffer and the phosphate buffer extraction methods have been used widely in Japan due to the high efficiency in time-consuming and labor for the extraction, they are suitable for the analysis routine and they also showed the significant positive correlation with Si content in rice (Imaizumi and Yoshida, 1958; Kato, 1998; Shigezumi et al., 2002; Yanai et al., 2016)

Therefore, in this chapter, the objectives of this study were to (i) assess the soil available Si status of soil surface by using three solution extraction methods including 0.1 M acetate buffer, 0.01 M and 0.04 M phosphate buffer solution methods, and (ii) evaluate relation between available Si and other soil properties in upland wheat production area on river terraces in the Tokachi district.

3.2. Materials and methods

3.2.1. Study site and samplings

Samplings in this study were placed in Shimizu town, which is located in the western part of the Tokachi district at the base of the Hidaka Mountain Range, Hokkaido, Japan (Figure 3.1). In Shimizu town, upland fields cover 14,900 ha. The major crops include wheat, sugar beets, potatoes, and beans. Winter wheat production was more than 18,000 tons in this area (Hokkaido Agriculture Policy Office, 2022).

Soil samples were collected from 40 wheat fields in total, along four different river terraces of different formation ages, including Lowland, Low terrace, Middle terrace, and High terrace, in the order of lower to higher elevations with younger to older formation age (Figure 3.1). The soil samples were collected from a one square meter area sampling plot which was established on each of the selected study field. during wheat maturity in July 2020 and 2021.

The soil samples were collected from the surface soil between 0 – 20 cm depth, and they were air-dried, and sieved through a 2-mm mesh, and any visible plant roots and remains were removed as much as possible.

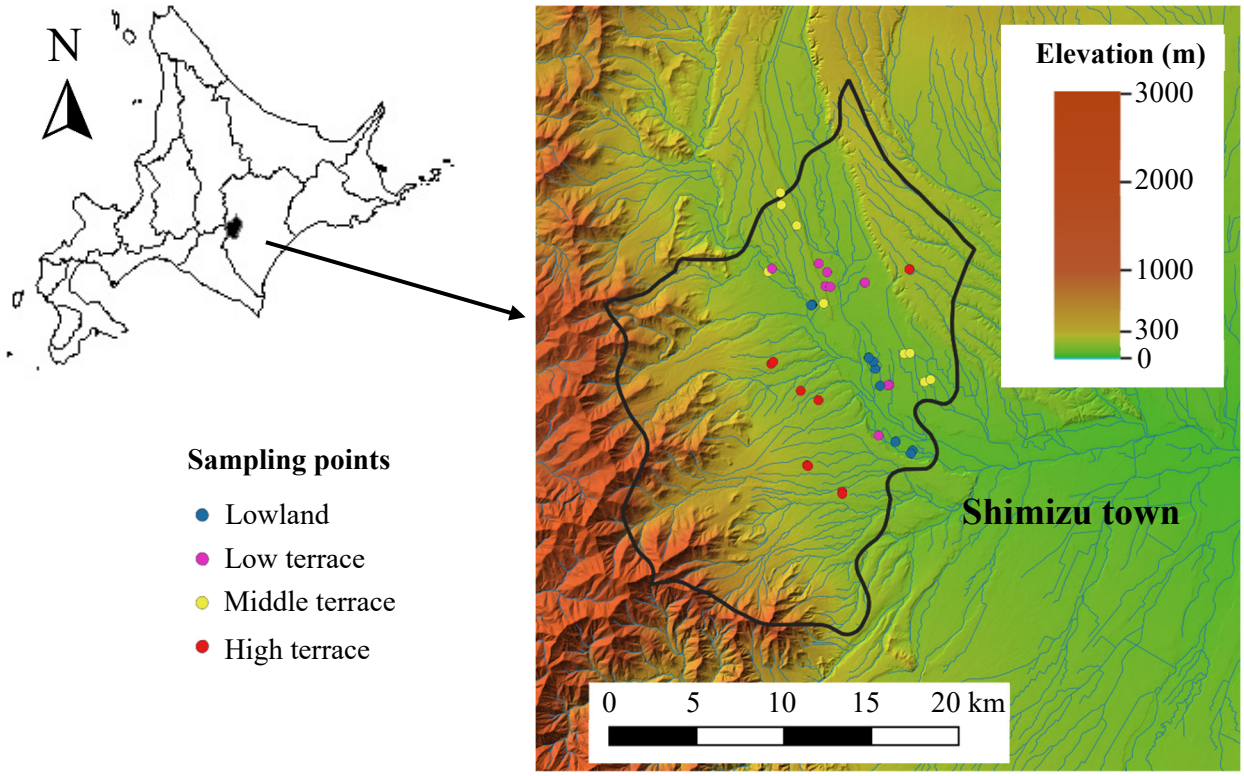

Figure 3.1. Surface soil sampling location in Shimizu town, Tokachi, Hokkaido.

3.2.2. Soil analysis

The dry combustion method measured total carbon (Total C) with a CHN automated elemental analyzer (Vario EL III, Elementar Analysensysteme, Hanua, Germany). The phosphate absorption coefficient (PAC) was determined by reacting soil with a solution containing 13.44 mg-P_2O_5 mL^{-1} for 24 hours. After the reaction, the remaining concentration of phosphate in the solution was measured using the vanadomolybdate yellow method with a spectrophotometer (UV mini-1240; Shimadzu Corporation, Kyoto, Japan).

Acid-oxalate extractable silicon (Si_o) was determined using a 0.2 mol L^{-1} acid ammonium oxalate solution at pH 3.0 (Blakemore et al., 1987), the concentration of Si in the extract was measured by a simultaneous inductively coupled plasma atomic emission

spectrometer (ICPE-9820, Shimadzu Corporation, Kyoto, Japan). The pH was measured using a 1:2.5 soil/water ratio.

Exchangeable cations and the cation exchange capacity (CEC) were determined by using a 1 mol L^{-1} ammonium acetate extraction method buffered at pH 7. An atomic adsorption spectrophotometer (AAS; Z-5010, Hitachi High-Tech Corporation, Tokyo, Japan) was used to determine the concentration of exchangeable cations. The CEC was measured using a formal titration method. Base saturation (BS) was calculated from the exchangeable cations and the CEC.

Available phosphate (P) was determined by the Truog method, and the concentration of phosphate in the extract was measured using the colorimetric molybdate blue method with a spectrophotometer (UV mini-1240; Shimadzu Corporation, Kyoto, Japan).

In this chapter, three buffer extraction methods, including the 0.1 M acetate buffer solution method (AB; pH 4.0) (Imaizumi and Yoshida, 1958; Kitta and Mizuochi, 1997; Yanai et al., 2016) and 0.02 M and 0.04 M phosphate buffers (PB2; pH 6.9 and PB4; pH 6.2) (Shigezumi et al., 2002; Yanai et al., 2016) were selected to evaluate available Si in these upland soils. These three buffer extraction methods had been developed for paddy soils, and they were also used to determine available Si in upland soils in some previous studies (Yanai et al., 2016; 2019). The two grams of air-dried soil sample were mixed with AB, PB2, or PB4 buffer solutions in a 50 ml centrifugation tube at a soil/solution ratio 1:10. The tubes were continuously shaken for five h at 40°C in the hot water bath. Then the Si concentration in the solution was determined using an ICP-AES (ICPE-9820; Shimadzu Corporation, Kyoto, Japan).

Statistical analyses were conducted using JMP Pro 16.1 (SAS Institute Inc., Cary, North California). The significant mean was tested using Tukey's honest significant difference

(HSD) test (p = 0.05). Pearson correlations were performed to determine the extent of relationships between available Si and soil properties.

3.3. Results and discussion

3.3.1. Soil surface characteristics in Shimizu, Tokachi

Overall, the soil surface samples collected from river terraces in Shimizu town, Tokachi district, disclosed a distinctive difference in soil characteristics between the four river terraces shown in Table 3.1. Total C was significantly lower in Lowland with a mean value of 15.6 g kg^{-1} compared to Low terrace, Middle terrace, and High terrace (80.6 g kg^{-1}, 73.9 g kg^{-1}, and 76.0 g kg^{-1} respectively). This reflected that Lowland's organic matter accumulation was significantly smaller than the other three terraces (Table 3.1). Similarly, the trend of total C was also found in the previous study (Kato et al., 2019; Kikuchi, 2008).

PAC is an index of the soil ability to fix phosphate and usually has been utilized to define andic soil properties when PAC is equal to or higher than 1500. PAC also has been used to classify the Andisol in Japanese soil classification (The Fifth Committee for Soil Classification and Nomenclature, 2017). In the Lowland, the PAC of all soil samples was lower than 1500; meanwhile, in the Middle terrace and High terrace, PAC was higher than 1500, and the mean value PAC of the Low terrace was 1360. This may relate to the difference in the soil parent materials and soil types.

Table 3.1. Descriptive statistics of the soil physiochemical properties of wheat fields in Shimizu town along different river terraces.

Soil properties	Unit	Lowland (n = 10) Mean ± SD†	Low terrace (n = 10) Mean ± SD†	Middle Terrace (n = 10) Mean ± SD†	High terrace (n = 10) Mean ± SD†
Total C	g kg^{-1}	15.6 ± 8.46 b	80.6 ± 29.4 a	73.9 ± 30.4 a	76.0 ± 24.4 a
PAC	-	500 ± 90.0 c	1360 ± 200 b	1880 ± 160 a	1970 ± 120 a
Si_o	g kg^{-1}	2.02 ± 0.71 c	3.50 ± 0.90 b	12.6 ± 5.13 a	14.9 ± 5.68 a
pH	-	5.7 ± 0.56 a	5.6 ± 0.25 a	5.8 ± 0.21 a	6.01 ± 0.34 a
CEC	$cmol_c$ kg^{-1}	15.4 ± 2.84 b	37.9 ± 8.57 a	36.0 ± 10.2 a	36.0 ± 8.10 a
Base saturation	%	65.4 ± 19.9 a	51.9 ± 7.86 ab	48.2 ± 7.86 b	54.8 ± 13.1 ab
Available P	mg P kg^{-1}	262 ± 102 a	240 ± 61.5 a	85.5 ± 44.9 b	99.1 ± 103 b

†SD; standard deviation. Different letters indicate significant differences between river terraces at $p < 0.05$ by the Tukey HSD test.

Si_o originating from amorphous to para-crystalline clay minerals (Blakemore et al., 1987) were significantly different in the soil of each terrace. The mean values of Sio increased in the order of the Lowland, Low terrace, Middle terrace, and High terrace, respectively (Table 3.1). The difference in Si_o contents indicated amorphous materials such as allophane and imogolite generated by the varied weathering and soil formation process derived from volcanic materials (Inoue and Huang, 1985; 1990; Shoji et al., 1994). These differences in soil inherence properties strongly reflect the differences in soil parent materials, soil formation processes, and the time of occurring formation at each terrace (Kato et al., 2019; Kikuchi, 2008).

The mean pH soils were slightly acidic and similar among four river terraces ranging from 5.6 to 6.0 (Table 3.1) which are within the range of the recommended soil pH for upland crop production in Hokkaido (pH 5.5 – 6.5) (Department of Agriculture, Hokkaido Government, 2020). The mean CEC of soils in the Low terrace, Middle terrace, and High terrace were similar and significantly larger than in Lowland, indicating the CEC was strongly related to humic substances which contribute to negative charge of nutrient absorption. Among river terraces, the BS of soils was very different and might be affected by soil formation processes and soil management practices such as lime application. The highest BS mean was 65.4 % in the Lowland and significantly higher than in the Middle terrace (48. 2 %). The Low, Middle, and High terraces were similar in BS (Table 3.1). This might reflect the influence of soil management of the farms and CEC. The mean available P of soils in the Lowland and Low terrace (means of available P were 262 and 240 mg P kg^{-1} respectively) were significantly greater than optimal range (43.6 – 130 mg P kg^{-1} or 10 – 30 mg P_2O_5 100 g^{-1}) (Hokkaido Agriculture Policy Office, 2020) and more than two times higher than the available P means of 85.5 and 99.1 mg P kg^{-1} in Middle terrace and High terrace respectively (Table 3.1). The PAC and agriculture practices, such as applications of

livestock manure and P chemical fertilizers, might influence the high available P contents in these soils. In particular, there was reported in previous findings that heavy fertilization of P applying to the upland Andosols in the Tokachi district could contribute to a massive accumulation of available and total P in plowing soil layers (Tani, 2010).

3.3.2 Available Si status of soil surface of wheat fields

Table 3.2 illustrates the descriptive statistics of the available Si contents in winter wheat growing along different river terraces in the Tokachi district obtained by three extraction solution methods; AB, PB2, and PB4. For the overall 40 samples, the available Si content measured by the AB method ranged from 13.0 to 241 mg kg^{-1}, and by the PB2 and PB4 varied from 17.8 to 238 mg kg^{-1} and from 19.5 to 342 mg kg^{-1}, respectively. These values were within the range of available Si in Japanese upland soils reported in previous findings (Yanai et al., 2016; Yanai et al., 2019).

Regarding the field locations along the river terraces, the soil available Si contents increased in the order of the Lowland, the Low terrace, the Middle terrace, and the High terrace, which followed the trend of Si_o and PAC means. Thus, the differences in the soil available Si along river terraces might be influenced by inherent soil properties such as Si_o. Statistically, soil available Si had been divided into two groups. The first group included Lowland and Low terrace, which their means of available Si were less than 100 mg kg^{-1}. In contrast, the second group contained the Middle and High terrace, whose available Si means were more significant than 100 mg kg^{-1} (Table 3.2).

According the soil available Si index of paddy soils for rice (Hatano et al., 2021), the optimal value for Si availability of soil is 75 mg Si kg^{-1} obtained by the acetate buffer extraction method. Which 45 % of soil available Si in our studied fields might be below the optimum for rice, especially in the Lowland (Appendix III).

Table 3.2. Soil available Si (mg kg^{-1}) of wheat fields obtained by three extraction methods along river terraces in Shimizu town, Tokachi district.

Extraction method		Lowland (n = 10)	Low terrace (n =10)	Middle terrace (n = 10)	High terrace (n = 10)
AB	Mean ± SD†	42.9 ± 23.3 b	56.3 ± 34.1 b	144 ± 51.4 a	164 ± 53.5 a
	Range	13.0 – 85.6	40.7 – 155	73.9 – 241	76.1 – 216
PB2	Mean ± SD†	33.4 ± 10.5 b	44.1 ± 17.5 b	105 ± 60.3 a	111 ± 40.9 a
	Range	17.8 – 46.0	29.7 – 84.9	54.2 – 238	62.0 – 164
PB4	Mean ± SD†	41.0 ± 15.0 b	66.3 ± 26.2 b	164 ± 83.9 a	177 ± 65.9 a
	Range	19.5 – 62.8	42.0 – 129	83.6 – 342	100 – 291

†SD; standard deviation. Difference letters indicate significant differences among river terraces at $p < 0.05$ by the Tukey HSD test.

3.3.3 Availability of Si and its relation to other soil properties

Figure 3.2 shows factor analysis for available Si obtained by three methods (AB, PB2, and PB4) and selected soil physiochemical properties. In this study, more than 47 % of the soil data set had been explained by factor group 1, which included soil available Si, Sio, pH, and available P. Factor group 2, including Total C, CEC, and Base saturation, explained 28 % of the data set. This could be clarified that soil properties were affected by soil mineralogical properties and soil C accumulation.

The correlation between the soil available contents and these selected soil physicochemical properties for all samples of four terraces was also investigated (Table 3.3), and a strong significant positive correlation was found between the available Si of three solution extraction methods and Sio contents. This indicates that the available Si of wheat fields could be strongly influenced by the soil parent materials and soil formation processes, particularly amorphous and para-crystalline minerals (Makabe et al., 2009; Wada and Inoue, 1974; Yanai et al., 2016). A weak correlation was also detected between the available Si and pH which agreed to previous findings, suggesting that the soil pH might be involved in a dissolution of the minerals and a subsequent release of Si (Haynes, 2019; Huang and Hseu, 2021; Sourideth et al., 2023; Yanai et al., 2016; Yanai et al., 2019).

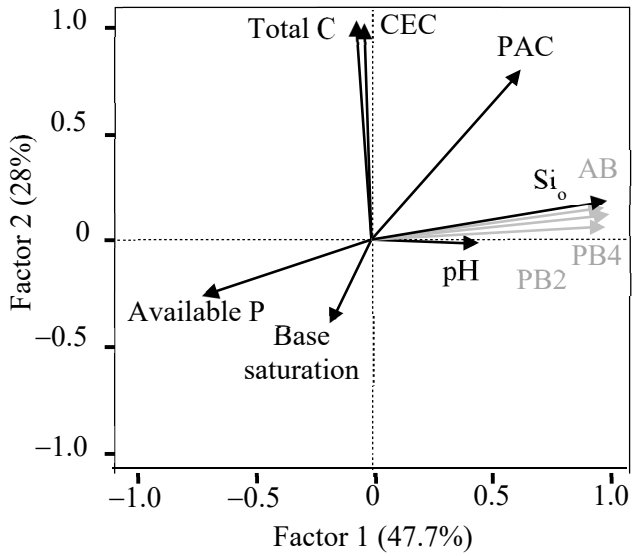

Figure 3.2. Factor analysis for soil available Si and soil physicochemical properties.

In addition, a strong negative correlation was observed between the available P and available Si obtained from three solution extractions methods, similar to the previous study of vertical Si distribution in the upland soil. As discussed in the last section, huge accumulated P content in the Tokachi district could be influenced by agricultural inputs (Tani, 2010), suggesting the possibility that anthropogenic activities exert on available Si concentrations in soils (Clymans et al., 2011; Guntzer et al., 2012).

Table 3.3. Pearson correlation coefficients between available Si and selected physiochemical soil properties.

Soil property	Acetate buffer (n = 40)	0.02 M Phosphate buffer (n = 40)	0.04 M Phosphate buffer (n = 40)
Total C	0.078	0.002	0.048
PAC	0.695***	0.617***	0.678***
Si_o	0.898***	0.840***	0.886***
pH	0.528**	0.396*	0.390*
CEC	0.131	0.028	0.087
Base saturation	− 0.088	− 0.198	− 0.232
Available P	− 0.641***	− 0.668***	− 0.688***

*, ** and *** indicate significant correlations at p <0.05, p <0.01 and p <0.001 respectively.

The figure 3.3 reflects the summaries of relationship between the soil available Si contents obtained by the acetate buffer method, the 0.02 M and 0.04 M phosphate buffer methods. The relationship among these three methods was positive and almost linear (Figure 3.2 and 3.3) which also found by Yanai (2016). In addition, the available Si determined by the acetate buffer showed strongest relationship with other soil parameters (Table 3.3).

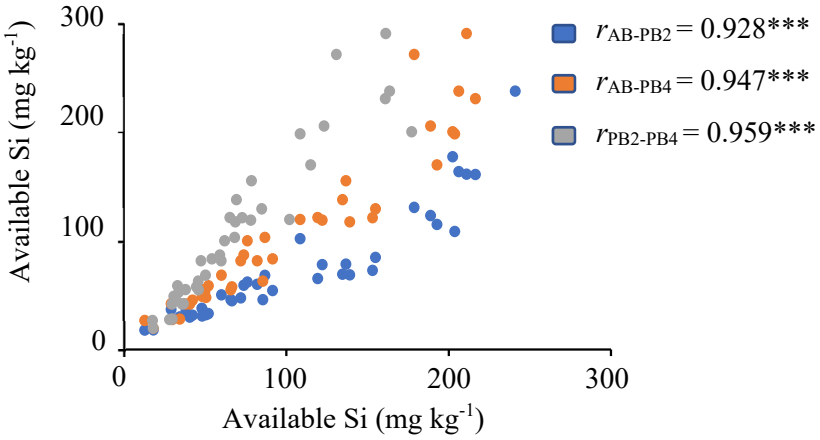

Figure 3.3. The relationship between the soil available Si contents obtained by the acetate buffer, the 0.02 M and 0.04 M phosphate buffer.

3.4. Summary

The results obtained on upland cultivated winter wheat fields provide us with the major findings on the soil Si availability varied from field to field and was remarkably higher in the fields located in the Middle terrace and High terrace compared to the Lowland and Low terrace. This variation in soil Si availability was contributed by the impacts of the soil parent materials and soil formation processes, particularly amorphous materials, as well as soil pH. The soil available Si obtained from 3 extraction methods was different in value however it follows similar trends.

CHAPTER 4. SILICON IN WHEAT AND ITS INTERACTION WITH AVAILABLE SI IN THE SOILS

4.1. Objectives

From the previous chapters, we can understand how much Si is available in the soil both in subsoil and surface soil, also which soil factors can affect their availability content. However, we still could not be confident that these soil available Si contents will be really available or not for plants until we evaluated Si in plants grown under these conditions.

Therefore, in this chapter, the objectives of this study were (i) to determine Si nutrition status and its distribution in wheat plants, (ii) to evaluate the responses of Si in wheat on the soil Si availability and other nutrients, and (iii) compare and identify probable methods to determine available Si for upland soils.

4.2. Materials and methods

4.2.1. Study sits and samplings

Wheat samples were collected from 40 wheat fields in total, along four different river terraces of different formation ages, including Lowland, Low terrace, Middle terrace, and High terrace, in the order of lower to higher elevations with younger to older formation age. A one square meter area sampling plot was established on each of the selected study fields. The wheat samples were collected simultaneously with soil samples during wheat maturity in July 2020 and 2021 that has been discussed in previous chapter (Figure 3.1, Figure 4.1).

Figure 4.1. Photograph of wheat and soil sampling area.

The wheat samples were harvested at 2 – 3 cm height above the soil surface, and they were air-dried in the greenhouse until the air-dried weight was stable. Wheat samples were then separated into three parts, stem, husk, and grain, and were oven-dried at 60 °C for at least 72 hours or until they reached staple weight, then determined biomass and ground for nutrient content analysis.

4.2.2. Wheat survey and analysis

The soil available Si obtained by three buffer extraction methods, including the 0.1 M acetate buffer solution method (AB; pH 4.0) (Imaizumi and Yoshida, 1958; Kitta and Mizuochi, 1997; Yanai et al., 2016) and 0.02 M and 0.04 M phosphate buffers (PB2; pH 6.9 and PB4; pH 6.2) (Shigezumi et al., 2002; Yanai et al., 2016) were evaluated and discussed in previous chapter.

Wheat samples after air drying in the green house, total stem number with panicles were counted, and 100 stems with the average weight were selected randomly. These 100 stems were processed to evaluate stem height, 3 node stems, the grain yield and grain yield

components (1000 grain weight, grain per panicle). After all agronomic measurements, samples were combined and separated into 3 parts: stem, husk and grain for further chemical analysis.

From ground wheat samples (stem, husk and grain), N concentration was determined by the dry combustion method with a CHN automated elemental analyzer (Vario EL III, Elementar Analysensysteme, Hanau, Germany). Furthermore, 0.5 g of ground wheat samples were Kjedahl acidic digested using Foss 2040 digestor (Foss Teacator 2040 Digestor unit, SpectraLab Scientific Inc. Canada), and the digested solution was filtrated using ashless filter paper. Afterward, P and K were quantified using the ICP-ESP (ICPE-9820; Shimadzu Corporation, Kyoto, Japan), while Si was measured using a gravimetric method, the filter paper was then ignited and weighed to determine Si content (Datnoff et al., 2001; Liang et al., 2015; Yoshida et al., 1976).

The weather information during wheat growing periods in 2020 and 2021 was provided by the Japanese meteorological agency. Statistical analyses were conducted using JMP Pro 16.1 (SAS Institute Inc., Cary, North California). The significant mean was tested using Tukey's honest significant difference (HSD) test (p = 0.05). Pearson correlations were performed to determine the extent of relationships between available Si and soil properties and Si contents in the wheat plants.

4.3. Results and discussion

4.3.1. Wheat agronomic properties and grain yield

The figure 4.2 a and b showed the difference in weather conditions during wheat growing season among two years 2020 and 2021. Generally, the total precipitation was similar between 2 years, however most of the precipitation of 2020 occurred in June and July, while in 2021 the major precipitation appeared in April and May and declined in June

and July. The sunshine hours were not much different except in June, the sunshine hour of 2020 was really dramatically lower compared to 2021. These differences in weather conditions strongly affect the grain yields of wheat (Figure 4.2 c). The significantly lower yield in 2020 may be related to the remarkably high rainfall in June and July 2020, which could increase the infestation of fungus diseases and the Low sunshine hour in June 2020 also decreased the photosynthesis rate consequence to low yield components and grain yields (Bingham et al., 2009; Fageria et al., 2010; Jia et al., 2021)

In this study, wheat grown in Shimizu town produced better yields compared the average of wheat production in Japan. The mean plant biomass wheat farms ranged from 1,292 to 1,459 g m^{-2} which mean grain yields ranged between 7070 and 7870 kg ha^{-1} depending on river terraces (Table 4.1) which were greater than the average wheat yields of 4990 and 5780 kg ha^{-1}) of Japan and Hokkaido respectively (MAFF, 2023). The differences in biomass and grain yield wheat grown among terraces could be noticed, even though the differences were not significant.

Our results showed that there were no significant differences in both biomass or grain yields between terraces within same years which within terraces, the biomass and grain yields of Lowland were pretty stable in Lowland, the biomass and grain yield gap between yields significantly increased from Low terrace to High terrace (Appendix IV). This could indicate that besides weather conditions, topography and soil types also significantly affect wheat production (Barzegar et al., 2002; Whalley et al., 2008).

There was no significant difference found in any yield components such as stem number, 1000 grain weight, grain number per spike among terraces (Table 4.1).

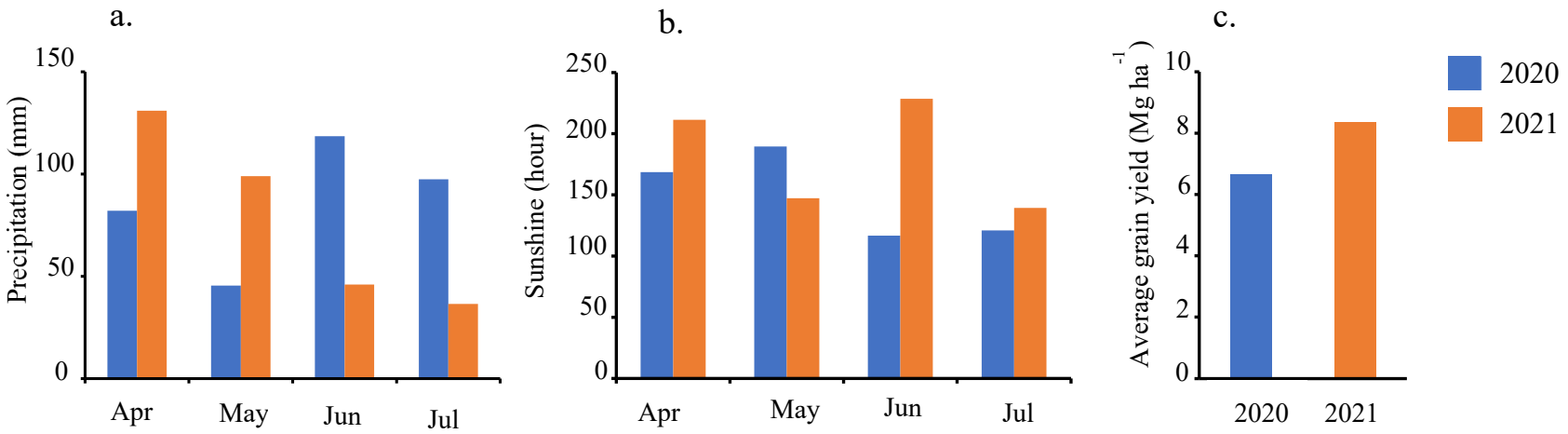

Figure 4.2. Weather condition (a. precipitation and b. sunshine hour) during growing season and average wheat grain yields (c).

Table 4.1. Descriptive statistics of plant biomass, grain yields and selected yield components of wheat grown along different river terraces.

Parameter	Unit	Lowland (n = 10)	Low terrace (n = 10)	Middle Terrace (n = 10)	High terrace (n = 10)
		Mean ± SD†	Mean ± SD†	Mean ± SD†	Mean ± SD†
Plant biomass	g m^{-2}	1292 ± 335 a	1426 ± 250 a	1459 ± 264a	1335 ± 278 a
Grain yield	kg ha^{-1}	7360 ± 1590 a	7870 ± 1380 a	7780 ± 1440 a	7070 ± 1450 a
Stem number	-	687 ± 173 a	706 ± 136 a	705 ± 140 a	634 ± 166 a
1000 Grain weight	g	35.1 ± 3.72 a	33.5 ± 3.50 a	34.1 ± 3.12 a	33.0 ± 1.85 a
Grain number per spike	_	15 ± 1.32 a	16 ± 0.78 a	16 ± 0.86 a	16 ± 1.10 a

†SD; standard deviation. Different letters indicate significant differences between river terraces at p <0.05 by the Tukey HSD test.

Table 4.2. Pearson correlation coefficients between soil available Si and agronomic properties of wheat fields.

Parameter	AB (n = 40)	PB2 (n = 40)	PB4 (n = 40)
Plant biomass	– 0.056	– 0.020	0.023
Grain yield	0.022	– 0.045	– 0.018
Stem number	– 0.191	– 0.239	– 0.234
1000 grain weight	0.014	0.130	0.095
Grain number per panicle	0.297	0.243	0.281

* indicates significant correlations at $p < 0.05$.

Table 4.2 showed the relation between soil available Si obtained by three solution extraction methods and plant agronomic properties. The results indicate that soil available Si had no effect on wheat biomass, grain yields and agronomic properties excluded 3rd node width. Soil available Si both measured by AB and PB4 showed weak positive relationship to 3rd node width. The increase of soil available Si may improve to the formation of phytolith and epidermis trichomes (Neu et al., 2017).

4.3.2. Si and essential nutrient uptake of wheat and their response to soil available Si

In this study, wheat Si uptake by winter wheat in upland soils varied from field to field, ranging from 3.00 to 21.0 g m^{-2}, with an average of 13.4 g m^{-2} (Table 4.3). The variation of Si uptake may be affected by plant genetic and environmental conditions (Cooke and Leishman, 2012; Miles et al., 2014; Schaller et al., 2016; Wu et al., 2006). The winter wheat Si uptake was remarkably greater than P uptake and similar to N and K (Figure 4.3). Wheat mainly stored Si in the stem and husk rather than the grain. In winter wheat, Si distribution was opposite to other nutrients such as N and P distribution. Wheat accumulated Si through phytoliths and leaf epidermis hairs (Trichomes) (Neu et al., 2017). Generally, Si

concentration in plants ranges between 0. 1 and 10 % of dry biomass, which may be exceeded the concentration of many macro elements (Epstein, 1999). In this study, the Si concentrations of winter wheat grown in upland soils varied between 3.34 to 13.1 g kg-1, with an average of 9.61 g kg-1. The highest concentration of Si was found in husks (mean = 27. 6 g kg-1), followed by Si concentration in stems and grains (means equaled 15.1 and 1.28 g kg-1, respectively) (Table 4.3). The high Si concentration in husks may be associated with a pre-harvest sprouting and disease resistance (Ma and Yamaji 2006).

Table 4.3. Descriptive statistics of the Si uptake and concentration of wheat grown in Shimizu town, Tokachi district.

Soil properties	Si uptake ($g\ m^{-2}$) (n = 40)		Si concentration ($g\ kg^{-1}$) (n = 40)	
	Mean ± SD†	Range	Mean ± SD†	Range
Whole plant‡	13.4 ± 4.39	3.00 – 21.0	9.61 ± 2.23	3.45 – 13.1
Stem	8.27 ± 3.20	0.99 – 14.6	15.1 ± 4.05	3.27 – 24.2
Husk	4.26 ± 1.29	1.32 – 7.07	27.6 ± 6.54	12.6 – 46.0
Grain	0.85 ± 0.32	0.19 – 1.53	1.28 ± 0.55	0.28 – 2.71

†SD; standard deviation. ‡Whole plant; means above-ground parts including only stem, husk, and grain.

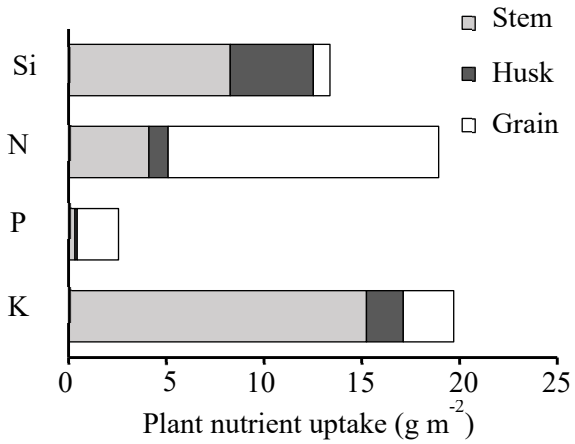

Figure 4.3. Plant nutrient uptake and their distribution in wheat

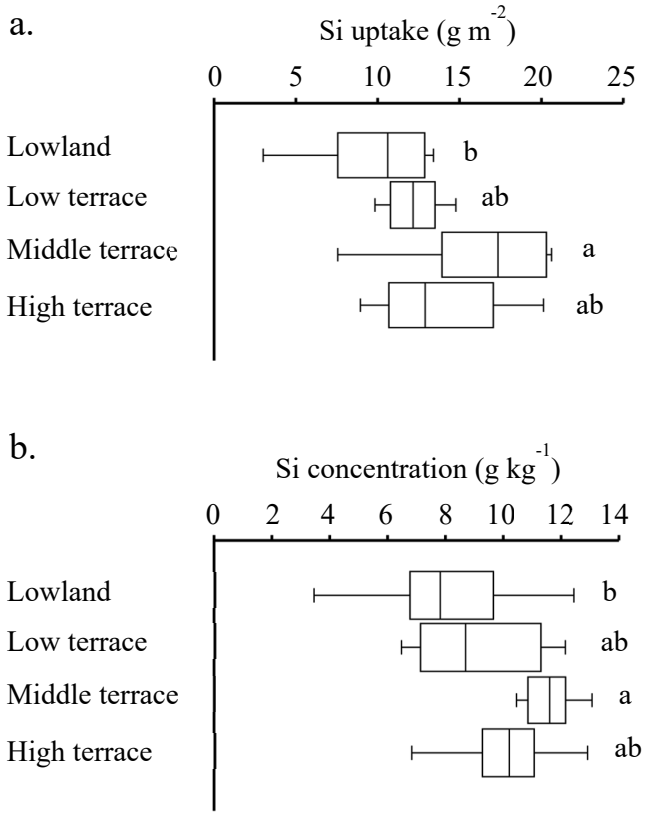

Figure 4.4. Box plots describing Si uptake (a) and concentration (b) of winter wheat grown along river terraces in Shimizu town. Different letters indicate significant differences between terraces at $p < 0.05$ by the Tukey HSD test.

Regarding the location of river terraces, winter wheat Si uptake and concentration differed significantly between terraces, as shown in Figure 4.4 (a and b), respectively. Winter wheat grown in the Middle terrace obtained the highest means for both Si uptake and Si concentration which was significantly higher than winter wheat grown in the Lowland. This may be related to the influence of the difference in soil physiochemical properties among terraces. As we found that the soil Si contents in Middle and High terraces were significant higher compared to Lowland in chapter 3, affecting in increase of uptake and concentration

of Si in wheat. Our findings were similar to previous studies found in wheat pot experiments and in rice (Kato and Owa, 1997; Liu et al., 2014; Neu et al., 2017).

The figure 4. 5 illustrates wheat nutrient uptake and concentration of wheat grown along different river terraces. These significant differences in Si uptake take among terraces reflecting the influences of soil Si availability hence soil types as have been discussed in previous chapters. The uptake and concentration of N and K were not different among the terraces, these indicate that N and K availability for wheat were sufficient in all terraces, this could be related to the fertilizer application following the fertilizer recommendation rate provided by the Hokkaido government (Department of Agriculture, Hokkaido Government, 2020). In contrast, the huge P uptake in the Lowland and the significant difference in P concentration between terraces may associated with the excessive P fertilizer application in this area (Tani 2010).

From the multiple regression analysis (Appendix V), which the depend valuable value of biomass and grain yield, where the independent valuable values include wheat essential nutrient and Si uptake. We found that the nutrient uptake of the essential elements (N, P, K and Mg) and Si can explain the biomass and grain yield production of wheat grown in Shimizu, Tokachi by 88 and 80 % respectively. Importantly, Si uptake showed significant effects in both biomass and grain yield. Specifically, in plant biomass, the effect is as strong as essential elements likes N and P.

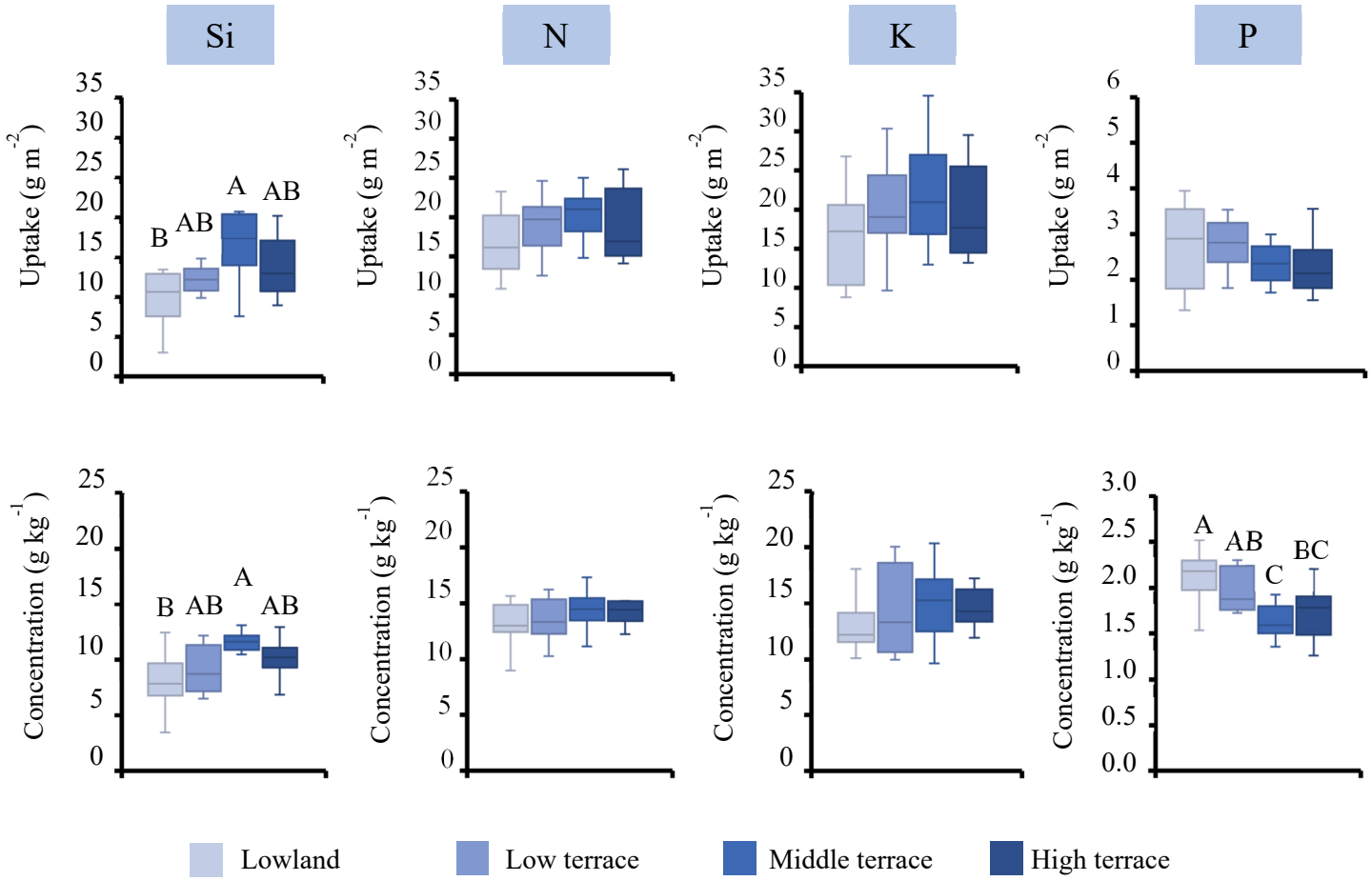

Figure 4.5. Nutrient uptake and concentration of wheat plants grown along river terraces. The alphabet indicates significant difference between terraces.

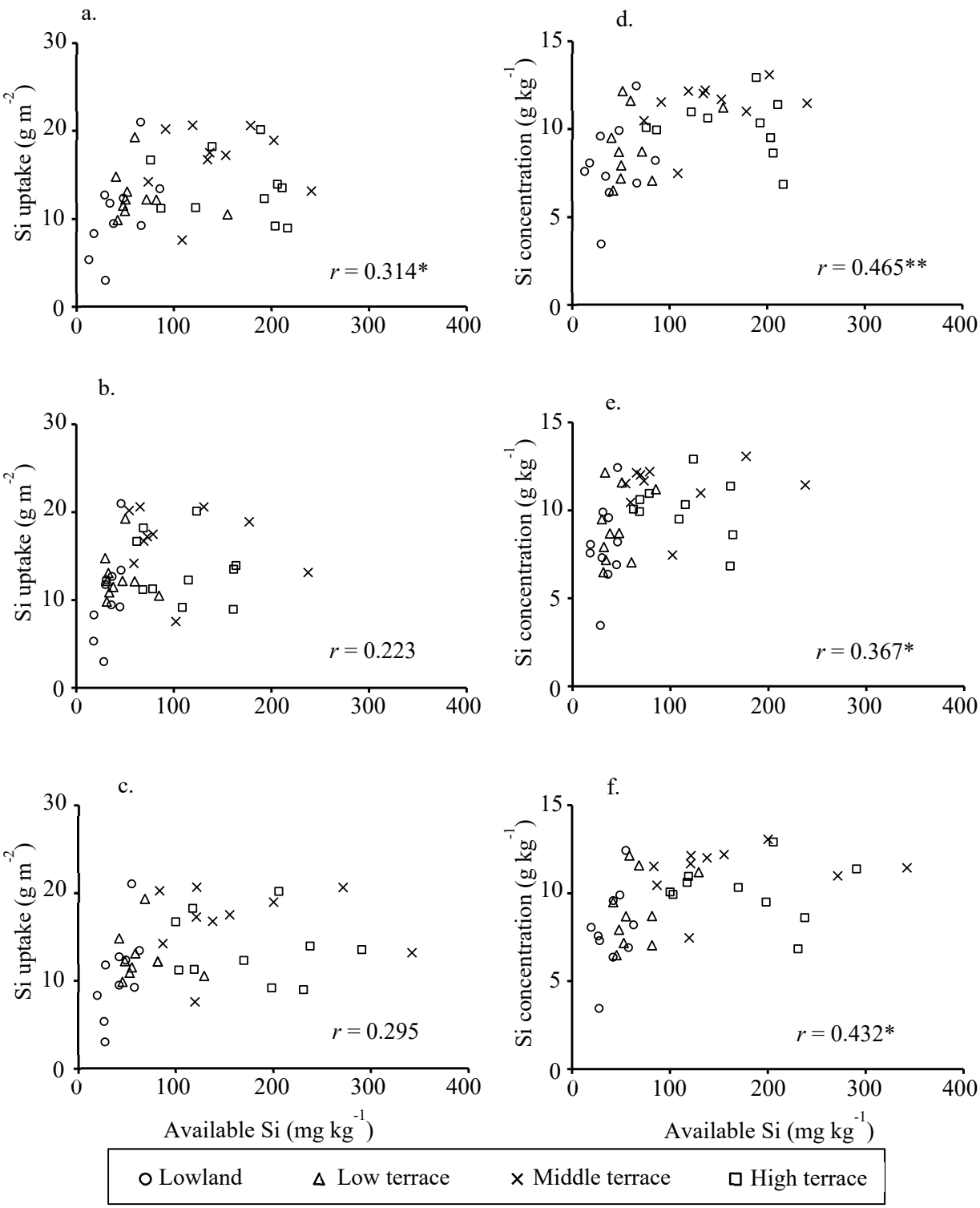

Figure 4.6. Si uptake and Si concentration of wheat plants respond to soil available Si extracted by acetate buffer (a and d), 0.02 M phosphate buffer (b and e), and 0.04 M phosphate buffer, respectively. * and **significant correlation at $p < 0.05$ and $p < 0.01$ respectively.

The effects of soil available Si extracted by three methods, AB, PB2, and PB4, on winter wheat Si uptake and concentration are shown in Figure 4.6 (a – f). The results showed that soil available Si extracted by three methods positively correlated to plant Si uptake and concentration, and the relationship was stronger with the Si concentration. An increase in Si availability increases plant Si concentration, especially in vegetative plant parts, which agrees with many previous studies (Cooke and Leishman, 2012; de Carvalho et al., 2022; Frazão et al., 2020; Lata-Tenesaca et al., 2021; Liang et al., 2005; Neu et al., 2017; Schaller et al., 2021). Neu et al. (2017) found that the concentration of Si in vegetative tissue were highest in leaf blades followed by leaf sheaths, culm and lowest in grain and root. Under high Si supply condition Si occur as phytoliths and further localized Si in strongly developed trichomes. Soil available Si extracted by the AB method obtained the highest correlation with the Si concentration in wheat among the three solution extraction methods. This suggested that the AB solution extraction method could be used to determine soil Si availability for upland soils.

In addition, we found that the significant negative correlation between Si and C content across the 40 fields in all wheat parts; stem, husk and grain, particularly in husk where the correlation very strong ($r = -0.832$) (Figure 4.7). Our findings are broadly in line with those who found previously in wheat in greenhouse condition and forestry species (Cooke and Leishman, 2012; Neu et al., 2017). There where been noticed that Si concentration was significantly correlated to C concentration as well as C based defense and Si could be served as a replacement for part of C compounds as it might have stabilizing function or photosynthetically active tissue.

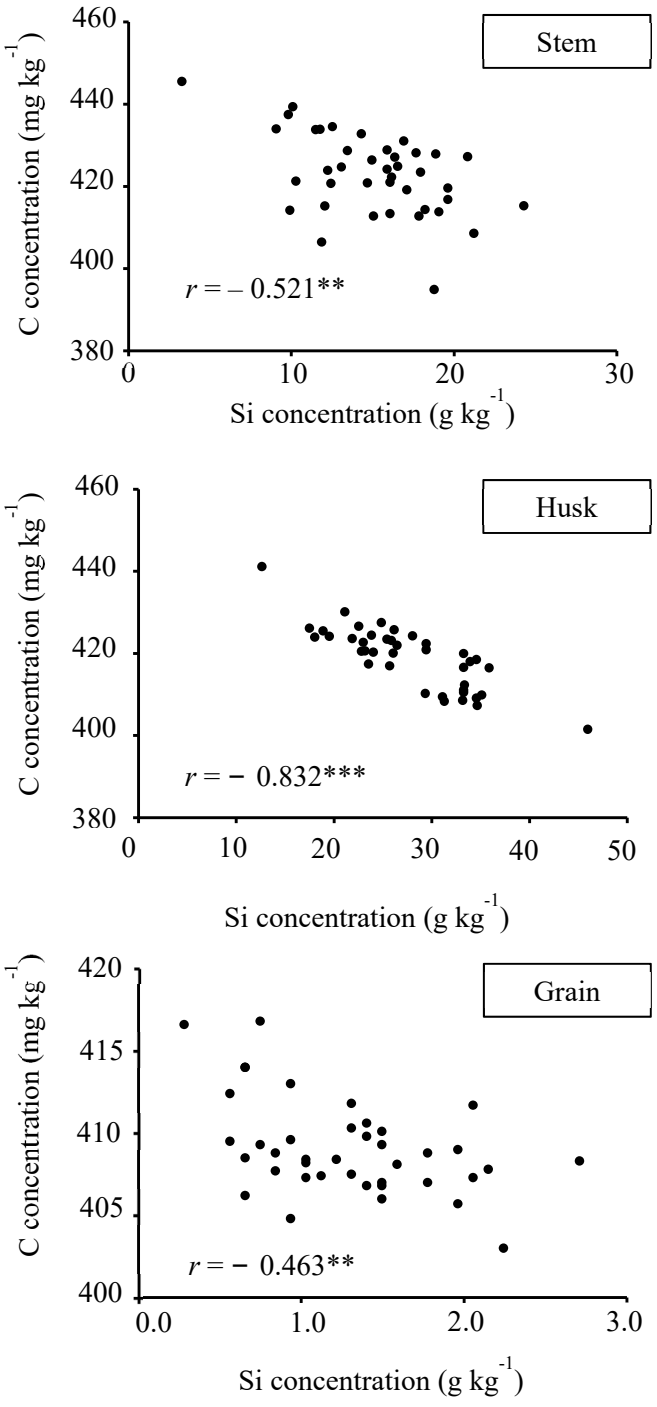

Figure 4.7. Correlations between Si concentration and C concentration in stem, husk and grain of winter wheat. ** and ***significant correlation at $p < 0.01$ and $p < 0.001$ respectively.

4.4. Summery

The results obtained on upland cultivated winter wheat fields provide us with the major findings on a mean Si uptake by winter wheat was 13.4 g m^{-2} and was considerably comparable to N and K uptake and greater than P. Winter wheat mainly stores Si in stems and husks, and the highest mean concentration of Si in wheat plants was 27.6 g kg^{-1} and found in husks, followed by stems and a very small amount of Si contain in their grains. The high concentration of Si in the husk and stems may be related to enhance plant physical protection to pests and diseases. In addition, among three solution extraction methods, acetate buffer solution method could be the most promising method to determine soil Si availability for upland soils.

CHAPTER 5. GENERAL CONCLUSION

The available Si content in upland soils varied from 13 – 377 mg kg^{-1} depending on location and extraction methods. The acetate buffer extraction method could be used to estimate plant available Si in the upland soils, especially for winter wheat. The allophane contributed as a source of available Si in the upland soils of Tokachi, Hokkaido, particularly, in the subsoils. Besides the amorphous minerals, pH also affects soil Si availability, especially pH KCL.

Wheat uptakes Si from the soil 134 kg ha^{-1} on average and contains 9.6 % in its biomass. Even though in our study, Si did not show a significant effect on wheat growth and quality. However, it is impossible to claim that Si does not affect wheat's production as numerous factors affect wheat plants in this study, such as farm management.

There is an interesting finding that, the tradeoff between Si and C in the husk. When husk contain high Si, it may save C and transfer to the grain. In addition, wheat Si uptake showed significant effect on both biomass and grain yields productions however Si is still neglected from the fertilizer recommendation rates.

Therefore, there is a need to further research for better nutrient balance management related to Si, including the different sources of Si supply and the mechanism of Si in wheat plants or other upland crops must be further studied in detail.

ABSTRACT

Silicon (Si) is known as an important element for cereal crops including wheat (*Triticum aestivum*) by enhancing resistance against stresses thereby increasing productivity. The Tokachi district of Hokkaido occupies 20 % of the national wheat production area with various soil types present, but the availability of soil Si in relation to the physicochemical and mineralogical properties of the soils and the relation to Si in plants in upland soils have not been assessed in detail. Our finding goals were; (i) to clarify the soil morphological features and characteristics of the soil profiles and to classify the soils developed on the river terrace. (ii) to evaluate the soil Si ability in both vertically in the subsoil and soil surface and to the assess the influence of other soil properties on soil Si availability, (iii) to assess the status of wheat Si uptake, concentration and understand their relation to the soil available and other nutrients. (iv) to evaluate soil Si solution extraction methods that could be used to determine Si for upland soil.

The 40 paired of soil and wheat samples were collected from farmers' fields of Shimizu town, Tokachi, Hokkaido in 2020 and 2021 along river terraces and four soil profiles were drug at different river terraces, Lowland, Low terrace, Middle terrace and High terraces. Surface soil samples at 20 cm depth and soil samples from all horizons of the four profiles were analysis for total C, phosphate absorption coefficient (PAC), cation exchangeable capacity, and soil mineralogical properties through selective dissolution methods and available soil Si using 0.1 M acetate buffer, 0.02 and 0.04 M phosphate buffer methods were also analyzed. Wheat samples were air dried and determined for plant agronomic properties, grain yields and biomass. Later wheat samples were separated into 3 parts stem, husk and grain then grounded for Si and nutrient contents.

From this study we found that soils, soil profiles developed on river terraces in the Shimizu town, Tokachi district revealed completely different morphological features and remarkably

different physicochemical and mineralogical properties. The soil formation processes and a significant difference in the vertical distribution of humic substances and amorphous minerals were strongly affected by the soil moisture regime in the lower horizons and the differences in the parent materials such as alluvial and volcanic deposits. According to the Japanese Soil Classification, these soil profiles, one of them could be classified Fluvic soils and other three were classified as Andosols, however one of the Andosols was classified as Inceptisols according to Soil Taxonomy due to a subtle difference in the criteria of the andic properties.

The vertical distribution of soil available Si contents were remarkably different in each horizon and were higher in the horizons where allophane formation was advance. The available Si of soil surface varied from field to field and notably higher in the fields located in the areas where allophane formation was more progressive as in Middle terrace and High terrace. From our results, suggesting that the amorphous minerals contributed as a source of available Si in the upland soils of Shimizu, Tokachi, Hokkaido. Increase of pH enhanced soil Si availability.

In average, wheat took up Si from the soils 13.4 g m^{-2} which was significant amount comparable to major essential element like N and K and remarkably higher than P. Wheat stored Si mainly in stem and husk and minor amount in grains. The highest concentration of Si was almost 28 g kg^{-1} of dry matter in husk, this might be related to protection the grain from biotic and abiotic stresses during harvest. It was important to note that soil available Si affected Si concentration in wheat rather than plant Si uptake. The negative correction between Si and C concentration from our finding supporting the theory that there is tradeoff between these 2 elements in wheat.

Among three extracted solution methods, acetate buffer method showed the most promising method for measuring soil available for upland soils, as soil available Si obtained by acetate buffer reflected better amount Si obtained in wheat plants. Even through the interesting in Si research has been increased and Si has showed the positive impact in plant productions, however the understanding on the mechanism on different source of Si supply and the limitation for uplands crops and the hypothesis of the depletion of Si in cropping system is still related, hence there is need to further research for better and nutrient balance management.

要約

ケイ素（Si）はコムギ（*Triticum aestivum*）を含む穀物類にとって重要な元素であり、生物的あるいは非生物的ストレスに対する耐性を高めることによって生産性を向上させる。北海道の十勝地域は、国内のコムギ生産の 20%を占める主産地であり、様々な種類の土壌が分布するが、土壌からの Si の可給性、可給性に及ぼす土壌の理化学性や鉱物特性の影響、およびコムギによる Si 吸収との関係などについてはあまり詳細が知られていない。本研究における目標は、1）十勝地域の河岸段丘上に生成する土壌の断面における形態学的な特徴や特性を明らかにすること、2）土壌の表層と下層における可給態 Si を評価し、土壌の特性と可給態 Si との関係を明らかにすること、3）コムギによる Si 吸収を調べ、土壌の可給態 Si や他の養分元素との関係を明らかにすること、4）普通畑土壌における可給態 Si を評価する最も適した抽出法を評価することとした。

北海道十勝地域の清水町において、2020 年と 2021 年に生産者圃場計 40 地点の調査を行った。また、河岸段丘上の 4 地点（低地、低位段丘、中位段丘、高位段丘）で土壌断面調査を行った。40 地点の生産者圃場では深さ 20cm までの表層土を採取し、土壌断面では層位ごとに試料を採取した。土壌試料については、全炭素量、リン酸吸収係数、陽イオン交換容量、および選択溶解法による鉱物学的特徴を調べた。また、0.1M 酢酸緩衝液、0.02M リン酸緩衝液、0.04M リン酸緩衝液を用いて、可給態 Si を分析した。コムギ地上部試料については、風乾した後に各種農業形質、子実収量、およびバイオマスなどを調べた。その後、コムギ試料は茎葉、もみ殻、子実の 3 部位に分け、粉砕して Si 濃度を測定した。

まず、清水町の河岸段丘上に生成した 4 地点土壌断面を調べた結果、形態学的特徴が著しく異なること、理化学性や鉱物学的特性が明らかに異なることなどが示された。とくに、腐植物質や非晶質・準晶質粘土鉱物の垂直分布は、母材の違い（沖積堆積物および火山放出物）と、下層における水分条件の違いを強く反映した。日本土壌分類体系によると、1 地点は低地土、残り 3 地点は黒ボク土に分類されたが、Soil Taxonomy では 1 地点の黒ボク土が Inceptisols に分類された。

土壌中の可給態 Si の垂直分布は各層位によって大きく異なり、アロフェンなどの生成が進んでいる層位で著しく多かった。表層土の可給態 Si は圃場ごとで大きく異なり、中位段丘や高位段丘などアロフェン生成が進んでいる地点で多かった。本研究の結果は、北海道十勝地域清水町の普通畑における可給態 Si の給源は非晶質・準晶質粘土鉱物であること、土壌 pH が高いと可給態 Si がより多いことが示された。

コムギによる土壌からの Si 吸収量は平均 13.4 g m^{-2} と、窒素やカリウムと同等の吸収量であり、リン吸収量よりも著しく多かった。コムギは、吸収した Si を主に茎葉やもみ殻に含んでおり、子実にはほとんど含まれなかった。もみ殻に含まれる Si は最も高い試料では 28 g kg^{-1} であり、この高濃度の Si が収穫まで子実を生物的および非生物的なストレスから保護している可能性が高い。土壌の可給態 Si は、コムギの Si 吸収量ではなく、Si 濃度に影響を及ぼした。また、コムギの Si 濃度と炭素濃度との間には負の相関関係が認められ、コムギにおいてこれら 2 つの元素がトレードオフの関係にあることが示唆された。

土壌の可給態 Si を評価するために、本研究で供試した 3 種類の緩衝液の中では、酢酸緩衝液が普通畑土壌の可給態 Si を評価するのに最も適しており、コムギに含

まれる Si 濃度と酢酸緩衝液法による土壌の可給態 Si との間には、より高い相関関係が認められた。土壌と作物における Si の研究が注目され、Si が作物の生産性にポジティブなインパクトを与えることが示されているが、土壌以外の Si 供給源の存在、作物生産における可給態 Si の制限などについては未解明な部分も多く残っており、より良い養分管理に向けたさらなる研究が求められる。

ACKNOWLEDGMENTS

Without the great supervision and cooperation that I received from supervisors, colleagues, friends as well as my family, this study project would not have been successful and have produced the results it has.

First and foremost, I would like to say a very big thank you to my best supervisor Prof. Masayuki Tani for giving me a great opportunity to pursue a Doctoral program at the Obihiro University of Agriculture and Veterinary Medicine and his great guidance and excellent supporter through all the steps of my studies. You have taught me a lot, and I value this information as a priceless gift in my life. I was able to continue with my study project to its finish because to your unwavering guidance and assistance. Thank you very much sensei.

I would like to express my deep gratitude to my co-supervisors, to Assistant Prof. Dr. Kinoshita Rintaro for his useful comments and suggestions to improve my works and inspiring me how to write technical papers. To Associate Prof. Dr. Daigo Aiuchi and Prof. Kazumitsu Onishi for their valuable comments and advice during my progress report and seminars which motivated me to widen my research from various perspectives.

I would also like to extend my heartfelt gratitude to Mr Jingo Shimada and all staffs of Ja Tokachi Shimizu for their guidance and facilitating the selection of the study fields.

Being a part of the Soil Science Laboratory is a wonderful honor for me. I would like to thanks to Miss Akari Kishimoto for her expert and technical guidance in the laboratory and fields activities who has helped me from the start.

I am also thankful to Dr. Hiroaki Shimada, and all of my lab members who have helped, supported, and shared constructive comments to improve my research.

To Elton Amadeus Francisco with whom I started this long journey, and who has supported me in both social and academic life. Thank you for this great friendship.

I am thankful to The Obihiro University of Agriculture for funding this project and to the farmers of Shimizu town for allowing us to use their fields.

I am grateful to Japan International Cooperation Agency (JICA) for supporting me with great scholarship. I would like to express my sincere gratitude to you for making my study possible. I was thrilled to learn of my selection for this honor, and I am deeply appreciative of your support.

To Dr Naomi Asagi from the Ibaraki University and Dr Chanthakhone Bualaphan from The National Agriculture and Forestry Research Institute of Laos, Thank you very much for your supports and encouragements.

To all my friends in Obihiro, Japan and Laos. Thank you very much for always supporting me, for cheering me on all the time. Without all your love and kindness, I couldn't pass the hard time during my Ph.D. study. I feel so warm and comfortable when we were together. I am glad to have enjoyed their friendship.

I am deeply grateful to my family for the everlasting love of family, especially to my super mom Sybounheung Noymany, thank you very much for your constant support, understanding, love and guidance all throughout my study. To my lovely daughter, Phetvilay Sourideth (Penguin) for your patience waiting during my absence for studying and for always giving me an extra motivation and positive energy to overcome all challenges.

Finally, for the memories of my lovely sister Mimi, father and grandpa, who left us forever without saying goodbye. I would like to tell you that there is no single moment in any day that I don't find myself missing you. Thank you very much to giving me a sweetheart, I still feel it. Your presence, love, kindness will forever be with us.

REFERNCE

Ali, S., Rizwan, M., Hussain, A., Zia ur Rehman, M., Ali, B., Yousaf, B., Wijaya, L., Alyemeni, M. N., and Ahmad, P. (2019). Silicon nanoparticles enhanced the growth and reduced the cadmium accumulation in grains of wheat (*Triticum aestivum* L.). Plant Physiology and Biochemistry 140, 1-8.

Alzahrani, Y., Kuşvuran, A., Alharby, H. F., Kuşvuran, S., and Rady, M. M. (2018). The defensive role of silicon in wheat against stress conditions induced by drought, salinity or cadmium. Ecotoxicology and environmental safety 154, 187-196.

Barzegar, A., Yousefi, A., and Daryashenas, A. (2002). The effect of addition of different amounts and types of organic materials on soil physical properties and yield of wheat. Plant and soil 247, 295-301.

Bingham, I., Walters, D., Foulkes, M., and Paveley, N. (2009). Crop traits and the tolerance of wheat and barley to foliar disease. Annals of Applied Biology 154, 159-173.

Blakemore, L. C., Searle PL., and Daly BK. (1987). Extractable iron, aluminium and silicon. In Methods for Chemical Analysis of Soils. Vol. 80, pp. p. 71 - 76. NZ Soil Bureau Scientific Report.

Camargo, M. S., and Keeping, M. G. (2021). Silicon in sugarcane: availability in soil, fertilization, and uptake. Silicon 13, 3691-3701.

Clymans, W., Struyf, E., Govers, G., Vandevenne, F., and Conley, D. (2011). Anthropogenic impact on amorphous silica pools in temperate soils. Biogeosciences 8, 2281-2293.

Cooke, J., and Leishman, M. R. (2012). Tradeoffs between foliar silicon and carbon‐based defences: evidence from vegetation communities of contrasting soil types. Oikos 121, 2052-2060.

Datnoff, L. E., Snyder, G. H., and Korndörfer, G. H. (2001). "Silicon in agriculture" Elsevier.

de Carvalho, J. S., Frazão, J. J., de Mello Prado, R., de Souza Júnior, J. P., and Costa, M. G. (2022). Silicon modifies C:N:P stoichiometry and improves the physiological efficiency and dry matter mass production of sorghum grown under nutritional sufficiency. Scientific Reports 12, 16082.

Debona, D., Rodrigues, F., Rios, J., Nascimento, K., and Silva, L. (2014). The effect of silicon on antioxidant metabolism of wheat leaves infected by *Pyricularia oryzae*. Plant pathology 63, 581-589.

Department of Agriculture, Hokkaido Government. (2020). Hokkaido fertilizer recommendations 2020. Hokkaido Agricultural Policy, Planning Department, Sapporo.

Department of Agriculture, Hokkaido Government. (2022). Hokkaido Annual Report of Agriculture Forestry and Fisheries Statistics 2020 - 2021. Vol. 2022. Hokkaido Agricultural Policy, Planning Department, Sapporo.

Dorneles, K. R., Dallagnol, L. J., Pazdiora, P. C., Rodrigues, F. A., and Deuner, S. (2017). Silicon potentiates biochemical defense responses of wheat against tan spot. Physiological and Molecular Plant Pathology 97, 69-78.

Epstein, E. (1994). The anomaly of silicon in plant biology. Proceedings of the National Academy of Sciences 91, 11-17.

Epstein, E. (1999). Silicon. Annual review of plant biology 50, 641-664.

Fageria, N. K., Baligar, V. C., and Jones, C. A. (2010). Growth and mineral nutrition of field crops. CRC press.

Frazão, J. J., Prado, R. d. M., de Souza Júnior, J. P., and Rossatto, D. R. (2020). Silicon changes C:N:P stoichiometry of sugarcane and its consequences for photosynthesis, biomass partitioning and plant growth. Scientific Reports 10, 12492.

Guntzer, F., Keller, C., and Meunier, J. D. (2012). Benefits of plant silicon for crops: a review. Agronomy for Sustainable Development 32, 201-213.

Hashimoto, Y., Kang, J., Matsuyama, N., and Saigusa, M. (2012). Path analysis of phosphorus retention capacity in allophanic and non‐allophanic Andisols. Soil Science Society of America Journal 76, 441-448.

Hatano, R., Shinjo, H., and Yusuke, T. (2021). "The Soils of Japan," Springer Nature Singapore Pte Ltd.

Haynes, R. J. (2019). What effect does liming have on silicon availability in agricultural soils? Geoderma 337, 375-383.

He, W., Yang, M., Li, Z., Qiu, J., Liu, F., Qu, X., Qiu, Y., and Li, R. (2015). High levels of silicon provided as a nutrient in hydroponic culture enhances rice plant resistance to brown planthopper. Crop Protection 67, 20-25.

Hellal, F., Zeweny, R., and Yassen, A. (2012). Evaluation of nitrogen and silicon application for enhancing yield production and nutrient uptake by wheat in clay soil. Journal of Applied Sciences Research, 686-692.

Huang, Y. C., and Hseu, Z. Y. (2021). Silicon availability in relation to soil properties in Inceptisols on uncultivated lands and paddy fields in Taiwan. Geoderma Regional 26, e00406.

Imaizumi, K., and Yoshida, S. (1958). Edaphological studies on silicon-supplying power of paddy soils. Bulletin National Institute Agriculture Science, B 8, 261-304.

Inoue, K., and Huang, P. M. (1985). Influence of citric acid on the formation of short-range ordered aluminosilicates. Clays and Clay Minerals 33, 312-322.

Inoue, K., and Huang, P. M. (1990). Perturbation of imogolite formation by humic substances. Soil Science Society of America Journal 54, 1490-1497.

Jackson, R. B., Schenk, H., Jobbagy, E., Canadell, J., Colello, G., Dickinson, R., Field, C., Friedlingstein, P., Heimann, M., and Hibbard, K. (2000). Belowground consequences of vegetation change and their treatment in models. Ecological Applications 10, 470-483.

Japanese Society of Pedology (2021). "Soil Survey Handbook (JPS)," Hakuyusha, Tokyo, Japan.

Jobbágy, E. G., and Jackson, R. B. (2001). The distribution of soil nutrients with depth: Global patterns and the imprint of plants. Biogeochemistry 53, 51-77.

Kanda, T., Takata, Y., Kohyama, K., and Obara, H. (2016). Soil map of Hokkaido developed with the comprehensive soil classification system of Japan, First Approximation: change of Andosols distribution area in forest. Japanese Journal of Soil Science and Plant Nutrition 87, 184-192.

Kato, N., and Owa, N. (1997). Dissolution of slag fertilizers in a paddy soil and Si uptake by rice plant. Soil science and plant nutrition, 43(2), 329-341.

Kato, T., Niwa, K., Kinoshita, R., Hashimoto, H., and Tani, M. (2019). Morphological features and physic-chemical properties of soil profiles developed on several river terraces different of formation age, Tokachi district, Hokkaido. Pedologist 63, 26-37.

Kikuchi, K. (1981). Interpretative classification of soils in the Tokachi district and their mapping and practical application for soil improvement. Report of Hokkaido Prefectural Agricultural Experiment Stations 34, 1-118.

Kikuchi, K. (2008). "Terraced soil and agriculture – How to utilize the Tokachi plain most effectively," Kokon Shoin Tokyo.

Kitta, Y., and Mizuochi, T. (1997). Simplification and refinement of the acetate extraction method for estimation of Si availability. Japanese Journal of Soil Science and Plant Nutrition 68, 589-594.

Kostic, L., Nikolic, N., Bosnic, D., Samardzic, J., and Nikolic, M. (2017). Silicon increases phosphorus (P) uptake by wheat under low P acid soil conditions. Plant and Soil 419, 447-455.

Lata-Tenesaca, L. F., de Mello Prado, R., de Cássia Piccolo, M., da Silva, D. L., and da Silva, J. L. F. (2021). Silicon modifies C:N:P stoichiometry, and increases nutrient use efficiency and productivity of quinoa. Scientific Reports 11, 9893.

Liang, Y., Nikolic, M., Bélanger, R., Gong, H., and Song, A. (2015). "Silicon in Agriculture: From Theory to Practice," Springer Dordrecht.

Liang, Y., Si, J., and Römheld, V. (2005). Silicon uptake and transport is an active process in *Cucumis sativus*. New Phytologist 167, 797-804.

Liu, X., Li, L., Bian, R., Chen, D., Qu, J., Wanjiru Kibue, G., Pan, G., Zhang, X., Zheng, J. and Zheng, J. (2014). Effect of biochar amendment on soil‐silicon availability and rice uptake. Journal of Plant Nutrition and Soil Science, 177(1), 91-96.

Ma, J. F., and Yamaji, N. (2006). Silicon uptake and accumulation in higher plants. Trends in plant science 11, 392-397.

Ma, J. F., and Takahashi, E. (2002). "Soil, fertilizer, and plant silicon research in Japan," Elsevier.

Machida, H., and Arai, F. (1992). Atlas of tephra in and around Japan. University of Tokyo Press, 276p.

MAFF (2023). The 96th Statistical Yearbook. Vol. February 2023. Ministry of Agriculture, Forestry and Fisheries of Japan, https://www.maff.go.jp/e/data/stat/nenji_index.htm.

Majumdar, S., and Prakash, N. B. (2022). Relationship of properties of rice and sugarcane soils and plant available silicon in Karnataka, South India. Silicon 14, 5647-5660.

Makabe S, Kakuda K, Sasaki Y, Ando T, Fujii H, Ando H., (2009). Relationship between mineral composition or soil texture and available silicon in alluvial paddy soils on the Shounai Plain, Japan. Soil Science and Plant Nutrition. 55, 300-308.

Miles, N., Manson, A. D., Rhodes, R., van Antwerpen, R., and Weigel, A. (2014). Extractable silicon in soils of the South African sugar industry and relationships with crop uptake. Communications in Soil Science and Plant Analysis 45, 2949-2958.

Neu, S., Schaller, J., and Dudel, E. G. (2017). Silicon availability modifies nutrient use efficiency and content, C:N:P stoichiometry, and productivity of winter wheat (*Triticum aestivum* L.). Scientific Reports 7, 40829.

Obara, H., Takata, Y., Kohyama, K., Ohkura, T., Maejima, Y., Watabayashi, S., and Kanda, T. (2016). A new soil map of Japan based on comprehensive soil classification system of Japan First Approximation. Nogyo Kankyo Gijutsu Kenkyusho Hokoku= Bulletin of National Institute for Agro-Environmental Sciences, 133-148.

Parfitt, R. L., and Wilson, A. (1985). Estimation of allophane and halloysite in three sequences of volcanic soils, New Zealand. Catena. Supplement (Giessen), 1-8.

Powell, J. J., McNaughton, S. A., Jugdaohsingh, R., Anderson, S. H. C., Dear, J., Khot, J., Mowatt, L., Gleason, K. L., Sykes, M., Thompson, R. P. H., Bolton-Smith, C., and Hodson, M. J. (2005). A provisional database for the silicon content of foods in the United Kingdom. British Journal of Nutrition 94, 804-812.

Rodgers‐Gray, B., and Shaw, M. (2004). Effects of straw and silicon soil amendments on some foliar and stem‐base diseases in pot‐grown winter wheat. Plant Pathology 53, 733-740.

Rodrigues, F. A., and Datnoff, L. E. (2015). "Silicon and plant diseases," Springer.

Saigusa, M., Shoji, S., and Otowa, M. (1991). Clay mineralogy of two Andisols showing a hydrosequence and its relationships to their physical and chemical properties. Pedologist 35, 21-33.

Schaller, J., Puppe, D., Kaczorek, D., Ellerbrock, R., and Sommer, M. (2021). Silicon cycling in soils revisited. Plants 10, 295.

Schaller, J., Schoelynck, J., Struyf, E., and Meire, P. (2016). Silicon affects nutrient content and ratios of wetland plants. Silicon 8, 479-485.

Shigezumi, M., Kitta, Y., Kubo, S., and Mizuochi, T. (2002). The evaluation of the available silica in paddy soil by the phosphate buffer extraction method. Japanese Journal of Soil Science and Plant Nutrition 73, 383-390.

Shoji, S., Nanzyo, M., and Dahlgren, R. (1994). "Volcanic ash soils: genesis, properties and utilization," Elsevier.

Soil Survey Staff (2014). Keys to Soil Taxonomy. USDA-Natural Resources Conservation Service, Washington, DC.

Sourideth, V., Kinoshita, R., Francisco, E. A., Onishi, K., Aiuchi, D., Shimada, J., and Tani, M. (2023). Vertical distribution of available silicon in soil profiles along river terraces of Tokachi, Hokkaido. Pedologist 67, No. 1, 35 – 46.

Sumida, H. (1991). Characteristics of silica dissolution and adsorption in paddy soils: Application to soil test for available silica. Japanese Journal of Soil Science and Plant Nutrition 62, 378-285.

Takahashi, T., and Dahlgren, R. A. (2016). Nature, properties and function of aluminum–humus complexes in volcanic soils. Geoderma 263, 110-121.

Tani, M. (2010). Nature and Land Use in Hokkaido. In "Hokkaido Agriculture and Soil Fertilizer", pp. 1-13. Hokkaido Branch of the Japan Society of Soil and Plant Nutrition, Kita Agricultural Association, Sapporo.

Tani, M., Mizota, C., Yagi, T., Kato, T., and Koike, M. (2010). Vertical distribution and accumulation of phosphate in virgin soils and arable soils of Tokachi district, Hokkaido. Japanese Journal of Soil Science and Plant Nutrition 81, 350-359.

The Fifth Committee for Soil Classification and Nomenclature (2017). Soil classification system of Japan.

Thorup-Kristensen, K., Salmerón Cortasa, M., and Loges, R. (2009). Winter wheat roots grow twice as deep as spring wheat roots, is this important for N uptake and N leaching losses? Plant and Soil 322, 101-114.

Wada K and Inoue A (1974). Adsorption of monomeric silica by volcanic ash soils. Soil Science and Plant Nutrition 20, 5–15.

Wedepohl, K. H. (1995). The composition of the continental crust. Geochimica et cosmochimica Acta 59, 1217-1232.

Whalley, W. R., Watts, C. W., Gregory, A. S., Mooney, S. J., Clark, L. J., and Whitmore, A. P. (2008). The effect of soil strength on the yield of wheat. Plant and Soil 306, 237-247.

White, R. G., and Kirkegaard, J. A. (2010). The distribution and abundance of wheat roots in a dense, structured subsoil–implications for water uptake. Plant, cell & environment 33, 133-148.

Wu, J., Geilfus, C.-M., Pitann, B., and Mühling, K.-H. (2016). Silicon-enhanced oxalate exudation contributes to alleviation of cadmium toxicity in wheat. Environmental and Experimental Botany 131, 10-18.

Wu, Q. S., Wan, X. Y., Su, N., Cheng, Z. J., Wang, J. K., Lei, C. L., Zhang, X., Jiang, L., Ma, J. F., and Wan, J. M. (2006). Genetic dissection of silicon uptake ability in rice (*Oryza sativa* L.). Plant Science 171, 441-448.

Yanai, J., Nakao, A., and Taniguchi, H. (2016). Evaluation of available silicon content and its determining factors of agricultural soils in Japan. Soil Science and Plant Nutrition 62, 511-518.

Yanai, J., Noguchi, N., Miyamaru, N., and Nakao, A. (2019). Evaluation of available silicate content and its determining factors in the soils of sugarcane fields in Okinawa, Japan. Japanese Journal of Soil Science and Plant Nutrition 90, 13-21.

Yoshida, S., Forno, D. A., Cock, J., and Gomez, K. (1976). "Laboratory manual for physiological studies of rice", International Rice Research Institute.

Appendix Table 1-1. Morphological description of Lowland soil profile.

Profile ID	S2021-09			Soil Classfication	Oxyaquic Udifluvents (USDA) Aquic Brown Lowland soils (JP)		Date	6-Aug-21			Surveyors	Tani, Kinishita, Kishimoto, Sourideth		
Survey Site	Lowland (LL) - Murase H					Owner	Murase H			Weather	Sunny	Vegetation, landuse, or sketch of surrounding environment		
Parent material	Alluvial			Mode of deposition	Alluvial fan		Latitude・Longitude		N 42.98195 E 142.95770			Winter wheat		
Topography	Lowland - flood plain, flat position					Elevation	106 m			Slope	Flat			
Erosion	slightly			Drainage	Poorly drained	Rock outcrop	none							
Horizon	Depth (cm)	Horizon boundary	Soil Color[a]	Mottling・Concretion[b]	Organic Matter[c]	Texture[d]	Rock fragment[e]	Soil Structure[f]	Stickiness[g]	Plasticity[h]	Compactness (mm)	Root biological feature[i]	Moisture condition[j]	Active aluminum	Remarks
Ap1	0-15	Smooth Clear	10YR 4/3	N	M	SL	N	0.2 - 0.5 cm CR 0.5 - 1 cm SB WE	VSS	VSP	16.7	VF, F C	MM	−	
Ap2	15-30	Smooth Clear	10YR 4/3	N	M	SL	N	0.2 - 0.5 cm SB CR VW	VSS	VSP	20.0	VF, F C	MM	−	
Ap3	30-39	Smooth Clear	2.5Y 4/4	N	L	SL	N	0.2 - 0.5 cm SB VW	VSS	VSP	25.7	VF, F VF	MM	−	
C	39-69	Smooth Clear	2.5Y 5/4	N	L	LS	N	SG	VSS	N	22.7	VF, F VF	MM	−	
Cg1	69-100	Smooth Gradual	10YR 4/6 (30%) 2.5Y 5/2 (70%)	FA TU FeM FA CL FeM (30%)	L	CoS/S FS/LS	N	SG	N/VSS	N	CoS/S 17.3 FS/LS 20.0	VF, F VF	MM	−	
Cg2	100 - 120+		10YR 4/6 (30%) 2.5Y 5/2 (70%)	FA TU FeM FA CL FeM (30%)	L	LS	N	SG	VSS	N	17	VF, F VF	MM	±	Wetter than Cg1

[a]Based on Munsell color chart. [b]N, none; FA, faint; DI, distinct; TU, tubular; CL, cloudy; FeM, Fe mottling. [c]L, low; M, medium; H, high; VH, very high . [d]SL, sandy loam; LS, loamy sand; S, sand; L, loam; CL, clay loam; LiC, light clay. [e]N, none; F, fresh; G, gravel; S, stone; LS, large stone; SR, subrounded. [f]VW, very weak; WE, weak; M, medium; CR, crumb; SB, subangular blocky; SG single grain. [g]N, none; VSS, very slight sticky; SS, slightly sticky. [h]N, none; VSP, very slightly plastic; SP, slightly plastic. [i]VF, very fine; F, fine; VF, very few; F, few; C, common. [j]MD, moderate dry; MM, moderate moist; M, moist; W, wet.

Appendix Table 1-2. Morphological description of Low terrace soil profile.

Profile ID	S2021-11			Soil Classfication	Andic Oxyaquic Humudepts (USDA) Endofluvic Wet Andosols (JP)		Date	6-Aug-21			Surveyors	Tani, Kinishita, Kishimoto, Sourideth		
Survey Site	Lower terrace (LT) - Murase T(6-1)					Owner	Murase T			Weather	Sunny	Vegetation, landuse, or sketch of surrounding environment		
Parent material	Volcanic ash/Alluvials			Mode of deposition	Eolian and Alluvial fan		Latitude・Longitude		N 42.96967 E 142.96790			Winter wheat		
Topography	Lower volcanic ash terrace flat position					Elevation	102 m			Slope	flat			
Erosion	slightly			Drainage	poorly drained	Rock outcrop	none							
Horizon	Depth (cm)	Horizon boundary	Soil Color[a]	Mottling・Concretion[b]	Organic Matter[c]	Texture[d]	Rock fragment[e]	Soil Structure[f]	Stickiness[g]	Plasticity[h]	Compactness (mm)	Root biological feature[i]	Moisture condition[j]	Active aluminum	Remarks
Ap1	0-15	Smooth clear	10YR 2/2	N	H	L	1 - 3 cm F, SR (2%)	0.5 - 1 cm SB 0.2 - 0.5 cm CR W	SS	SP	13.7	VF, F M	MM	++	
Ap2	15-30	Wavy clear	10YR 2/2	N	H	L	1 - 3 cm F, SR (2%)	0.5 - 1 cm SB 0.2 - 0.5 cm CR W - M	SS	SP	23.3	VF, F C	MM	++	
Ap2/2B/ 2A	30-38	Smooth abrupt	10YR 2/2(Ap2) 10YR 4/6(B) 10YR 2/1(2A)	N	H	SL (B) CL	N	0.5 - 1 cm SB W - M	VSS (B) SS	VSP (B) SP	24.0 19..0	VF, F F	MM	(++) Ap2 (+++) 2B (+++) 2A	
2Cg1	38-48	Smooth clear	10YR 4/6 (50%) 10YR 5/1 (50%)	D TU Fe (50%)	L	CL	1 - 3 cm F (1%)	M	SS	SP	24.7	VF, F VF	MM	−	
2Cg2	48-80	Smooth clear	10YR 4/6 (10%) 2.5Y 5/1 (90%)	D TU Fe (10%)	L	LiC	5 - 10 cm F, SR (5%)	M	VSS	VSP	21.3	VF, F VF	MM	−	
2Cg3	80-100+		10YR 4/6 (50%) 10YR 5/1 (50%)	F TU Fe (30%)	L	CL	5 - 20 cm F, SR (30%)	SG	VSS	N	14.0	N	W	−	

[a]Based on Munsell color chart. [b]N, none; FA, faint; DI, distinct; TU, tubular; CL, cloudy; FeM, Fe mottling. [c]L, low; M, medium; H, high; VH, very high . [d]SL, sandy loam; LS, loamy sand; S, sand; L, loam; CL, clay loam; LiC, light clay. [e]N, none; F, fresh; G, gravel; S, stone; LS, large stone; SR, subrounded. [f]VW, very weak; WE, weak; M, medium; CR, crumb; SB, subangular blocky; SG single grain. [g]N, none; VSS, very slight sticky; SS, slightly sticky. [h]N, none; VSP, very slightly plastic; SP, slightly plastic. [i]VF, very fine; F, fine; VF, very few; F, few; C, common. [j]MD, moderate dry; MM, moderate moist; M, moist; W, wet.

Appendix Table 1-3. Morphological description of Middle terrace soil profile.

Profile ID	S2021-13		Soil Classfication	Aquic Melandands (USDA) Humic Allophanic Andosols		Date	6-Aug-21			Surveyors	Tani, Kinishita, Kishimoto, Sourideth		
Survey Site	Middle terrace (MT) - Sasaki				Owner	Sasaki			Weather	Partly cloudy	Vegetation, landuse, or sketch of surrounding environment		
Parent materia	Volcanic ash		Mode of deposition	Eolian		Latitude・Longitude		N 42.98622 E142.98355			Winter wheat		
Topography	Flat middle volcanic ash terrace				Elevation	116 m			Slope	flat			
Erosion	slightly		Drainage	poorly drained	Rock outcrop	none							
Horizon	Depth (cm)	Horizon boundary	Soil Color[a]	Mottling・Concretion[b]	Organic Matter[c]	Texture[d]	Rock fragment[e]	Soil Structure[f]	Stickiness[g]	Plasticity[h]	Compactness (mm)	Root biological feature[i]	Moisture condition[j]	Active aluminum	Remarks[k]
Ap1	0-15	Smooth clear	10YR 1.7/1	N	VH	L	N	0.5 - 1.5 cm SB 0.2 - 0.5 cm CR W	VSS	VSP	14.3	VF, F M	MM	++	
Ap2	15-35	Smooth clear	10YR 1.7/1	N	VH	L	N	0.5 - 1.5 cm SB 0.2 - 0.5 cm CR W - M	VSS	VSP	19.5	VF, F C	MM	++	
2A	35-46	Smooth clear	N 1.5/0	N	VH	L	N	0.5 - 1.5 cm SB 0.2 - 0.5 cm CR W	VSS	VSP	24.0	VF, F F	MM	++	Ta - c
3B	46-61	Wavy clear	10YR 5/4	N	L	CL	N	0.2 - 1 cm SB VW	VSS	VSP	20.7	VF VF	MM - MD	+++	Ta - d
4Cg1	61-91	Smooth gradual	2.5 Y 6/1 (90%) 7.5YR 5/6 (10%)	D TU Fe (10%)	L	LiC	N	M	SS-S	P	24.7	VF VF	MM	—	
4Cg2	91-110+		2.5 Y 5/2 (90%) 7.5YR 5/6 (10%)	D TU Fe (10%)	L	CL	N	M	SS	SP-P	24.3	N	MM - MD	—	

[a]Based on Munsell color chart. [b]N, none; FA, faint; DI, distinct; TU, tubular; CL, cloudy; FeM, Fe mottling. [c]L, low; M, medium; H, high; VH, very high . [d]SL, sandy loam; LS, loamy sand; S, sand; L, loam; CL, clay loam; LiC, light clay. [e]N, none; F, fresh; G, gravel; S, stone; LS, large stone; SR, subrounded. [f]VW, very weak; WE, weak; M, medium; CR, crumb; SB, subangular blocky; SG single grain. [g]N, none; VSS, very slight sticky; SS, slightly sticky. [h]N, none; VSP, very slightly plastic; SP, slightly plastic. [i]VF, very fine; F, fine; VF, very few; F, few; C, common. [j]MD, moderate dry; MM, moderate moist; M, moist; W, wet. [k]Ta-c, Tarumae C; Ta-d, Tarumae D.

Appendix Table 1-4. Morphological description of High terrace soil profile.

Profile ID	S2021-04		Soil Classfication	Typic Hapludands (USDA) Haplic Allophanic Andosols		Date	6-Aug-21			Surveyors	Tani, Kinishita, Kishimoto, Sourideth		
Survey Site	High terrace (HT) - Nakamura				Owner	Nakamura			Weather	Partly cloudy	Vegetation, landuse, or sketch of surrounding environment		
Parent material	Volcanic ash		Mode of deposition	Eolian	Latitude・Longitude		N 43.0530 E142.90424				Winter wheat		
Topography	Flat upper volcanic ash terrace				Elevation	188 m			Slope	Flat			
Erosion	Very slight		Drainage	Well drained	Rock outcrop	None							
Horizon	Depth (cm)	Horizon boundary	Soil Color[a]	Mottling・Concretion[b]	Organic Matter[c]	Texture[d]	Rock fragment[e]	Soil Structure[f]	Stickiness[g]	Plasticity[h]	Compactness (mm)	Root biological feature[i]	Moisture condition[j]	Active aluminum	Remarks[k]
Ap1	0 -13	Smooth clear	10YR 3/3	N	H	L	N	0.5 - 1.5 cm SB 0.2 - 0.5 cm CRW	VSS	SP	12.7	VF, FM	MM	++	
Ap2	13-32	Smooth abrupt	10YR 3/3	N	H	L	N	0.5 - 1.5 cm SB 0.2 - 0.5 cm CRW-M	VSS	SP	19.3	VF, FC	MM	++	
2B	32-42	Wavy clear	10YR 4/6	N	L	L	N	0.5 - 1 cm SBW	VSS	VSP	21.0	VF, FF	MM	+++	Ta _c
3B1	42-72	Wavy clear	10YR 5/6	N	L	L	N	0.5 - 1.5 cm SBW - M	VSS	SP	25.0	VF, FVF	MM	+++	En_a
3B2	72-104+		10YR 5/6	N	L	L	F, SR 5 cm (1%)	0.5 - 1.5 cm SBW	VSS	VSP	24.0	VF, FVF	MM	+++	En_a

[a]Based on Munsell color chart. [b]N, none; FA, faint; DI, distinct; TU, tubular; CL, cloudy; FeM, Fe mottling. [c]L, low; M, medium; H, high; VH, very high . [d]SL, sandy loam; LS, loamy sand; S, sand; L, loam; CL, clay loam; LiC, light clay. [e]N, none; F, fresh; G, gravel; S, stone; LS, large stone; SR, subrounded. [f]VW, very weak; WE, weak; M, medium; CR, crumb; SB, subangular blocky; SG single grain. [g]N, none; VSS, very slight sticky; SS, slightly sticky. [h]N, none; VSP, very slightly plastic; SP, slightly plastic. [i]VF, very fine; F, fine; VF, very few; F, few; C, common. [j]MD, moderate dry; MM, moderate moist; M, moist; W, wet. [k]Ta-c, Tarumae C; En-a, Eniwa A.

Appendix Table 2-1. Mineralogical properties of soil profile along river terraces in the Tokachi district.

Sample ID	Horizon	Depth	TC[a]	TN[b]	Al_o[c]	Fe_o[c]	Si_o[c]	Al_p[d]	Fe_p[d]	Al_o[c] +1/2Fe_o[c]	Al/Si	Allophane	PAC[e]
		cm	g kg^{-1}							%		g kg^{-1}	
Lowland													
LL-1	Ap1	0 - 15	13.3	1.53	4.59	8.62	2.24	0.9	2.60	0.89	1.70	15.2	600
LL-2	Ap2	15 - 30	13.5	1.52	3.80	7.91	1.67	0.77	2.50	0.78	1.89	12.1	630
LL-3	Ap3	30 - 39	9.49	1.19	4.55	8.05	2.28	0.6	2.35	0.86	1.78	16.0	630
LL-4	C	39 - 69	5.75	0.80	4.02	8.30	2.20	0.36	1.64	0.82	1.73	15.1	750
LL-5	Cg1	69 - 100	3.49	0.54	2.73	8.75	1.88	0.08	0.83	0.71	1.47	11.8	590
LL-6	Cg2	100 - 120+	2.75	0.49	3.14	7.65	2.13	0.10	0.78	0.70	1.49	13.5	490
Low terrace													
LT-1	Ap1	0 - 15	58.8	4.42	11.5	20.7	3.16	5.94	6.30	2.18	1.82	22.4	1390
LT-2	Ap2	15 - 30	63.6	4.63	12.4	23.2	3.51	6.08	5.61	2.40	1.88	25.4	1440
LT-3	Ap2/2B/ 2A	30 - 38	50.1	2.94	11.6	42.5	4.82	4.20	4.60	3.29	1.60	31.7	1650
LT-4	2Cg1	38 - 48	5.17	0.57	2.72	10.6	1.89	0.06	0.70	0.80	1.47	11.9	810
LT-5	2Cg2	48 - 80	4.38	0.57	2.12	3.84	1.16	0.09	0.52	0.40	1.82	8.2	610
LT-6	2Cg3	80 - 100+	6.91	0.71	4.45	7.0	2.54	0.46	1.11	0.80	1.64	16.9	300
Middle terrace													
MT-1	Ap1	0 - 15	88.4	5.97	23.8	11.7	6.71	9.48	5.46	2.97	2.22	55.5	2150
MT-2	Ap2	15 - 35	90.3	5.96	23.5	12.0	6.53	10.1	6.03	2.94	2.14	52.3	2090
MT-3	2A	35 - 46	99.0	6.02	24.6	15.7	6.75	11.0	6.74	3.24	2.10	53.2	2310
MT-4	3B	46 - 61	48.6	3.80	77.2	4.54	32.1	8.73	1.36	7.95	2.22	266	2680
MT-5	4Cg1	61 - 91	5.28	0.54	2.88	7.37	1.01	0.25	1.10	0.66	2.71	10.6	980
MT-6	4Cg2	91 - 110+	3.28	0.48	2.82	8.19	1.66	0.01	1.09	0.69	1.77	11.5	1050
High terrace													
HT-1	Ap1	0 - 13	42.6	3.64	39.6	14.3	16.5	4.9	1.67	4.67	2.19	135	2210
HT-2	Ap2	13 - 32	44.0	3.73	40.9	17.6	17.0	4.80	1.71	4.97	2.21	140	2190
HT-3	2B	32 - 42	10.3	1.06	40.6	12.7	19.6	3.28	0.31	4.69	1.98	147	2280
HT-4	3B1	42 - 72	8.53	0.85	40.9	17.6	17.0	2.89	0.21	4.97	2.36	150	2260
HT-5	3B2	72 - 104+	11.4	0.88	40.9	17.6	17.0	3.40	0.25	4.97	3.28	254	2610

[a]TC; total C. [b]TN; total N. [c]Al_o, Fe_o, and Si_o; oxalate-extractable Al, Fe, and Si, respectively. [d]Al_p and Fe_p; pyrophosphate-extractable Al and Fe, respectively.

[e]PAC; phosphate absorption coefficient.

Appendix Table 2-2. Physiochemical properties and available Si of soil profile along river terraces in the Tokachi district.

Sample ID	Horizon	Depth	pH		Available P[a]	CEC[b]	Exchangeable			Base saturation	Ca saturation	Available Si[c]		
							K	Ca	Mg			AB	PB2	PB4
		cm	H_2O	KCl	mg kg^{-1}		mg kg^{-1}			%	%	mg kg^{-1}		
Lowland														
LL-1	Ap1	0 - 15	6.12	4.80	328	8.62	350	2064	338	83.3	61.1	46.8	47.8	64.0
LL-2	Ap2	15 - 30	6.16	5.19	360	7.91	428	2364	360	92.0	68.0	54.2	106.5	69.4
LL-3	Ap3	30 - 39	6.26	5.11	258	8.05	361	2151	335	89.9	66.4	56.7	75.9	80.7
LL-4	C	39 - 69	6.30	5.02	64.2	8.30	225	2314	347	94.8	72.2	93.0	62.1	157.2
LL-5	Cg1	69 - 100	6.54	5.08	56.0	8.75	64.2	1953	187	82.6	69.0	88.6	147.2	148.2
LL-6	Cg2	100 - 120+	6.59	5.09	66.4	7.65	91.1	1674	206	86.4	68.8	65.8	115.1	123.2
Low terrace														
LT-1	Ap1	0 - 15	5.33	4.36	195	20.7	133	1989	241	40.8	33.0	43.7	36.3	64.3
LT-2	Ap2	15 - 30	5.34	4.38	149	23.2	347	1852	191	39.6	31.2	50.3	44.4	81.5
LT-3	Ap2/2B/ 2A	30 - 38	5.63	4.60	23.0	42.5	241	2379	314	47.8	37.6	100.2	116.1	162.0
LT-4	2Cg1	38 - 48	5.96	4.34	1.68	10.6	133	2286	588	98.5	67.6	77.7	129.0	175.4
LT-5	2Cg2	48 - 80	6.12	4.32	2.64	3.84	62.6	1705	523	95.3	62.3	51.9	86.2	123.9
LT-6	2Cg3	80 - 100+	5.92	4.29	19.0	7.0	69.4	756	195	68.9	46.7	40.8	50.9	55.5
Middle terrace														
MT-1	Ap1	0 - 15	5.74	4.77	151	6.1	9.48	3347	372	50.3	41.1	60.3	72.1	120.5
MT-2	Ap2	15 - 35	5.68	4.69	149	10.3	10.1	3114	365	45.6	36.6	63.7	68.9	113.0
MT-3	2A	35 - 46	5.72	4.63	0.32	6.5	11.0	3065	360	42.3	33.8	64.9	90.4	141.2
MT-4	3B	46 - 61	5.38	4.71	1.19	5.09	8.73	921	125	16.1	10.7	274.6	104.5	520.2
MT-5	4Cg1	61 - 91	4.92	3.50	5.05	6.18	0.25	2021	458	64.7	44.2	92.2	128.6	428.6
MT-6	4Cg2	91 - 110+	4.91	3.36	1.70	15.69	0.01	2316	656	70.9	46.0	93.5	174.8	245.0
High terrace														
HT-1	Ap1	0 - 13	5.62	4.91	52.0	14.3	134	1904	237	45.5	36.5	137.0	161.8	284.9
HT-2	Ap2	13 - 32	5.76	4.87	59.5	17.6	203	1726	190	42.2	33.8	159.5	171.4	506.6
HT-3	2B	32 - 42	6.18	5.34	2.80	12.7	147	1049	134	40.3	31.1	290.9	282.2	535.2
HT-4	3B1	42 - 72	6.37	5.48	0.32	17.6	58.6	853	91.1	34.4	27.7	319.7	251.2	543.6
HT-5	3B2	72 - 104+	6.43	5.46	0.33	17.6	46.3	838	66.8	27.8	23.8	377.0	252.1	562.1

[a]Available P using the Troug method. [b]CEC; cation exchange capacity. [c]AB; acetate buffer method (0.1 M acetate buffer, pH 4.0), PB2 and PB4; phosphate buffer method (0.02M phosphate buffer, pH 6.9 and 0.04 phosphate buffer, pH 6.2)

Appendix Table 3-1. Sample ID, farm name, soil type, and location of the sampling site.

Year	Sample ID	Farm name	Soil type	Level of river terrace	Longitude	Latitude	Elevation (m)
2020	S2020-01	Nitta	Lowland soils	Middle terrace	N 43° 1'40.07"	E 142°53'3.46"	143
2020	S2020-02	Tamoto	Wet Andosols	High terrace	N 42°58'50.91"	E 142°53'11.00"	202
2020	S2020-03	Ito	Peat soils	Middle terrace	N 43° 3'42.83"	E 142°53'36.47"	194
2020	S2020-04	Nakamura	Andosols	Middle terrace	N 43° 3'4.96"	E 142°54'15.04"	188
2020	S2020-05	Shiraishi	Andosols	Middle terrace	N 43° 0'41.84"	E 142°55'23.13"	162
2020	S2020-06	Shiraishi	Lowland soils	Lowland	N 43° 0'39.82"	E 142°54'54.46"	129
2020	S2020-07	Suzuki	Peat soils	Low terrace	N 43° 1'13.72"	E 142°55'27.56"	144
2020	S2020-08	Fukuoka	Lowland soils	Low terrace	N 43° 1'55.28"	E 142°55'10.68"	145
2020	S2020-09	Yamaguchi	Thapt Andosols	Low terrace	N 43° 1'20.13"	E 142°57'6.68"	130
2020	S2020-10	Murase	Lowland soils	Lowland	N 42°58'41.83"	E 142°57'33.10"	105
2020	S2020-11	Murase	Lowland soils	Lowland	N 42°59'2.32"	E 142°57'16.57"	108
2020	S2020-12	Murase	Thapt Andosols	Low terrace	N 42°58'12.25"	E 142°58'8.72"	115
2020	S2020-13	Sasaki	Thapt Andosols	Middle terrace	N 42°59'9.39"	E 142°58'45.99"	116
2020	S2020-14	Akama	Wet Andosols	Middle terrace	N 42°58'17.76"	E 142°59'36.91"	107
2020	S2020-15	Kohata	Andosols	High terrace	N 43° 1'44.90"	E 142°58'59.49"	212
2020	S2020-16	Kamiya	Lowland soils	Lowland	N 42°56'27.73"	E 142°58'24.10"	88
2020	S2020-17	Nonomura	Lowland soils	Lowland	N 42°56'11.64"	E 142°59'6.92"	85
2020	S2020-18	Inuikawa	Andosols	High terrace	N 42°55'44.43"	E 142°54'41.20"	218
2020	S2020-19	Sato	Wet Andosols	High terrace	N 42°58'1.26"	E 142°54'25.33"	175
2020	S2020-20	Tomita	Andosols	High terrace	N 42°54'55.68"	E 142°56'9.59"	178
2021	S2021-01	Nitta	Lowland soils	Low terrace	N 43° 1'45.85"	E 142°53'12.93"	144
2021	S2021-02	Tamoto	Wet-Andosols	High terrace	N 42°58'54.57"	E 142°53'16.04"	198
2021	S2021-03	Ito	Wet-Andosols	Middle terrace	N 43° 4'5.38"	E 142°53'34.05"	198
2021	S2021-04	Nakamura	Andosols	Middle terrace	N 43° 3'4.78"	E 142°54'15.29"	186
2021	S2021-05	Shiraishi	Lowland soils	Lowland	N 43° 0'38.52"	E 142°54'52.04"	135
2021	S2021-06	Suzuki	Peak soils	Low terrace	N 43° 1'12.37"	E 142°55'39.96"	140
2021	S2021-07	Fukuoka	Wet-Andosols	Low terrace	N 43° 1'39.36"	E 142°55'31.62"	144
2021	S2021-08	Yamaguchi	Andosols	Low terrace	N 43° 1'20.18"	E 142°57'7.01"	131
2021	S2021-09	Murase H	Lowland soils	Lowland	N 42°58'55.01"	E 142°57'27.74"	106
2021	S2021-10	Murase T (3-1)	Lowland soils	Lowland	N 42°59'2.25"	E 142°57'16.73"	108
2021	S2021-11	Murase T (6-1)	Andosols	Low terrace	N 42°58'11.74"	E 142°58'4.56"	101
2021	S2021-12	Miyakawa	Lowland soils	Lowland	N 42°58'10.50"	E 142°57'45.28"	102
2021	S2021-13	Sasaki	Wet-Andosols	Middle terrace	N 42°59'10.56"	E 142°59'0.74"	118
2021	S2021-14	Akama	Wet-Andosols	Middle terrace	N 42°58'21.84"	E 142°59'52.44"	114
2021	S2021-15	Kohata	Andosols	High terrace	N 43° 1'44.35"	E 142°58'58.84"	215
2021	S2021-16	Kamiya	Lowland soils	Low terrace	N 42°56'39.13"	E 142°57'41.27"	90
2021	S2021-17	Nonomura	Lowland soils	Lowland	N 42°56'6.10"	E 142°59'2.52"	83
2021	S2021-18	Inuikawa	Andosols	High terrace	N 42°55'42.95"	E 142°54'43.78"	213
2021	S2021-19	Sato	Andosols	High terrace	N 42°57'44.04"	E 142°55'9.96"	168
2021	S2021-20	Tomita	Andosols	High terrace	N 42°54'51.83"	E 142°56'10.27"	176

Appendix Table 3-2. Mineralogical properties of upland soils along river terraces in the Tokachi district.

Sample ID	Level of river terrace	TC[a]	TN[b]	Al_o[c]	Fe_o[c]	Si_o[c]	Al_p[d]	Fe_p[d]	Al_o[c]+1/2Fe_o[c]	Allophane	PAC[e]
					g kg^{-1}				%	g kg^{-1}	
S2020-01	Middle terrace	89.5	6.05	24.5	10.8	6.51	10.2	6.51	2.99	4.91	1740
S2020-02	High terrace	74.6	5.19	38.1	11.8	14.6	7.19	3.64	4.41	5.66	1920
S2020-03	Middle terrace	118	7.95	38.2	15.3	10.3	13.8	7.04	4.58	4.59	2150
S2020-04	Middle terrace	42.1	3.62	42.1	16.2	17.3	5.19	1.65	5.02	4.95	1810
S2020-05	Middle terrace	21.8	1.99	44.0	13.0	22.8	3.73	0.55	5.05	5.06	1780
S2020-06	Lowland	19.3	1.56	5.66	4.25	1.75	2.68	2.20	0.78	3.91	420
S2020-07	Low terrace	128	7.48	14.5	10.3	3.93	8.25	6.86	1.97	4.54	1630
S2020-08	Low terrace	48.1	3.15	10.5	19.5	4.86	3.67	7.07	2.03	4.71	1170
S2020-09	Low terrace	86.5	5.98	11.4	15.0	3.11	5.95	7.19	1.89	4.74	1320
S2020-10	Lowland	14.1	1.57	5.23	8.10	2.74	1.16	2.55	0.93	5.18	500
S2020-11	Lowland	14.0	1.59	5.31	8.04	2.78	1.27	2.64	0.93	4.64	500
S2020-12	Low terrace	71.2	4.54	10.6	14.2	3.30	5.24	6.73	1.77	4.37	1120
S2020-13	Middle terrace	81.1	5.92	33.9	15.5	11.9	8.71	5.34	4.17	4.85	1930
S2020-14	Middle terrace	96.3	6.83	33.6	15.8	10.9	9.20	6.36	4.15	5.13	1700
S2020-15	High terrace	55.3	4.34	40.8	15.5	16.3	6.28	2.94	4.86	4.99	1940
S2020-16	Lowland	12.3	1.44	5.69	7.77	3.01	1.38	2.33	0.96	4.84	570
S2020-17	Lowland	11.7	1.38	5.53	7.70	2.67	1.51	2.65	0.94	4.12	550
S2020-18	High terrace	106	7.31	28.8	10.0	8.37	10.9	5.47	3.38	5.08	2000
S2020-19	High terrace	103	6.90	22.9	9.27	5.87	10.9	5.81	2.75	4.48	1890
S2020-20	High terrace	67.2	5.27	48.3	15.7	20.1	7.25	3.21	5.62	5.17	2080
S2021-01	Low terrace	61.5	4.25	12.2	7.23	2.61	5.33	3.92	1.58	4.81	1240
S2021-02	High terrace	70.7	5.30	32.6	12.2	11.8	5.72	3.11	3.87	5.41	1690
S2021-03	Middle terrace	64.2	4.96	37.7	14.1	13.1	7.36	4.30	4.48	4.90	1920
S2021-04	Middle terrace	42.5	3.65	40.4	17.6	17.1	4.54	1.60	4.92	4.90	1880
S2021-05	Lowland	38.3	3.12	5.58	6.91	1.30	2.62	3.07	0.90	4.49	540
S2021-06	Low terrace	134	6.86	14.9	7.35	2.37	10.9	5.59	1.86	4.51	1680
S2021-07	Low terrace	77.9	5.26	18.5	13.2	5.09	7.97	6.54	2.51	4.51	1580
S2021-08	Low terrace	80.5	5.58	13.6	14.5	3.76	6.11	6.31	2.08	4.71	1350
S2021-09	Lowland	12.4	1.47	3.72	7.06	1.62	0.56	2.13	0.72	5.18	650
S2021-10	Lowland	13.6	1.56	4.07	6.83	1.80	0.86	2.50	0.75	4.47	480
S2021-11	Low terrace	68.2	5.24	11.9	11.2	3.04	5.83	5.13	1.75	4.53	1250
S2021-12	Lowland	12.5	1.40	3.84	6.84	1.55	1.01	2.38	0.73	4.36	470
S2021-13	Middle terrace	84.3	5.69	22.5	11.6	6.65	8.17	4.35	2.83	4.65	1770
S2021-14	Middle terrace	100	6.53	30.6	12.5	9.38	10.4	5.89	3.69	4.69	2130
S2021-15	High terrace	55.8	4.50	44.0	14.8	19.3	5.04	2.38	5.14	5.07	2040
S2021-16	Low terrace	49.8	3.67	10.0	8.58	3.09	3.97	4.65	1.42	5.02	1220
S2021-17	Lowland	7.88	1.00	3.00	5.59	1.01	0.91	1.58	0.58	3.68	330
S2021-18	High terrace	117	7.94	34.2	11.4	10.1	11.6	5.41	3.99	4.95	2120
S2021-19	High terrace	43.9	3.87	48.0	16.3	22.3	4.38	1.78	5.61	5.23	2000
S2021-20	High terrace	66.4	5.27	45.6	13.4	20.4	5.89	2.89	5.23	5.28	2050

[a]TC; total C. [b]TN; total N. [c]Al_o, Fe_o, and Si_o; oxalate-extractable Al, Fe, and Si, respectively. [d]Al_p and Fe_p; pyrophosphate-extractable Al and Fe, respectively. [e]PAC; phosphate absorption coefficient. [d]CEC; cation exchange capacity.

Appendix Table 3-3. Soil nutrient properties of upland soils along river terraces in the Tokachi district.

Sample ID	Level of river terrace	pH		Available P[a]	CEC[b]	Exchangeable			Base saturation	Ca saturation
		H_2O	KCl			K	Ca	Mg		
				mg kg^{-1}	$cmol_c$ kg^{-1}	mg kg^{-1}			%	%
S2020-01	Middle terrace	6.02	4.91	135	40.5	311	3,798	389	56.0	45.9
S2020-02	High terrace	6.72	5.66	49.3	35.3	352	4,522	511	77.6	62.9
S2020-03	Middle terrace	5.50	4.59	39.9	46.6	196	2,871	255	35.9	30.2
S2020-04	Middle terrace	5.89	4.95	53.3	22.8	204	1,805	205	49.3	38.9
S2020-05	Middle terrace	5.89	5.06	27.9	19.6	366	1,090	204	40.8	27.3
S2020-06	Lowland	4.97	3.91	225	13.1	174	717	75.8	35.1	26.9
S2020-07	Low terrace	5.59	4.54	154	50.3	199	3,974	303	44.8	38.7
S2020-08	Low terrace	6.02	4.71	293	34.3	157	3,219	346	55.6	46.0
S2020-09	Low terrace	5.66	4.74	278	41.9	435	4,087	520	61.0	47.8
S2020-10	Lowland	6.54	5.18	374	15.6	642	2,130	270	92.5	67.0
S2020-11	Lowland	5.91	4.64	281	14.7	376	1,683	298	79.5	56.0
S2020-12	Low terrace	5.24	4.37	163	28.3	182	1,678	261	38.5	29.0
S2020-13	Middle terrace	5.63	4.85	115	37.4	359	3,188	371	52.4	41.7
S2020-14	Middle terrace	6.08	5.13	106	43.2	407	4,710	396	63.5	53.4
S2020-15	High terrace	5.82	4.99	48.2	27.4	183	2,169	201	46.6	38.8
S2020-16	Lowland	6.00	4.84	227	16.5	185	1,825	326	73.8	54.3
S2020-17	Lowland	5.47	4.12	176	14.5	294	1,288	237	62.3	43.4
S2020-18	High terrace	5.92	5.08	105	45.3	206	4,615	348	57.5	49.9
S2020-19	High terrace	5.45	4.48	115	44.6	174	2,891	205	36.6	31.8
S2020-20	High terrace	6.06	5.17	41.4	35.2	198	2,744	220	45.0	38.2
S2021-01	Low terrace	5.95	4.81	300	32.6	337	2,863	266	52.7	43.0
S2021-02	High terrace	6.31	5.41	380	38.1	430	4,675	539	74.8	60.2
S2021-03	Middle terrace	5.89	4.90	81.6	34.2	426	2,491	350	47.7	35.7
S2021-04	Middle terrace	5.75	4.90	48.3	25.0	117	1,807	203	44.0	35.4
S2021-05	Lowland	5.20	4.49	474	21.3	293	2,093	219	60.5	48.2
S2021-06	Low terrace	5.46	4.51	307	53.6	131	4,380	301	45.8	40.1
S2021-07	Low terrace	5.66	4.51	189	38.0	178	3,072	203	45.4	39.6
S2021-08	Low terrace	5.60	4.71	298	38.6	606	3,535	478	59.4	44.9
S2021-09	Lowland	6.36	5.18	297	17.1	319	2,266	346	86.8	64.8
S2021-10	Lowland	5.77	4.47	237	15.8	389	1,551	267	68.6	48.0
S2021-11	Low terrace	5.34	4.53	220	31.4	380	2,634	396	54.8	41.1
S2021-12	Lowland	5.72	4.36	206	14.9	451	1,265	250	63.4	41.5
S2021-13	Middle terrace	5.51	4.65	167	42.1	283	3,380	388	49.0	39.4
S2021-14	Middle terrace	5.61	4.69	82.2	48.3	298	3,610	308	43.9	36.6
S2021-15	High terrace	5.84	5.07	34.4	28.0	206	2,203	216	47.0	38.6
S2021-16	Low terrace	5.85	5.02	194	29.6	100	2,790	491	61.0	46.3
S2021-17	Lowland	4.88	3.68	119	10.2	177	422	83.4	31.6	20.3
S2021-18	High terrace	5.79	4.95	108	48.1	247	3,804	488	48.6	38.8
S2021-19	High terrace	6.00	5.23	40.7	24.3	275	2,166	217	54.2	43.8
S2021-20	High terrace	6.16	5.28	69.8	34.2	368	3,378	341	59.6	48.4

[a]Available P; available phosphorus by Troug method. [b]CEC; cation exchange capacity.

Appendix Table 3-4. Available Si of upland soils along river terraces in the Tokachi district.

Sample ID	Farm name	Level of river terrace	AB[a]	PB2[b]	PB4[b]
			mg kg^{-1}		
S2020-01	Nitta	Middle terrace	73.9	59.1	86.9
S2020-02	Tamoto	High terrace	193	115	170
S2020-03	Ito	Middle terrace	109	102	120
S2020-04	Nakamura	Middle terrace	202	177	200
S2020-05	Shiraishi	Middle terrace	241	238	342
S2020-06	Shiraishi	Lowland	13.0	17.8	26.6
S2020-07	Suzuki	Low terrace	60.1	50.4	68.5
S2020-08	Fukuoka	Low terrace	155	84.9	129.3
S2020-09	Yamaguchi	Low terrace	52.1	33.1	58.6
S2020-10	Murase	Lowland	85.6	45.9	62.8
S2020-11	Murase	Lowland	48.3	30.9	48.9
S2020-12	Murase	Low terrace	48.1	38.0	55.1
S2020-13	Sasaki	Middle terrace	135	69.4	138
S2020-14	Akama	Middle terrace	153	72.8	121
S2020-15	Kohata	High terrace	204	109	198
S2020-16	Kamiya	Lowland	66.6	44.8	57.7
S2020-17	Nonomura	Lowland	29.2	36.8	42.1
S2020-18	Inuikawa	High terrace	122	78.3	119
S2020-19	Sato	High terrace	86.9	68.2	103
S2020-20	Tomita	High terrace	211	161	291
S2021-01	Nitta	Low terrace	42.3	31.5	45.5
S2021-02	Tamoto	High terrace	139	68.7	117
S2021-03	Ito	Middle terrace	137	78.7	155
S2021-04	Nakamura	Middle terrace	179	131	271
S2021-05	Shiraishi	Lowland	29.9	28.2	27.5
S2021-06	Suzuki	Low terrace	40.7	29.7	42.0
S2021-07	Fukuoka	Low terrace	72.0	47.5	81.7
S2021-08	Yamaguchi	Low terrace	50.6	31.9	47.9
S2021-09	Murase H	Lowland	65.9	46.0	54.9
S2021-10	Murase T (3-1)	Lowland	38.3	35.9	42.0
S2021-11	Murase T (6-1)	Low terrace	50.0	34.0	52.9
S2021-12	Miyakawa	Lowland	34.6	29.9	28.1
S2021-13	Sasaki	Middle terrace	91.6	54.2	83.6
S2021-14	Akama	Middle terrace	119	65.4	122
S2021-15	Kohata	High terrace	189	123	206
S2021-16	Kamiya	Low terrace	82.2	60.0	81.7
S2021-17	Nonomura	Lowland	18.2	18.1	19.5
S2021-18	Inuikawa	High terrace	76.1	62.0	100
S2021-19	Sato	High terrace	216	161	231
S2021-20	Tomita	High terrace	206	164	238

[a]AB; acetate buffer method (0.1 M acetate buffer, pH 4.0). [b]PB2 and PB4; phosphate buffer method (0.02M phosphate buffer, pH 6.9 and 0.04 phosphate buffer, pH 6.2)

Appendix Table 4-1. Agronomic properties of winter wheat grown in the Tokachi district.

Sample ID	Level of river terrace	Stem number	Stem Height	Ear length	Third node		
			cm		Length cm	Width mm	Strength kg
S2020-01	Middle terrace	653	64.2	9.35	11.7	3.94	0.387
S2020-02	High terrace	560	59.1	8.48	11.6	3.82	0.444
S2020-03	Middle terrace	679	53.8	7.89	10.2	3.19	0.346
S2020-04	Middle terrace	650	65.7	8.95	11.9	3.78	0.315
S2020-05	Middle terrace	447	66.8	8.98	11.3	3.93	0.503
S2020-06	Lowland	314	52.0	8.21	9.04	3.40	0.484
S2020-07	Low terrace	791	69.3	8.71	12.6	3.91	0.351
S2020-08	Low terrace	505	50.7	8.55	8.98	3.24	0.438
S2020-09	Low terrace	582	62.4	9.58	10.9	3.78	0.327
S2020-10	Lowland	836	70.4	8.65	12.6	3.71	0.281
S2020-11	Lowland	851	61.7	9.05	10.5	3.53	0.381
S2020-12	Low terrace	688	56.3	9.41	10.3	3.50	0.226
S2020-13	Middle terrace	649	71.8	9.31	11.9	3.69	0.258
S2020-14	Middle terrace	773	70.2	9.13	12.2	3.68	0.233
S2020-15	High terrace	392	66.3	9.28	10.8	3.80	0.397
S2020-16	Lowland	702	57.5	8.60	11.3	3.47	0.284
S2020-17	Lowland	639	60.9	8.29	11.6	3.54	0.334
S2020-18	High terrace	570	66.5	8.63	12.0	3.65	0.303
S2020-19	High terrace	537	63.4	8.93	11.4	3.73	0.453
S2020-20	High terrace	567	64.4	8.03	11.0	3.35	0.364
S2021-01	Low terrace	645	68.7	8.47	10.8	3.93	0.366
S2021-02	High terrace	876	73.2	8.14	13.4	4.17	0.255
S2021-03	Middle terrace	667	72.5	8.51	12.9	3.95	0.264
S2021-04	Middle terrace	710	77.2	8.47	13.3	4.20	0.400
S2021-05	Lowland	579	54.4	7.42	9.5	3.19	0.260
S2021-06	Low terrace	651	70.6	8.12	12.13	3.93	0.352
S2021-07	Low terrace	604	70.3	8.21	11.8	3.80	0.329
S2021-08	Low terrace	936	68.6	7.73	12.78	3.71	0.181
S2021-09	Lowland	785	82.6	7.94	13.5	3.77	0.238
S2021-10	Lowland	881	66.6	8.08	11.8	3.55	0.166
S2021-11	Low terrace	866	70.1	8.43	12.4	3.62	0.177
S2021-12	Lowland	725	79.8	8.49	11.6	3.67	0.290
S2021-13	Middle terrace	835	74.4	8.53	12.7	3.99	0.218
S2021-14	Middle terrace	985	72.8	8.22	12.9	3.65	0.093
S2021-15	High terrace	675	73.9	8.55	12.6	3.92	0.247
S2021-16	Low terrace	787	78.0	8.04	12.5	3.70	0.233
S2021-17	Lowland	555	58.4	6.75	9.9	3.08	0.309
S2021-18	High terrace	731	75.4	8.41	14.0	4.06	0.216
S2021-19	High terrace	511	73.8	8.64	12.8	4.11	0.287
S2021-20	High terrace	917	73.9	7.62	13.2	3.71	0.182

Appendix Table 4-2. Biomass, grain yield, and yield componets of winter wheat grown in the Tokachi district.

Sample ID	Level of river terrace	Biomass				Grain yield	1000 grains weight	Grain number
		Stem	Husk	Grain	Plant			
		g m^{-2}				kg $10a^{-1}$	g	grain/ear
S2020-01	Middle terrace	544	167	646	1358	700	34.5	9
S2020-02	High terrace	483	126	581	1190	632	36.2	8
S2020-03	Middle terrace	342	126	546	1013	595	37.2	8
S2020-04	Middle terrace	556	167	723	1447	789	34.7	9
S2020-05	Middle terrace	430	125	594	1149	650	38.1	9
S2020-06	Lowland	209	80	414	704	451	37.3	8
S2020-07	Low terrace	679	205	780	1664	851	33.5	9
S2020-08	Low terrace	289	125	523	937	570	35.9	9
S2020-09	Low terrace	423	157	497	1078	543	31.8	10
S2020-10	Lowland	657	192	785	1634	857	35.8	9
S2020-11	Lowland	452	157	635	1244	693	37.7	9
S2020-12	Low terrace	451	170	701	1322	765	35.4	9
S2020-13	Middle terrace	569	166	658	1392	717	33.8	9
S2020-14	Middle terrace	634	180	661	1474	720	32.1	9
S2020-15	High terrace	390	122	453	964	495	32.5	9
S2020-16	Lowland	493	147	695	1336	759	36.8	9
S2020-17	Lowland	474	148	704	1326	769	36.3	8
S2020-18	High terrace	418	126	484	1028	526	33.2	9
S2020-19	High terrace	430	136	560	1127	613	33.7	9
S2020-20	High terrace	465	132	591	1188	643	35.7	8
S2021-01	Low terrace	603	155	760	1518	841	34.2	8
S2021-02	High terrace	753	174	790	1717	871	30.5	8
S2021-03	Middle terrace	592	154	688	1434	758	32.7	9
S2021-04	Middle terrace	721	173	981	1875	1087	37.7	8
S2021-05	Lowland	304	104	459	867	509	27.4	7
S2021-06	Low terrace	597	159	802	1558	887	36.8	8
S2021-07	Low terrace	534	149	717	1399	795	34.7	8
S2021-08	Low terrace	629	172	738	1539	820	28.3	8
S2021-09	Lowland	731	154	804	1688	891	36.0	8
S2021-10	Lowland	566	179	740	1485	821	29.2	8
S2021-11	Low terrace	618	178	721	1517	798	26.9	8
S2021-12	Lowland	608	158	845	1611	936	35.5	8
S2021-13	Middle terrace	721	185	847	1753	936	31.8	9
S2021-14	Middle terrace	779	171	748	1698	830	28.1	8
S2021-15	High terrace	647	165	747	1559	828	30.7	9
S2021-16	Low terrace	662	160	902	1724	1001	37.3	8
S2021-17	Lowland	321	105	605	1031	670	38.8	7
S2021-18	High terrace	715	158	782	1656	869	33.2	8
S2021-19	High terrace	508	140	660	1308	733	32.2	9
S2021-20	High terrace	667	175	775	1617	863	32.4	8

Appendix Table 4-3. Carbon (C) uptake, concentration, and their distribution of winter wheat grown along river terraces in the Tokachi district.

Sample ID	Level of river terrace	C uptake				C concentration			
		Stem	Husk	Grain	Plant	Stem	Husk	Grain	Plant
		g m^{-2}				g kg^{-1}			
S2020-01	Middle terrace	230	70.8	263	564	422	424	407	415
S2020-02	High terrace	206	53.1	237	497	427	422	408	417
S2020-03	Middle terrace	147	54.0	223	424	429	430	410	419
S2020-04	Middle terrace	231	70.4	299	601	415	421	414	415
S2020-05	Middle terrace	181	52.3	241	474	420	418	406	413
S2020-06	Lowland	92	34.2	169	295	439	426	408	420
S2020-07	Low terrace	286	84.5	316	687	421	412	406	413
S2020-08	Low terrace	123	52.9	211	387	427	422	403	413
S2020-09	Low terrace	175	65.9	203	444	413	420	408	412
S2020-10	Lowland	279	81.2	319	679	424	424	407	416
S2020-11	Lowland	195	65.8	257	518	431	420	405	416
S2020-12	Low terrace	192	72.5	286	550	426	427	408	416
S2020-13	Middle terrace	237	70.2	268	575	417	423	407	413
S2020-14	Middle terrace	263	75.6	272	610	414	420	412	414
S2020-15	High terrace	165	51.8	184	401	424	425	407	416
S2020-16	Lowland	216	61.8	282	560	437	420	406	419
S2020-17	Lowland	203	61.5	288	553	429	417	409	417
S2020-18	High terrace	175	53.4	198	427	419	423	409	415
S2020-19	High terrace	183	57.8	230	470	425	424	410	417
S2020-20	High terrace	199	55.2	240	495	428	418	407	416
S2021-01	Low terrace	262	65.6	309	637	434	424	407	419
S2021-02	High terrace	311	71.6	324	706	413	411	410	411
S2021-03	Middle terrace	245	63.0	281	589	414	409	408	411
S2021-04	Middle terrace	308	70.9	401	780	428	409	408	416
S2021-05	Lowland	135	46.1	188	369	446	441	409	426
S2021-06	Low terrace	258	65.1	327	650	433	410	408	418
S2021-07	Low terrace	227	60.8	293	581	425	408	409	415
S2021-08	Low terrace	261	72.3	302	635	415	421	409	413
S2021-09	Lowland	309	61.7	327	699	423	402	407	414
S2021-10	Lowland	238	76.0	305	619	421	424	412	417
S2021-11	Low terrace	256	75.2	298	629	414	423	413	415
S2021-12	Lowland	264	67.4	345	676	434	427	408	420
S2021-13	Middle terrace	297	76.0	348	721	413	410	411	411
S2021-14	Middle terrace	308	70.1	308	686	395	410	412	404
S2021-15	High terrace	264	67.2	306	638	409	407	410	409
S2021-16	Low terrace	287	66.7	369	723	434	417	409	419
S2021-17	Lowland	139	43.9	248	431	435	417	410	418
S2021-18	High terrace	301	65.9	324	691	421	416	414	417
S2021-19	High terrace	214	59.6	275	548	421	426	417	419
S2021-20	High terrace	271	71.6	323	666	406	409	417	412

Appendix Table 4-4. Nitrogen (N) uptake, concentration, and their distribution of winter wheat grown along river terraces in the Tokachi district.

Sample ID	Level of river terrace	N uptake				N concentration			
		Stem	Husk	Grain	Plant	Stem	Husk	Grain	Plant
		g m^{-2}				g kg^{-1}			
S2020-01	Middle terrace	5.11	1.37	14.4	20.9	9.39	8.20	22.3	15.4
S2020-02	High terrace	2.87	0.79	11.9	15.5	5.95	6.30	20.4	13.0
S2020-03	Middle terrace	2.99	1.07	11.8	15.8	8.73	8.49	21.6	15.6
S2020-04	Middle terrace	4.24	1.45	15.5	21.2	7.62	8.64	21.4	14.6
S2020-05	Middle terrace	2.31	0.74	11.8	14.8	5.38	5.89	19.8	12.9
S2020-06	Lowland	1.37	0.49	9.0	10.9	6.53	6.15	21.8	15.5
S2020-07	Low terrace	3.99	1.43	15.5	20.9	5.87	6.96	19.9	12.6
S2020-08	Low terrace	1.33	0.90	10.3	12.5	4.60	7.22	19.7	13.4
S2020-09	Low terrace	4.65	1.19	10.6	16.5	11.0	7.58	21.4	15.3
S2020-10	Lowland	3.95	1.41	15.2	20.5	6.01	7.35	19.3	12.6
S2020-11	Lowland	2.43	1.09	11.6	15.2	5.38	6.98	18.3	12.2
S2020-12	Low terrace	4.41	1.60	14.4	20.4	9.78	9.43	20.6	15.5
S2020-13	Middle terrace	4.49	1.17	13.3	19.0	7.89	7.07	20.3	13.7
S2020-14	Middle terrace	4.70	1.27	15.1	21.1	7.41	7.09	22.9	14.3
S2020-15	High terrace	3.55	0.74	9.83	14.1	9.11	6.12	21.7	14.6
S2020-16	Lowland	3.01	0.82	13.7	17.5	6.10	5.60	19.7	13.1
S2020-17	Lowland	2.45	0.70	13.9	17.1	5.17	4.74	19.8	12.9
S2020-18	High terrace	3.92	1.04	10.7	15.7	9.37	8.26	22.1	15.2
S2020-19	High terrace	2.64	0.79	11.8	15.3	6.14	5.78	21.1	13.5
S2020-20	High terrace	2.35	0.61	11.6	14.5	5.05	4.59	19.6	12.2
S2021-01	Low terrace	3.82	0.88	15.3	20.1	6.34	5.71	20.2	13.2
S2021-02	High terrace	7.99	1.29	16.8	26.1	10.6	7.41	21.3	15.2
S2021-03	Middle terrace	6.36	1.17	14.0	21.5	10.7	7.59	20.3	15.0
S2021-04	Middle terrace	2.75	0.67	17.5	20.9	3.81	3.87	17.8	11.1
S2021-05	Lowland	1.89	0.48	10.3	12.7	6.22	4.57	22.5	14.6
S2021-06	Low terrace	1.96	0.78	13.2	16.0	3.28	4.93	16.5	10.3
S2021-07	Low terrace	3.39	0.86	14.3	18.6	6.36	5.80	20.0	13.3
S2021-08	Low terrace	6.04	1.24	15.1	22.4	9.60	7.22	20.5	14.6
S2021-09	Lowland	2.30	0.54	12.3	15.1	3.15	3.53	15.3	9.0
S2021-10	Lowland	6.21	1.37	15.7	23.3	11.0	7.62	21.2	15.7
S2021-11	Low terrace	8.00	1.25	15.4	24.6	12.9	7.05	21.3	16.2
S2021-12	Lowland	2.67	0.55	16.9	20.1	4.40	3.46	20.0	12.5
S2021-13	Middle terrace	6.01	1.14	17.9	25.0	8.34	6.16	21.1	14.3
S2021-14	Middle terrace	11.1	1.39	17.0	29.4	14.2	8.15	22.7	17.3
S2021-15	High terrace	6.85	1.05	15.8	23.7	10.6	6.36	21.1	15.2
S2021-16	Low terrace	2.63	0.63	16.2	19.4	3.97	3.92	17.9	11.3
S2021-17	Lowland	1.40	0.40	11.8	13.6	4.36	3.78	19.6	13.2
S2021-18	High terrace	5.98	0.95	16.7	23.7	8.36	5.98	21.4	14.3
S2021-19	High terrace	3.45	1.02	13.7	18.2	6.79	7.32	20.8	13.9
S2021-20	High terrace	6.85	1.08	15.6	23.5	10.26	6.21	20.1	14.5

Appendix Table 4-5. Phosphorus (P) uptake, concentration, and their distribution of winter wheat grown along river terraces in the Tokachi district.

Sample ID	Level of river terrace	P uptake				N concentration			
		Stem	Husk	Grain	Plant	Stem	Husk	Grain	Plant
		g m^{-2}				g kg^{-1}			
S2020-01	Middle terrace	0.23	0.12	1.76	2.12	0.42	0.74	2.73	1.56
S2020-02	High terrace	0.17	0.07	1.87	2.12	0.36	0.59	3.23	1.78
S2020-03	Middle terrace	0.14	0.11	1.69	1.95	0.41	0.91	3.10	1.92
S2020-04	Middle terrace	0.23	0.16	2.20	2.58	0.41	0.94	3.05	1.79
S2020-05	Middle terrace	0.09	0.06	1.56	1.72	0.22	0.49	2.63	1.49
S2020-06	Lowland	0.13	0.08	1.56	1.77	0.62	1.05	3.76	2.51
S2020-07	Low terrace	0.30	0.18	2.48	2.96	0.44	0.87	3.18	1.78
S2020-08	Low terrace	0.08	0.10	1.64	1.82	0.28	0.79	3.14	1.94
S2020-09	Low terrace	0.38	0.16	1.86	2.39	0.89	1.03	3.73	2.22
S2020-10	Lowland	0.69	0.29	2.96	3.95	1.05	1.54	3.78	2.42
S2020-11	Lowland	0.25	0.16	2.38	2.79	0.55	1.04	3.75	2.24
S2020-12	Low terrace	0.22	0.16	2.00	2.37	0.49	0.91	2.85	1.80
S2020-13	Middle terrace	0.19	0.13	1.77	2.09	0.33	0.75	2.70	1.50
S2020-14	Middle terrace	0.15	0.11	1.73	2.00	0.24	0.59	2.63	1.35
S2020-15	High terrace	0.22	0.07	1.52	1.81	0.57	0.59	3.35	1.88
S2020-16	Lowland	0.34	0.11	2.56	3.01	0.68	0.78	3.68	2.25
S2020-17	Lowland	0.21	0.08	2.41	2.70	0.44	0.51	3.43	2.04
S2020-18	High terrace	0.19	0.11	1.53	1.82	0.45	0.85	3.16	1.77
S2020-19	High terrace	0.12	0.06	1.37	1.55	0.29	0.43	2.44	1.37
S2020-20	High terrace	0.13	0.05	1.85	2.03	0.28	0.37	3.14	1.71
S2021-01	Low terrace	0.65	0.16	2.61	3.43	1.08	1.06	3.44	2.26
S2021-02	High terrace	0.84	0.21	1.11	2.16	1.12	1.18	1.40	1.26
S2021-03	Middle terrace	0.34	0.11	2.16	2.60	0.57	0.69	3.14	1.82
S2021-04	Middle terrace	0.14	0.05	2.81	3.00	0.20	0.28	2.86	1.60
S2021-05	Lowland	0.25	0.05	1.03	1.33	0.82	0.50	2.24	1.53
S2021-06	Low terrace	0.24	0.11	2.84	3.18	0.40	0.68	3.54	2.04
S2021-07	Low terrace	0.23	0.08	2.15	2.45	0.43	0.52	3.00	1.75
S2021-08	Low terrace	0.79	0.19	2.55	3.53	1.25	1.10	3.46	2.29
S2021-09	Lowland	0.73	0.16	2.78	3.67	1.00	1.06	3.46	2.18
S2021-10	Lowland	0.49	0.20	2.49	3.18	0.87	1.14	3.36	2.14
S2021-11	Low terrace	0.38	0.10	2.18	2.66	0.62	0.56	3.02	1.75
S2021-12	Lowland	0.74	0.15	2.62	3.51	1.21	0.97	3.10	2.18
S2021-13	Middle terrace	0.34	0.11	2.42	2.87	0.48	0.58	2.86	1.64
S2021-14	Middle terrace	0.58	0.14	1.96	2.68	0.75	0.82	2.62	1.58
S2021-15	High terrace	0.46	0.12	2.49	3.08	0.71	0.74	3.34	1.97
S2021-16	Low terrace	0.27	0.06	2.64	2.97	0.41	0.36	2.92	1.72
S2021-17	Lowland	0.08	0.03	1.70	1.82	0.26	0.26	2.82	1.76
S2021-18	High terrace	0.34	0.09	2.08	2.51	0.48	0.56	2.66	1.52
S2021-19	High terrace	0.22	0.10	2.06	2.38	0.43	0.74	3.12	1.82
S2021-20	High terrace	0.57	0.15	2.84	3.56	0.85	0.88	3.66	2.20

Appendix Table 4-6. Potassium (K) uptake, concentration, and their distribution of winter wheat grown along river terraces in the Tokachi district.

Sample ID	Level of river terrace	K uptake				K concentration			
		Stem	Husk	Grain	Plant	Stem	Husk	Grain	Plant
		g m^{-2}				g kg^{-1}			
S2020-01	Middle terrace	15.1	1.67	2.58	19.4	27.8	10.0	3.99	14.3
S2020-02	High terrace	10.8	1.34	2.47	14.6	22.4	10.7	4.25	12.3
S2020-03	Middle terrace	9.31	1.31	2.35	13.0	27.2	10.4	4.32	12.8
S2020-04	Middle terrace	13.6	1.71	3.15	18.4	24.4	10.2	4.36	12.7
S2020-05	Middle terrace	9.81	1.20	2.39	13.4	22.8	9.6	4.03	11.7
S2020-06	Lowland	5.73	1.00	2.07	8.8	27.4	12.5	5.00	12.5
S2020-07	Low terrace	15.8	2.16	3.29	21.2	23.2	10.5	4.22	12.7
S2020-08	Low terrace	6.06	1.16	2.44	9.7	21.0	9.3	4.67	10.3
S2020-09	Low terrace	15.3	2.15	2.42	19.9	36.2	13.7	4.87	18.5
S2020-10	Lowland	20.0	2.53	3.64	26.2	30.4	13.2	4.64	16.0
S2020-11	Lowland	11.9	1.77	3.09	16.8	26.4	11.3	4.86	13.5
S2020-12	Low terrace	13.4	1.86	2.96	18.3	29.8	11.0	4.22	13.8
S2020-13	Middle terrace	17.6	2.22	2.72	22.6	31.0	13.4	4.14	16.2
S2020-14	Middle terrace	21.2	2.18	2.79	26.1	33.4	12.1	4.22	17.7
S2020-15	High terrace	9.51	1.55	2.14	13.2	24.4	12.7	4.72	13.7
S2020-16	Lowland	10.5	1.94	3.18	15.6	21.2	13.2	4.57	11.7
S2020-17	Lowland	12.8	1.95	2.89	17.6	27.0	13.2	4.11	13.3
S2020-18	High terrace	13.1	1.36	1.98	16.5	31.4	10.8	4.08	16.0
S2020-19	High terrace	12.4	1.34	2.10	15.8	28.8	9.8	3.75	14.0
S2020-20	High terrace	10.7	1.13	2.31	14.1	23.0	8.5	3.91	11.9
S2021-01	Low terrace	17.7	2.05	3.02	22.8	29.4	13.3	3.98	15.0
S2021-02	High terrace	25.9	2.42	1.21	29.5	34.4	13.9	1.53	17.2
S2021-03	Middle terrace	19.1	2.41	2.57	24.1	32.2	15.6	3.74	16.8
S2021-04	Middle terrace	13.1	1.78	3.14	18.0	18.2	10.3	3.20	9.6
S2021-05	Lowland	8.14	1.13	0.99	10.3	26.8	10.8	2.16	11.8
S2021-06	Low terrace	11.5	2.03	3.13	16.7	19.3	12.8	3.90	10.7
S2021-07	Low terrace	12.7	1.87	2.64	17.2	23.8	12.6	3.68	12.3
S2021-08	Low terrace	24.0	2.24	2.88	29.2	38.2	13.0	3.90	18.9
S2021-09	Lowland	14.4	1.56	2.76	18.7	19.6	10.1	3.44	11.1
S2021-10	Lowland	20.7	3.46	2.63	26.8	36.6	19.3	3.56	18.0
S2021-11	Low terrace	24.6	2.87	2.90	30.4	39.8	16.1	4.02	20.0
S2021-12	Lowland	14.9	1.49	2.32	18.8	24.6	9.5	2.74	11.6
S2021-13	Middle terrace	24.1	2.75	2.83	29.7	33.4	14.9	3.34	16.9
S2021-14	Middle terrace	29.6	2.76	2.17	34.5	38.0	16.1	2.90	20.3
S2021-15	High terrace	17.3	1.87	2.70	21.9	26.8	11.3	3.62	14.1
S2021-16	Low terrace	13.0	1.67	2.49	17.1	19.6	10.5	2.76	9.9
S2021-17	Lowland	7.44	1.17	1.78	10.4	23.2	11.1	2.94	10.1
S2021-18	High terrace	20.9	1.68	2.38	24.9	29.2	10.6	3.04	15.1
S2021-19	High terrace	14.0	2.14	2.73	18.9	27.6	15.3	4.14	14.5
S2021-20	High terrace	21.9	2.27	3.04	27.2	32.8	13.0	3.92	16.8

Appendix Table 4-7. Calcium (Ca) uptake, concentration, and their distribution of winter wheat grown along river terraces in the Tokachi district.

Sample ID	Level of river terrace	Ca uptake				Ca concentration			
		Stem	Husk	Grain	Plant	Stem	Husk	Grain	Plant
		g m^{-2}				g kg^{-1}			
S2020-01	Middle terrace	1.75	0.15	0.21	2.12	3.22	0.92	0.33	1.56
S2020-02	High terrace	1.16	0.10	0.15	1.41	2.40	0.79	0.27	1.19
S2020-03	Middle terrace	1.12	0.11	0.17	1.40	3.28	0.87	0.31	1.38
S2020-04	Middle terrace	2.39	0.14	0.24	2.77	4.30	0.85	0.33	1.92
S2020-05	Middle terrace	1.20	0.10	0.17	1.48	2.80	0.83	0.29	1.29
S2020-06	Lowland	0.62	0.10	0.15	0.87	2.98	1.21	0.37	1.24
S2020-07	Low terrace	1.86	0.17	0.25	2.28	2.74	0.82	0.32	1.37
S2020-08	Low terrace	0.91	0.10	0.21	1.21	3.14	0.80	0.39	1.29
S2020-09	Low terrace	1.15	0.15	0.16	1.47	2.72	0.98	0.33	1.36
S2020-10	Lowland	2.12	0.19	0.26	2.56	3.22	0.99	0.33	1.57
S2020-11	Lowland	1.28	0.17	0.22	1.66	2.82	1.06	0.35	1.34
S2020-12	Low terrace	1.40	0.16	0.22	1.78	3.10	0.94	0.31	1.34
S2020-13	Middle terrace	1.85	0.18	0.22	2.25	3.26	1.08	0.33	1.62
S2020-14	Middle terrace	2.27	0.22	0.22	2.71	3.58	1.21	0.33	1.84
S2020-15	High terrace	1.33	0.12	0.15	1.61	3.42	1.02	0.33	1.67
S2020-16	Lowland	1.47	0.12	0.22	1.81	2.98	0.82	0.31	1.35
S2020-17	Lowland	1.31	0.14	0.21	1.65	2.76	0.95	0.29	1.25
S2020-18	High terrace	1.35	0.15	0.15	1.64	3.22	1.16	0.30	1.59
S2020-19	High terrace	1.32	0.12	0.15	1.60	3.08	0.91	0.27	1.42
S2020-20	High terrace	1.25	0.11	0.17	1.53	2.68	0.85	0.29	1.29
S2021-01	Low terrace	1.69	0.21	0.22	2.12	2.80	1.39	0.29	1.40
S2021-02	High terrace	2.32	0.19	0.09	2.59	3.08	1.06	0.11	1.51
S2021-03	Middle terrace	2.01	0.17	0.21	2.39	3.40	1.12	0.30	1.67
S2021-04	Middle terrace	2.13	0.16	0.27	2.57	2.96	0.94	0.28	1.37
S2021-05	Lowland	0.77	0.11	0.09	0.97	2.54	1.10	0.19	1.12
S2021-06	Low terrace	1.23	0.13	0.20	1.56	2.06	0.82	0.25	1.00
S2021-07	Low terrace	1.58	0.16	0.22	1.96	2.96	1.07	0.30	1.40
S2021-08	Low terrace	1.98	0.16	0.23	2.37	3.14	0.96	0.31	1.54
S2021-09	Lowland	1.91	0.15	0.23	2.30	2.62	1.00	0.29	1.36
S2021-10	Lowland	2.04	0.23	0.23	2.50	3.60	1.30	0.32	1.69
S2021-11	Low terrace	1.92	0.20	0.25	2.37	3.10	1.15	0.35	1.56
S2021-12	Lowland	1.49	0.14	0.21	1.85	2.46	0.91	0.25	1.15
S2021-13	Middle terrace	1.84	0.18	0.28	2.30	2.56	0.96	0.33	1.31
S2021-14	Middle terrace	3.37	0.23	0.22	3.82	4.32	1.33	0.30	2.25
S2021-15	High terrace	2.42	0.18	0.21	2.82	3.74	1.12	0.29	1.81
S2021-16	Low terrace	1.71	0.16	0.27	2.14	2.58	1.00	0.30	1.24
S2021-17	Lowland	0.81	0.12	0.17	1.11	2.52	1.17	0.29	1.07
S2021-18	High terrace	2.13	0.15	0.23	2.52	2.98	0.97	0.30	1.52
S2021-19	High terrace	1.73	0.15	0.18	2.06	3.40	1.06	0.28	1.58
S2021-20	High terrace	2.39	0.20	0.25	2.84	3.58	1.14	0.33	1.76

Appendix Table 4-8. Magnesium (Mg) uptake, concentration, and their distribution of winter wheat grown along river terraces in the Tokachi district.

Sample ID	Level of river terrace	Mg uptake				Mg concentration			
		Stem	Husk	Grain	Plant	Stem	Husk	Grain	Plant
		g m^{-2}				g kg^{-1}			
S2020-01	Middle terrace	0.723	0.077	0.614	1.41	1.33	0.46	0.95	1.04
S2020-02	High terrace	0.617	0.049	0.596	1.26	1.28	0.39	1.03	1.06
S2020-03	Middle terrace	0.469	0.058	0.562	1.09	1.37	0.46	1.03	1.08
S2020-04	Middle terrace	0.905	0.066	0.734	1.70	1.63	0.39	1.02	1.18
S2020-05	Middle terrace	0.468	0.050	0.543	1.06	1.09	0.40	0.92	0.92
S2020-06	Lowland	0.088	0.015	0.452	0.56	0.42	0.19	1.09	0.79
S2020-07	Low terrace	0.529	0.067	0.733	1.33	0.78	0.33	0.94	0.80
S2020-08	Low terrace	0.244	0.043	0.531	0.82	0.85	0.34	1.02	0.87
S2020-09	Low terrace	0.465	0.063	0.567	1.10	1.10	0.40	1.14	1.02
S2020-10	Lowland	0.466	0.061	0.801	1.33	0.71	0.32	1.02	0.81
S2020-11	Lowland	0.291	0.053	0.686	1.03	0.64	0.34	1.08	0.83
S2020-12	Low terrace	0.652	0.085	0.736	1.47	1.45	0.50	1.05	1.11
S2020-13	Middle terrace	0.683	0.066	0.615	1.36	1.20	0.40	0.94	0.98
S2020-14	Middle terrace	0.577	0.059	0.572	1.21	0.91	0.33	0.87	0.82
S2020-15	High terrace	0.501	0.048	0.473	1.02	1.29	0.40	1.05	1.06
S2020-16	Lowland	0.549	0.041	0.768	1.36	1.11	0.28	1.11	1.02
S2020-17	Lowland	0.358	0.039	0.736	1.13	0.76	0.27	1.05	0.85
S2020-18	High terrace	0.495	0.053	0.482	1.03	1.18	0.42	1.00	1.00
S2020-19	High terrace	0.422	0.045	0.451	0.92	0.98	0.33	0.81	0.82
S2020-20	High terrace	0.445	0.039	0.588	1.07	0.96	0.30	1.00	0.90
S2021-01	Low terrace	0.420	0.082	0.694	1.20	0.70	0.53	0.91	0.79
S2021-02	High terrace	0.684	0.072	0.302	1.06	0.91	0.41	0.38	0.62
S2021-03	Middle terrace	0.754	0.070	0.694	1.52	1.27	0.46	1.01	1.06
S2021-04	Middle terrace	0.755	0.062	0.856	1.67	1.05	0.36	0.87	0.89
S2021-05	Lowland	0.145	0.022	0.238	0.40	0.48	0.21	0.52	0.47
S2021-06	Low terrace	0.282	0.047	0.704	1.03	0.47	0.29	0.88	0.66
S2021-07	Low terrace	0.397	0.051	0.652	1.10	0.74	0.34	0.91	0.79
S2021-08	Low terrace	0.551	0.051	0.720	1.32	0.88	0.30	0.98	0.86
S2021-09	Lowland	0.498	0.048	0.715	1.26	0.68	0.31	0.89	0.75
S2021-10	Lowland	0.508	0.070	0.684	1.26	0.90	0.39	0.92	0.85
S2021-11	Low terrace	0.560	0.059	0.707	1.33	0.91	0.33	0.98	0.87
S2021-12	Lowland	0.397	0.039	0.665	1.10	0.65	0.25	0.79	0.68
S2021-13	Middle terrace	0.657	0.067	0.762	1.49	0.91	0.36	0.90	0.85
S2021-14	Middle terrace	0.973	0.073	0.587	1.63	1.25	0.43	0.78	0.96
S2021-15	High terrace	1.065	0.078	0.762	1.91	1.65	0.48	1.02	1.22
S2021-16	Low terrace	0.698	0.067	0.754	1.52	1.05	0.42	0.84	0.88
S2021-17	Lowland	0.169	0.043	0.532	0.74	0.53	0.41	0.88	0.72
S2021-18	High terrace	0.827	0.072	0.610	1.51	1.16	0.46	0.78	0.91
S2021-19	High terrace	0.480	0.056	0.603	1.14	0.94	0.40	0.91	0.87
S2021-20	High terrace	0.726	0.072	0.873	1.67	1.09	0.41	1.13	1.03

Appendix Table 4-9. Silicon (Si) uptake, concentration, and their distribution of winter wheat grown along river terraces in the Tokachi district.

Sample ID	Level of river terrace	Si uptake				Si concentration			
		Stem	Husk	Grain	Plant	Stem	Husk	Grain	Plant
		g m^{-2}				g kg^{-1}			
S2020-01	Middle terrace	8.79	4.68	0.72	14.2	16.16	28.02	1.12	10.46
S2020-02	High terrace	7.89	3.70	0.71	12.3	16.34	29.42	1.21	10.33
S2020-03	Middle terrace	4.60	2.65	0.31	7.56	13.45	21.11	0.56	7.46
S2020-04	Middle terrace	13.5	4.92	0.47	18.9	24.28	29.42	0.65	13.07
S2020-05	Middle terrace	8.44	4.32	0.39	13.1	19.61	34.56	0.65	11.44
S2020-06	Lowland	2.11	2.10	1.12	5.3	10.09	26.15	2.71	7.57
S2020-07	Low terrace	10.9	6.84	1.53	19.3	16.06	33.34	1.96	11.59
S2020-08	Low terrace	6.01	3.31	1.17	10.5	20.83	26.43	2.24	11.20
S2020-09	Low terrace	6.80	5.22	1.07	13.1	16.06	33.25	2.15	12.14
S2020-10	Lowland	8.04	4.19	1.17	13.4	12.24	21.86	1.49	8.20
S2020-11	Lowland	7.65	4.08	0.59	12.3	16.91	26.06	0.93	9.90
S2020-12	Low terrace	6.74	3.82	0.92	11.5	14.94	22.51	1.31	8.69
S2020-13	Middle terrace	11.2	4.21	1.35	16.7	19.61	25.40	2.05	12.01
S2020-14	Middle terrace	11.5	4.32	1.36	17.2	18.21	24.00	2.05	11.68
S2020-15	High terrace	6.19	2.30	0.68	9.16	15.88	18.87	1.49	9.50
S2020-16	Lowland	4.84	3.35	1.04	9.23	9.81	22.79	1.49	6.91
S2020-17	Lowland	7.53	3.79	1.38	12.7	15.88	25.68	1.96	9.58
S2020-18	High terrace	7.14	3.27	0.86	11.3	17.09	25.87	1.77	10.96
S2020-19	High terrace	7.11	3.24	0.84	11.2	16.53	23.82	1.49	9.93
S2020-20	High terrace	8.21	4.48	0.83	13.5	17.65	33.90	1.40	11.38
S2021-01	Low terrace	5.47	3.02	1.35	9.83	9.06	19.52	1.77	6.48
S2021-02	High terrace	11.3	5.79	1.11	18.2	15.04	33.25	1.40	10.61
S2021-03	Middle terrace	11.3	5.11	1.09	17.5	19.05	33.16	1.59	12.20
S2021-04	Middle terrace	13.6	5.99	1.01	20.6	18.87	34.56	1.03	10.98
S2021-05	Lowland	0.99	1.32	0.69	3.00	3.27	12.61	1.49	3.45
S2021-06	Low terrace	8.53	5.58	0.67	14.8	14.29	35.12	0.84	9.49
S2021-07	Low terrace	6.98	4.66	0.54	12.2	13.08	31.29	0.75	8.70
S2021-08	Low terrace	7.58	3.98	0.62	12.2	12.05	23.16	0.84	7.92
S2021-09	Lowland	13.1	7.07	0.83	21.0	17.93	45.95	1.03	12.44
S2021-10	Lowland	5.81	3.23	0.41	9.46	10.27	18.03	0.56	6.37
S2021-11	Low terrace	6.12	4.09	0.67	10.9	9.90	22.98	0.93	7.17
S2021-12	Lowland	6.98	3.92	0.87	11.8	11.49	24.84	1.03	7.30
S2021-13	Middle terrace	12.9	6.16	1.19	20.2	17.84	33.25	1.40	11.52
S2021-14	Middle terrace	14.6	5.01	0.98	20.6	18.77	29.33	1.31	12.14
S2021-15	High terrace	13.7	5.71	0.70	20.1	21.20	34.65	0.93	12.91
S2021-16	Low terrace	7.79	3.76	0.59	12.1	11.77	23.54	0.65	7.04
S2021-17	Lowland	4.01	3.50	0.79	8.31	12.52	33.25	1.31	8.06
S2021-18	High terrace	10.5	5.68	0.51	16.7	14.66	35.87	0.65	10.07
S2021-19	High terrace	6.32	2.44	0.18	8.94	12.42	17.47	0.28	6.84
S2021-20	High terrace	7.91	5.44	0.58	13.9	11.86	31.10	0.75	8.61

Appendix III. Soil available Si index of paddy soils

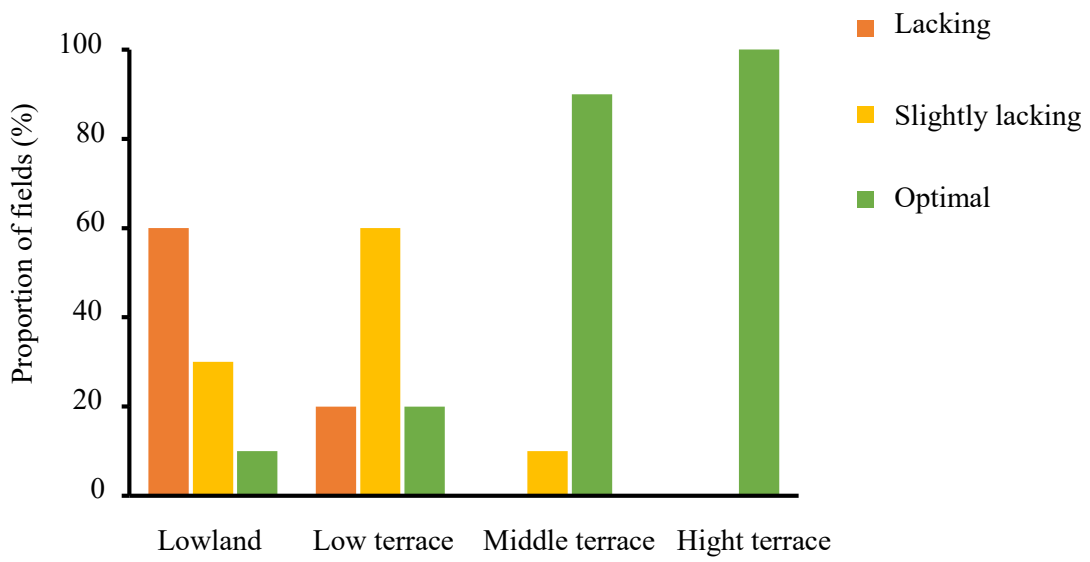

Status of soil available Si in Shimizu town (AB method), Tokachi. Based on a soil available Si index for rice paddy fields (Hatano et al., 2021). Lacking Si – soil with an available Si content less than 47 mg kg^{-1}, slightly lacking Si – soil with an available Si content between 47 – 75 mg kg^{-1} and soil with an available Si content of above 75 mg kg^{-1} is optimal.

Appendix IV. Wheat biomass and grain yields

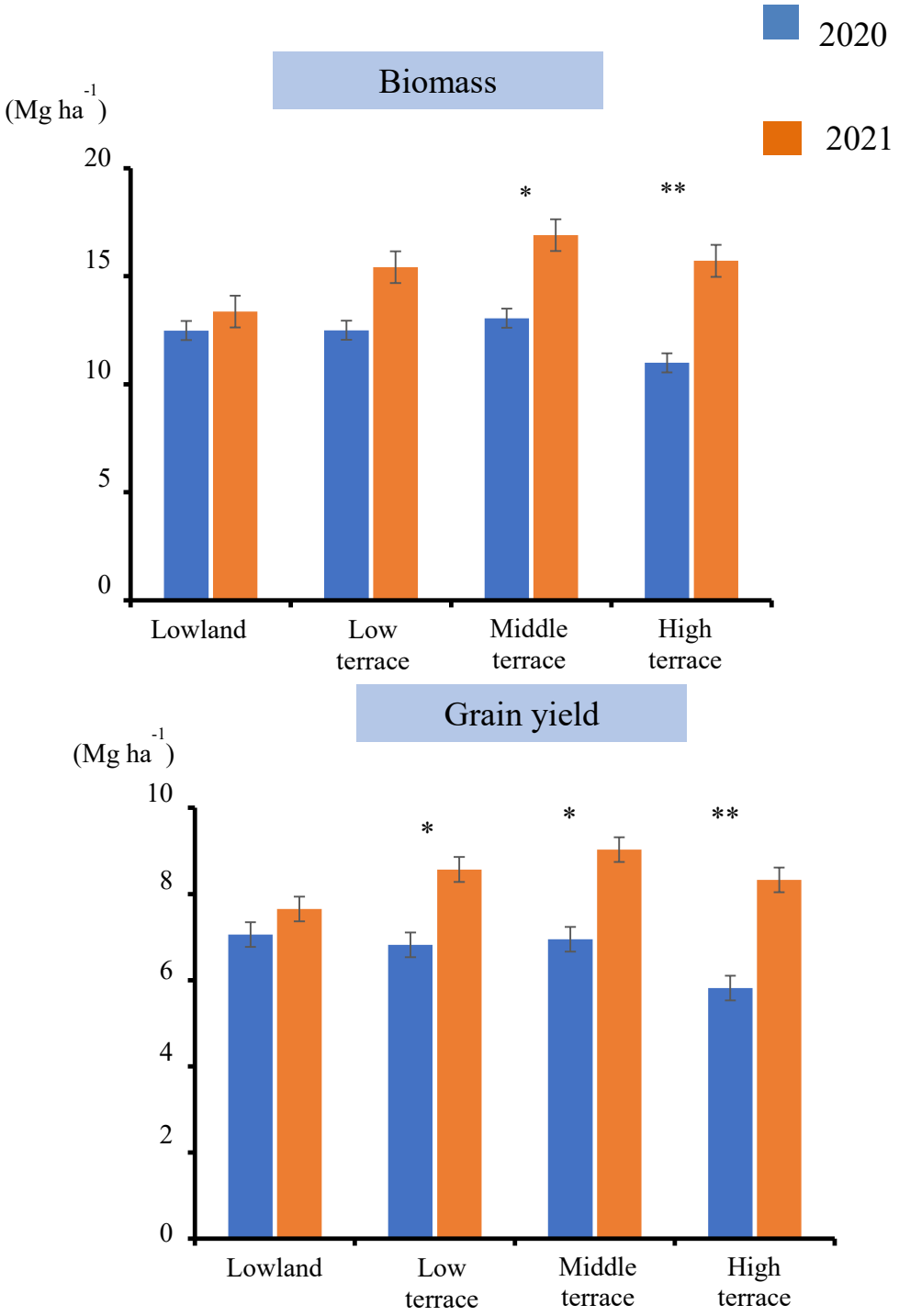

Appendix V. Multiple – regression analysis

$$Y_{Biomass} = 51X_{N\text{-}uptake} + 218X_{P\text{-}uptake} - 15X_{K\text{-}uptake} - 188X_{Mg\text{-}uptake} + 27X_{Si\text{-}uptake} + 26.7$$

$$(R^2 = 0.88, p < 0.01)$$

$$Y_{yield} = 39X_{N\text{-}uptake} + 53X_{P\text{-}uptake} - 20X_{K\text{-}uptake} - 143X_{Mg\text{-}uptake} + 12X_{Si\text{-}uptake} + 26.6$$

$$(R^2 = 0.80, p < 0.01)$$

Effect summary table

Source	P value	
	Biomass	Yield
N	**<0.001**	**<0.001**
P	**<0.001**	**<0.001**
K	0.06	**<0.001**
Mg	0.09	0.05
Si	**<0.001**	**<0.01**